[redacted]

(10)

NACA

RESEARCH MEMORANDUM

AN INVESTIGATION OF THE STREAM-TUBE POWER LOSSES AND AN IMPROVEMENT OF THE DIFFUSER-ENTRANCE NOSE IN THE LANGLEY 8-FOOT TRANSONIC TUNNEL

By Richard T. Whitcomb, Melvin M. Carmel,
and Francis G. Morgan, Jr.

Langley Aeronautical Laboratory
Langley Field, Va.

NATIONAL ADVISORY COMMITTEE
FOR AERONAUTICS

WASHINGTON

July 30, 1952

[redacted]

NATIONAL ADVISORY COMMITTEE FOR AERONAUTICS

RESEARCH MEMORANDUM

AN INVESTIGATION OF THE STREAM-TUBE POWER LOSSES AND AN IMPROVEMENT OF THE DIFFUSER-ENTRANCE NOSE IN THE LANGLEY 8-FOOT TRANSONIC TUNNEL

By Richard T. Whitcomb, Melvin M. Carmel, and Francis G. Morgan, Jr.

SUMMARY

Surveys of the distribution of total pressure, total temperature, and static pressure have been made at a number of stations in the slotted test section and diffuser of the Langley 8-foot transonic tunnel with early and improved diffuser-entrance noses installed at the ends of the slots. The results of these surveys and the development of the improved noses are described.

With the early diffuser-entrance nose installed, a large part of the power loss associated with the installation of the slotted test section was caused by the inefficient induction of the part of the stream tube outside the slots into the diffuser. The installation of improved diffuser-entrance noses substantially reduced the losses associated with the induction of the stream tube into the diffuser. With the improved diffuser-entrance nose installed, the increase in power loss due to the addition of the slots is most pronounced in the forward portions of the slotted throat.

INTRODUCTION

A slotted test section has recently been installed in the Langley 8-foot transonic tunnel. The slots reduce tunnel wall blockage and allow continuous operation of the tunnel through the speed of sound to low-supersonic Mach numbers (ref. 1). The results of the calibration of the flow in the test section are presented in reference 2. The power required to operate the tunnel with the slotted section at a given Mach number was considerably greater than that necessary for operation of the tunnel with a closed throat. Specifically, at a Mach number of 1.10,

the power requirement was almost twice as great as that which would have been needed for the tunnel with a closed throat operating at that speed.

In order to determine the sources of the power losses associated with installation of the slots, surveys of the distributions of total pressure, total temperature, and static pressure were made at a number of stations in the slotted test section and diffuser of the Langley 8-foot transonic tunnel. In order to reduce the associated losses, a revised diffuser-entrance nose has been developed. The surveys have been repeated with the final configuration of the revised diffuser-entrance nose installed to provide the basis for further reductions in the tunnel power requirements.

SYMBOLS

M	local Mach number
M_o	mean Mach number at center line of test region
M_{TC}	Mach number based on total pressure at center line of stream and static pressure in test chamber
V	local velocity
p_l	local static pressure
p_{tc}	test-chamber static pressure
p_a	atmospheric pressure
ρ_l	local mass density
ρ_H	mass density after increasing pressure of local element to local total pressure isentropically
ρ_{p_a}	mass density after increasing pressure of local element to atmospheric pressure isentropically
H	local total pressure
ΔH	local total pressure deficiency with relation to atmospheric pressure

[redacted]

ΔE	power required to raise total pressures of all elements passing through a stream-tube cross section to atmospheric pressure isentropically
ΔE_l	power required to raise total pressures of all elements passing through a stream-tube cross section to atmospheric pressure; based on measurement obtained at a single survey station
E_K	kinetic power of a stream tube in the test region assuming the conditions are uniform across the section
r	radial distance from center line of tunnel
R_l	local radius of stream tube
θ	angular segment of circular stream-tube section (table I)
y'	lateral distance from center line of a slot at wall
z	vertical distance from panel surface
b	lateral distance from center line of slot to center line of panel at wall
a	distance from surface of panel to radius through center line of slot; normal to panel (table I)
A	local enclosed cross-sectional area
A_o	area at tunnel minimum section
γ	ratio of specific heats; 1.40 for air

APPARATUS

Tunnel and Diffuser-Entrance Nose

The Langley 8-foot transonic tunnel is a continuous circuit tunnel as shown in figure 1. The stagnation pressure is maintained at essentially atmospheric pressure by the vent tower. The major part of diffusion occurs ahead of the first set of turning vanes downstream of the test section. The slotted test section of the tunnel is shown in figure 2 and is described more completely in reference 1. The diffuser-entrance-nose configuration used during the development of slot shape

[redacted]

(ref. 1) and the survey of the distributions of the test-section Mach number (ref. 2) is shown in figure 3(a). This nose, which was referred to as "nose A" in reference 2, will be designated "original nose" throughout this paper. The final diffuser-entrance nose configuration, which was derived during the development tests described herein, is shown in figure 3(b). This nose, which was referred to as "nose B" in reference 2, will be designated "final revised nose" herein.

The final revised noses were placed between steel plates parallel in the region of the noses 3.5 inches apart, which simplified the adjustment of the positions of the various noses. (See fig. 4.) Ahead of the noses, the plates are curved outward, fairing into the test-section structure at a station 93 inches downstream from the origin of the slots. Outlines of the various nose shapes which were investigated during the development of the final configuration are presented in figure 5.

Survey Equipment

Point values of the total pressure and total temperature were measured using probes as shown in figure 6. The design of the total-pressure probes was such that the total pressures were measured with negligible error, except for losses due to normal shock at Mach numbers greater than 1.0 at angles up to 20° from the direction of flow. The total-temperature probe allowed a direct measurement of the total temperature without any significant correction. Angles of downwash and sidewash in the slots were measured using claw-type yaw meters. (See fig. 7.)

The probes were supported in the tunnel by 12 rakes. At the end of the diffuser, the probes were supported by a 14-foot-long rake, which completely spanned the tunnel. In the forward region of the diffuser, surveys were made with 2-foot-span rakes as shown on the right of figure 7(a). In the test section, investigations were made with 1-foot-span rakes as shown in the center of figure 7(a). At the origin of the slots, the surveys were made with 6-inch rakes, as shown in the left of figure 7(a). In the slots in the region of the diffuser-entrance noses, surveys were made with a rake, shown in the center of figure 7(b), which spanned the slot. In the slots ahead of the noses, the surveys were made with rakes, shown on the right and left of figure 7(b), which could be rotated and moved normal to the tunnel axes. Surveys of the losses caused by the model support system were obtained with a 1-foot rake attached to the downstream end of this support.

Static pressures were measured along the center line of the tunnel during some of the test runs by use of orifices installed in a

2-inch-diameter tube. (See ref. 2.) During other test runs, the 45° sweptback wing-body model shown in figure 8, was installed in the test region with the nose 70 inches downstream of the slot origin.

METHODS

Measurements

With the original diffuser-entrance noses installed, total-pressure and temperature surveys were made along radial lines at the streamwise and lateral locations listed in table I. Static pressures were measured at the center line of the tunnel on the center line of a nose and along the center line of a panel in the vicinity of the diffuser-entrance nose; they were also measured at the survey stations in the diffuser. During the surveys with the original diffuser-entrance nose installed, a small model which had an insignificant effect on the flow near the test-section wall was at the center line of the test section.

During the development tests of the revised diffuser-entrance nose, static pressures were measured along a line on one of the side walls of the diffuser-entrance-nose combination and along a line near the edge of one of the panels in the vicinity of the nose (fig. 3(b)) in addition to measurements at the same locations as with the original nose. For these tests, runs were made with either the 45° sweptback wing-body model (fig. 8) or the static survey tube installed in the test region. The conditions for the various test runs are listed in figure 5.

With the final revised diffuser-entrance nose installed, total pressure and temperature surveys were made at the stations listed in table II. The wing-body model shown in figure 8 was in the test section during all these surveys. This model had a definite effect on the flow near the tunnel wall which resulted in a change in the energy losses associated with the tunnel boundary layer.

Because of a mixing in the slots and in the diffuser, the local static pressures, total pressures, and flow angularities in these regions fluctuate by relatively large amounts. Inasmuch as the frequency responses of the manometer leads and liquid columns are generally much lower than the fluctuations of the pressures, the manometer readings usually indicate nearly constant pressures. It can be shown that these nearly constant pressures are not exactly the mean pressures; however, for the accuracy required in the present analysis, the manometer reading may be assumed to be equal to the mean pressures. The fluctuations of the total pressure near the outer edge of the boundary layer in the diffuser are, at times, of the same order as the responses of the manometers. For these conditions, the manometer readings varied by as

[redacted]

much as 10 percent at times. To compensate partially for these fluctuations, the averages of three manometer readings were used in the reduction of the data.

Attempts were made to measure static pressures in the stream with static probes on the rakes which were previously described. Because of the irregular and unsteady nature of the flow near the wall, however, these pressure measurements were found to be unreliable and were not used in the calculations of the local Mach numbers. Local static pressures in the stream were estimated on the basis of the pressures measured on the wall and along the center line of the tunnel. Measurements made with the yaw heads indicate that even in the slot the average cross flows are small. Therefore, no corrections have been applied to the data to account for these stream deviations.

During the initial investigation of the slotted throat in the Langley 8-foot transonic tunnel, tests were made with the slots closed with wooden filler blocks to obtain power measurements for the directly comparable closed-throat wind tunnel. During these tests, power-loss surveys were made at the end of the diffuser with the rake described in the section on "Apparatus." Surveys were not made in the test region or forward portion of the diffuser.

Reduction of Data

Method of computation.- Using the measured values of local total pressure, total temperature, and static pressure, the energies required to raise the total pressures of all elements passing through the various stream-tube cross sections to atmospheric pressure isentropically have been calculated for each streamwise measurement station. An attempt was made to determine the actual energy losses from one survey station to another by determining the total energy of the stream at each station. However, the results of such a process proved to be extremely inaccurate because the values of the losses desired are very small compared with the total energy values, so that small errors in the total energy results produced very large errors in the loss values.

The energy required to raise the pressure of a unit mass to atmospheric pressure is defined as

$$e_m = \frac{\gamma}{\gamma - 1}\left(\frac{p_a}{\rho_{p_a}} - \frac{H}{\rho_H}\right)$$

[redacted]

The energy required for a unit area per unit time, or the power, is

$$e_a = \frac{\gamma}{\gamma - 1} \rho_l V \left(\frac{p_a}{\rho_{p_A}} - \frac{H}{\rho_H} \right)$$

$$= \frac{\gamma}{\gamma - 1} V \left[p_a \left(\frac{\rho_l}{\rho_{p_A}} \right) - H \left(\frac{\rho_l}{\rho_H} \right) \right]$$

By use of this last relation, unit values of power were obtained for the points of total-pressure measurement. To calculate these powers, the local Mach numbers, velocities, and density ratios were determined by using tables based on one-dimensional flow relations for a compressible fluid. The total power required for a given circular stream tube is

$$\Delta E = \int_0^{2\pi} \int_0^{R_l} e_a r \, dr \, d\theta$$

Surveys made at a number of circumferential stations for one streamwise station (table I) indicated that the losses were approximately the same on each segment of the tunnel bounded by radii through the center lines of a slot and panel. The measurements and computations were, therefore, simplified without a significant loss in accuracy by using the expression

$$\Delta E = 24 \int_0^{\frac{\pi}{12}} \int_0^{R_l} e_a r \, dr \, d\theta$$

The energy required for the measurement stations in the dodecagonal-shaped portions of the enclosed stream tube was integrated as follows:

$$\Delta E = 24 \int_0^b \int_0^a e_a \, dz \, dy'$$

At the measurement station in the test section, the power of the stream tube outside the slots was summarized in a similar manner.

[redacted]

In order to reduce the total power values to nondimensional form, these values were divided by the equation

$$E_K = \frac{\gamma}{\gamma - 1}(A\rho V)_{TC}\left(\frac{p_a}{\rho_{p_a}} - \frac{P_{TC}}{\rho_{TC}}\right)$$

$$= \frac{\gamma}{\gamma - 1}(AV)_{TC}\left(p_a \frac{\rho_{TC}}{\rho_{p_a}} - p_{TC}\right)$$

which is the kinetic power of a stream tube in the test region if the conditions are assumed to be uniform across the section with the total pressure equal to atmospheric pressure; the temperature equal to that at the center line of the entrance cone; and the velocity, static density, and stream-tube area equal to the values obtained by reducing the pressure in the stream isentropically to the pressure in the test chamber. This test-chamber pressure is approximately equal to the mean static pressure in the slotted test section. (See ref. 2.) The variation of this kinetic power with Mach number for the indicated reference temperatures is presented in figure 9.

Adjustments for variations in stream tube.- Because of the mixing in the regions of the slots, a small proportion of the kinetic power and momentum of the tunnel stream tube is transferred to the essentially still air just outside the slot. The entrained extraneous air moves, with the stream tube, past the measurement station in the slot to the diffuser-entrance nose. Because of the irregular nature of the flow near the slots, part of this extraneous air is carried into the tunnel diffuser instead of part of the original stream tube; however, the major portion of this air is rejected into the test chamber below the diffuser-entrance noses. To provide the most satisfactory indication of the origin of the power losses overcome by the fan, the summation of energy losses at the measurement station in the slot should include only that for the air induced into the diffuser. It is impossible to accomplish this summation exactly on the basis of the limited data available. An approximation has been obtained, however, by summarizing the energy losses of the air with a mass equal to that of the original stream tube above a line perpendicular to the slot plane of symmetry (designated "c" in table II).

The flow was reversed over the major part of the surface of the original diffuser-entrance nose. At the 145-inch measurement station, the region of reversed flow extended from the surface of the nose into

[redacted]

the tunnel proper. This reversed air also constituted part of the air moving in the stream direction above the nose. Obviously, in the summation of the power losses of the tunnel stream tube, the losses in this recirculating air should not be included. However, as for the flow in the slots, the cross section occupied by this recirculating air, and thus the losses for the stream tube, cannot be determined exactly. A reasonably close estimate of the losses at this station has been obtained by summarizing the losses of the air, with a mass equal to that of the original stream tube, passing above the panels between lines vertical to the panels (designated "d" in table I).

The determinations of the cross-sectional areas occupied by the mass of the tunnel stream tube are affected by the temperatures, total pressures, and static pressures at all points at the reference minimum station and at the measurement stations. Measured values of these quantities were not available for all points which required that estimated values be used for some points. As a result, the computed stream-tube areas are probably in error. Because of these differences, as well as errors in the estimations of distribution of these areas as mentioned previously, the final total power-loss values for the 90-inch and 145-inch stations are less reliable than the values for other stations.

Allowance for model support system.- The losses measured at the end of the central support were relatively minor and have not been included in the summation of the losses in the vicinity of the support. A loss equal to that measured at the end of the support has been subtracted from that measured across the entire cross section at the end of the diffuser.

Effect of Temperature Variations on Results

The radial distributions of local total temperature measured at the center line of the panel at the various streamwise stations are presented in figure 10. Except for station 337, the temperatures presented at the center line of the individual survey stations were actually measured in the entrance cone ahead of the test region. The mean temperature levels at the various stations differ by perceptible amounts because of the differences in atmospheric temperature present during the various test runs. These differences did not have a direct effect on the nondimensional power losses since they affect the numerator and denominator of the power expression in the same proportions.

These temperature results (fig. 10) indicate marked variations in temperature from the wall to the center line of the tunnel at all streamwise stations for Mach numbers of 0.60 and 1.10. The variations are most severe at the origin of the slotted throat and, in general, become progressively less pronounced at stations farther downstream. This temperature variation is associated with the method used to cool the tunnel,

by which atmospheric air is induced into the circuit at the air-exchange tower around the periphery of the stream tube. The mixing in the low-velocity stream between the tower and the test section is relatively slight, and, as a result, the temperature gradient initiated at the tower persists to the test section. A comparison of the temperatures measured at given stations during different runs indicates that the lateral temperature gradients are affected by the length of a run and the outside temperature. Such variations cause changes in the nondimensional power-loss results obtained from the total pressure and temperature surveys. These changes result primarily from a shift of the absolute losses in the boundary layer, based on the temperatures near the wall, compared with the reference loss, which is based on the temperature at the center line of the tunnel. They are also caused by changes of the mixing phenomena in the diffuser associated with the variations of the radial density and velocity gradients. In an attempt to reduce the variations in the data measured during the various test runs due to changes in the temperature gradients, data obtained for the various Mach numbers were recorded on the same sequence during each run.

RESULTS AND DISCUSSION

Survey of Power Losses With the Original Diffuser-Entrance Nose

The fan power required to operate the tunnel with a slotted test section and the original diffuser-entrance nose at a Mach number of 0.60 is approximately 1.22 times greater than that required for the same tunnel with a closed throat. (See fig. 11.) This ratio increases as the Mach number is increased, reaching a value of 2.04 at the maximum attainable Mach number of 1.13. (These data were obtained from ref. 2.)

Axial distribution of power losses.- The developments of the power losses in the tunnel circuit with a slotted throat and the original diffuser-entrance nose installed are presented in figure 12. These losses are in terms of the sum of the powers required to raise the local point total pressures to atmospheric pressure. The developments of the losses for the tunnel with a closed throat at a Mach number of 1.00 are also indicated. The experimental power-loss values for the closed throat at the origin of the slots and 9.8 feet (117 in.) downstream of the origin for a Mach number of 1.00 were obtained from data measured at the center line of the panels of the slotted throat with the final revised diffuser-entrance nose installed. An examination of the total-pressure data measured near the panels for this condition indicates that the boundary layer at the center line of the panel at the 117-inch station is only slightly affected by the presence of the slot, and the data measured here are indicative of the boundary-layer losses for a closed throat.

[redacted]

The increase in the power losses in the slotted test section at a Mach number of 1.00 is approximately 60 percent greater than the loss for the closed throat because of mixing in the slots. In the vicinity of the diffuser-entrance nose of the slotted throat, the losses are considerably more severe than in the comparable region of the closed throat. The large losses in this region may be attributed primarily to the presence of reversed or separated flow over the diffuser-entrance nose. Tuft surveys indicate the flow is reversed on the nose from the 14.2-foot (170-inch) streamwise station forward to the leading edge of the nose. The total-pressure measurement at the 12.1-foot (145-inch) streamwise station indicates that the region of reversed flow extends from the surface of the nose to a point several inches inside the tunnel wall, the region expanding with increase in Mach number. The tuft and total-pressure measurements indicate that this local, reversed, or separated flow does not lead to separation on the diffuser wall. The losses in the diffuser downstream of the slotted test section are greater than those for the diffuser with the closed throat for a Mach number of 1.00. This additional loss is due to the lower energy of the air induced into the diffuser with the slotted throat.

When the Mach number is increased from 0.60 to 1.00, the nondimensional losses in the slotted test section increase by approximately 14 percent. (See fig. 12.) This change must be caused by an increase in the losses associated with mixing at the higher subsonic Mach numbers, inasmuch as the nondimensional skin-friction losses on the panel decrease and the geometry of the stream tube in the test region remains essentially the same. When the Mach number is increased from 1.00 to 1.10, the nondimensional losses in the slotted test section increase further to approximately 30 percent. This increase is due primarily to the expansion of the stream tube into the slot which is required to obtain this supersonic Mach number. The additional loss is slightly greater than the power loss involved in throttling the air which expands through the slots from a total pressure of atmospheric to that of the test chamber.

The pressures measured on the panel (fig. 13) indicate an abrupt adverse gradient at approximately the 146-inch streamwise station at a Mach number of 0.60, which suggests that increased diffusion causes part of the large losses in this region of the diffuser-entrance nose for this condition. At a test-section Mach number of 1.10, the gradients in this same region are slight, and a severe discontinuity in the Mach number distribution along the center line of the tunnel occurs downstream of the 144-inch streamwise station. (See fig. 13.) The near-sonic Mach number downstream of the discontinuity indicates that it is not associated with a full normal shock. This discontinuity is probably the result of a merging of oblique shocks initiated by the compressive disturbances emanating from the vicinity of the slots ahead of the leading edges of the diffuser-entrance noses. The total-pressure measurements obtained at the 169-inch streamwise station indicate that this discontinuity causes

insignificant power losses. The acceleration of the flow ahead of this discontinuity is associated with the gradual divergence of the panel walls, at an angle greater than the 5° of the test region, starting at about the 100-inch station. (See ref. 1.)

Lateral and radial distribution of losses.- Lateral variations of the power required to raise the total pressures of stream-tube elements to atmospheric pressure, based on pressure and temperature measurements obtained at single survey stations, are presented in figure 14. These data provide an indication of the lateral distributions of the power losses. Because of the reversed flow over the diffuser-entrance nose, data obtained near the slot at the 145-inch streamwise station are of little value and have not been presented. The data for Mach numbers of 0.60 and 1.10 indicate that, at the 145-inch station, the losses are greatest in the proximity of the slot, as might be expected since the mixing in the slot causes a large local loss which is added to the general skin-friction loss.

Between the 145-inch and the 169-inch stations, the losses at the center line of the panel increase abruptly while those at the center line of the slot decrease, although the major portion of the large loss developing in this region is probably due to mixing above the diffuser entrance nose. This trend continues farther downstream so that, at the 241-inch station, the losses at rake positions behind the panel exceed those behind the slot. Apparently, a strong cross flow of low-energy air from the region behind the slot to that behind the panel is present. This cross flow may be attributed to the differences in panel and slot pressures shown in figure 13. This lateral transfer of low-energy air is more pronounced at a Mach number of 0.60 than at a Mach number of 1.10.

The radial variations of total-pressure deficiencies measured at the various stations in the diffuser (fig. 15) indicate the expected rapid thickening of the boundary layer associated with the flow against the positive pressure gradient (fig. 16). At the diffuser exit, the boundary layer extends to the center line of the tunnel.

Development of Revised Diffuser-Entrance Noses

Basic concept.- If the reversed flow on the diffuser-entrance nose, as described in the previous section, had not been present, a strong positive pressure gradient would have existed ahead of, and in the vicinity of, the nose. The reversal of the flow, which caused the large energy losses in the vicinity of the nose, resulted from the fact that the mixing air in the region of slots has insufficient streamwise kinetic energy to move continually downstream against this pressure gradient. This reversal of the flow reduced the expansion of the main stream tube in the vicinity of the nose and thus delayed the development

of a strong positive pressure gradient on the tunnel wall and diffuser-entrance nose to stations farther downstream, the 160-inch station for a Mach number of 1.10, as indicated by figure 13. With this delay and the increased rate of mixing resulting from the reversed flow, sufficient energy is transferred to the low-energy air of the main stream tube before it reaches the region of the severe positive pressure gradient to allow it to continue downstream against this gradient.

The energy losses in the vicinity of the diffuser-entrance nose could be reduced if the required transfer of energy were accomplished without the need for the region of reversed flow. Continuous flow could be maintained if the geometry of the tunnel in the region downstream of the slots were altered such that the positive gradient would be sufficiently gradual without reversal. With such a gradient, the rate of increase of total pressure of the low-energy air from slots due to mixing would be greater than the rate of increase in the static pressure and the forward velocity would be maintained. The basic form of the gradual pressure gradient is obtained by the proper distribution of cross-sectional area along the tunnel axis. In addition, the losses downstream of slots should be reduced by designing the size and shape of the entrance to the diffuser such that it induces and directs all portions of the stream tube with a minimum of distortion.

Results with final revised diffuser-entrance nose.- The final configuration of revised diffuser-entrance-nose combinations developed to accomplish the above objectives is shown in figure 3(b). With these combinations in place, the cross-sectional area of the tunnel was approximately constant from the beginning of the diffuser-entrance nose at the 115-inch streamwise station to approximately the 150-inch station (fig. 17), the area being 8 percent greater than that of the minimum section. Tuft surveys indicated that the flow did not reverse at any point on the surfaces of this diffuser-nose combination at the maximum test Mach number, the condition for which this combination was designed. At lower Mach numbers, the flow reversed in small regions near the leading edge of the upper surface of the nose. The nondimensional power losses $\Delta E/E_K$ at the end of the diffuser for various Mach numbers with the final revised diffuser-entrance nose installed are considerably less than those with the original nose in place. At a Mach number of 1.10, it is 20 percent less. (See fig. 18.)

Pressures measured at the center line of the final diffuser-entrance nose at a Mach number of 1.10 (fig. 19) indicate a gradual positive pressure gradient from near the leading edge to the 140-inch streamwise stations. Beyond the 140-inch station, the positive gradients become severe. The axial extent of the region of the desired gradual adverse gradients on the final diffuser-entrance noses is comparable to that produced on the original noses by the separation of the flow. (See fig. 19.)

[redacted]

The more forward location of the leading edge of the final diffuser-entrance nose compared with that for the original nose results in a reduction of the open area of the slots which leads to a small but significant reduction in the mixing losses. Also, with the final diffuser-entrance nose in place, diffusion on the panel wall started at approximately the 110-inch streamwise station at a Mach number of 1.10, whereas, with the original nose, it started downstream of the 165-inch streamwise station (fig. 19). The initiation of diffusion at a more forward station, of course, allows more gradual diffusion and reduces the extent of the region in which near-stream velocities are present. Both of these factors probably reduce the power losses.

As a result of moving the leading edge of the diffuser-entrance nose forward, the compressive disturbances emanating from the vicinity of the slots ahead of the noses merge at the center line of the tunnel to form a positive gradient at the 126-inch station. (See fig. 19.) This discontinuity is upstream of the region where the stream at the center line was accelerated with the original nose. Consequently, the magnitude of the discontinuity is considerably less with the final nose than with the original nose. Since the shock losses caused by the stronger discontinuity with the original noses were insignificant (fig. 15(c)), any reduction in these losses associated with the lessening of the pressure discontinuity should have little effect on the total power loss.

Pressure distributions with final revised diffuser nose.- The detailed pressure distributions for the final diffuser-entrance noses (fig. 20) indicate that, at a Mach number of 1.15, which is close to the design condition of 1.16, a positive pressure gradient is present in the slot ahead of the leading edge of the diffuser-entrance nose. This gradient indicates that the cross-sectional area enclosed by the nose combination is somewhat greater than that occupied by the low-energy air of the stream tube ahead of the nose, so that the stream air must decelerate to pass through the nose combination without separation. At lower Mach numbers, the area occupied by the stream tube ahead of the nose is even less, which requires a greater expansion of the stream tube to the area enclosed by the nose combination. This results in more severe pressure changes.

The gradual positive pressure gradients on the panel at Mach numbers of 1.10 and 1.15 from approximately the 115-inch to the 125-inch stations (fig. 20) are associated with the deceleration in the slot. At a Mach number of 0.60, the positive pressure gradient on the panel associated with the deceleration in the slot extends forward of the 70-inch streamwise station. The negative pressure gradient on the panel between the 125-inch and the 130-inch streamwise stations is associated with the curvature of the wall in this region. The pressure differences between the center line of the panel and the center line of the slot in the -

region between the 125-inch and the 160-inch stations are caused primarily by the reversed curvature of the diffuser-entrance nose. (See fig. 3(b).)

The effect of the deceleration of the flow in the slots results in a deceleration of the flow in the tunnel. At supersonic stream Mach numbers, this effect is carried downstream and produces no changes in the Mach number distribution at the center line of the test region. (See fig. 21.) The discontinuity of the Mach number distribution at the center line of the tunnel at approximately the 117-inch station for a Mach number of 1.154 is associated with disturbances produced by the initiation of the side walls for the diffuser-entrance noses at the 90-inch station. At subsonic Mach numbers, the effect of the strong deceleration in the slots (fig. 20) produces a gradual deceleration of the flow at the center line of the tunnel in the test region (fig. 21).

Effects of variations of revised diffuser-entrance-nose shapes.- The diffuser-entrance-nose configurations 2 to 9 in fig. 5 were tested during the development of the final noses. Comparisons of the maximum Mach numbers obtained with 19,000 horsepower indicate that, at approximately this maximum power condition the effects of these changes in nose configuration were slight, so that the highest maximum Mach number was only 0.005 greater than the lowest. This small effect might be expected since, for all these revised configurations, no severe reversed flow was present on the noses. These results indicate that the maximum Mach number could be slightly increased by reducing the radius of the leading edges of the noses, by moving the points of tangency of the noses with the diffuser wall forward, and, within certain limits, by increasing the distance between the leading edge of the diffuser-entrance nose and the surface of the tunnel. The major effects of variations of tunnel stream temperature on the comparisons shown in figures 5 and 22 have been eliminated by dividing the measured powers by the square root of the ratio of the stream temperature to arbitrarily selected reference temperatures for each Mach number. (See fig. 9.) The effects of variations of atmospheric pressure have been eliminated by dividing the measured powers by the ratios of the atmospheric pressure to standard atmospheric pressure.

The pressure distributions on the panel and diffuser-entrance nose and the center-line Mach number distributions are only slightly altered by the forward movement of the point of tangency of the diffuser-entrance nose with the diffuser wall. (See fig. 23.) A decrease in the distance between the leading edge of the diffuser-entrance nose and the surface of the tunnel from 9.7 inches to 7 inches reduces the positive gradients ahead of the diffuser-entrance nose. This factor results in a reduction of the mixing losses in the slot. Because of this reduction, the configuration with the smaller distance from the tunnel (fig. 22) requires less power at Mach numbers less than 1.137; however, this configuration change also nearly eliminated the gradual positive pressure

[redacted]

gradient on the panel as far downstream as the 140-inch station, so that the adverse gradient farther downstream became more severe. This increased gradient probably caused increased diffusion losses. The change in the configuration delayed the deceleration of the flow at the center line of the tunnel, allowing the flow to accelerate before it was decelerated. This delay resulted in a more severe discontinuity in the Mach number distribution which probably increases the shock losses. Most importantly, because of the higher velocities in the vicinity of the diffuser-entrance noses with the noses nearer to the tunnel wall, the flow in this region approached the choked condition at a lower test section Mach number. Power requirements for the tunnel with the noses closer to the tunnel wall, therefore, increased abruptly at a Mach number of 1.135 (fig. 22) so that, at the maximum power condition, the maximum Mach number attainable with this configuration was less than that with the noses in a more open position.

Effect of installation of test model.- The results presented in figures 5 and 22 indicate that higher Mach numbers are attainable with a given power when the sweptback wing-body model was in the test region than when the survey tube was installed. A comparison of the pressure distributions on the panel with the model and survey tube in the tunnel at a Mach number of 1.15 (fig. 24) indicate that the addition of the model caused a series of pressure changes between the 105-inch and the 135-inch stations. The reduction in power may result from the reduction of the adverse pressure gradients in the slots ahead of the diffuser-entrance noses associated with these pressure changes.

Modification for satisfactory subsonic operation.- With the revised diffuser-entrance noses installed, the Mach number gradient at the center line of the test section at subsonic Mach numbers caused by the deceleration of the flow in the slots is sufficiently large to be unacceptable for model testing. With the special diffuser-entrance-nose configuration (no. 10) installed, it is possible to obtain test-section Mach number distributions of acceptable uniformity at subsonic speeds. (See fig. 25.) This improvement results from the reduction of the cross-sectional area enclosed by the noses to values slightly greater than the area of the stream tube in the slotted region. The use of this diffuser-entrance-nose configuration for supersonic testing is limited, however, by choking the flow in the vicinity of the nose at a Mach number of 1.08. In order to obtain a configuration that has the same aerodynamic characteristics as this special nose at subsonic speeds, flaps were installed in the surfaces of the noses as shown in figure 3(b). For subsonic and sonic testing, these flaps are opened to the position shown. With these flaps open, entrained air from the test chamber moves into the forward portions of the entrance-nose combinations and back into the chamber under the flaps. Because of this secondary flow, the cross-sectional area occupied by the stream tube within the nose combination approaches the area of the tube ahead of the noses and only a slight deceleration of the flow occurs

ahead of the nose (fig. 26). As a result, the associated deceleration of the flow at the center line of the test region was acceptably small. (See fig. 25.)

Survey of Energy Losses in Tunnel with the Final Diffuser-Entrance Nose

Axial distributions of losses.- The development of the power losses in the tunnel circuit with the final revised diffuser-entrance noses installed is presented in figure 27. With the revised nose in place, the losses in the vicinity of the nose are relatively small compared with those present in the locality of the original nose. (See fig. 12.) The development of loss in this region and in the diffuser (fig. 27) is similar to that to be expected downstream of a closed throat. The losses for the slotted-throat condition are associated primarily with the same phenomena as those for the closed-throat condition, skin friction, and normal diffusion effects. As for the closed throat condition, the major part of the total power loss occurs in the diffuser.

At a Mach number of 1.00, the nondimensional loss for the closed throat and the approach to the throat up to the 9.8-foot station is 0.024, whereas the loss at the end of the diffuser downstream of the closed throat is 0.060. The comparable values for the slotted test section are 0.038 and 0.101. These data provide a direct indication of various diffuser efficiencies for this Mach number. The efficiency of the diffuser in recovering the kinetic energy of the stream tube between the 9.8-foot and 69-foot stations is 96.4 percent with the closed throat and 93.7 percent with the slotted test section. These efficiencies are approximately equal to the differences between the nondimensional power deficiencies at the entrance and exit of the diffuser. The efficiency of the diffuser acting as an induction pump to raise the total pressure of the low-energy air entering the diffuser to nearly atmospheric pressure is 40 percent with the closed throat and 38 percent with the slotted test section. These pump efficiencies are equal to the ratios of the nondimensional power deficiencies at the entrance and exit of the diffuser. The efficiency of the diffuser in overcoming the additional total-power deficiencies at the entrance caused by the installation of the slots is 34 percent. These efficiencies are equal to the ratios of the differences between nondimensional power deficiencies for the slots open and closed at the entrance and exit to the diffuser. The efficiency of this additional function of the diffuser is lower than that for the initial function with the closed throat, even though no additional skin-friction loss is associated with this additional function. This decrease in efficiency is probably due to the irregular lateral distribution of losses at the entrance to the diffuser downstream of the slotted test section. (See fig. 28.)

The results presented in figure 27 indicate that appreciable losses develop between the end of the diffuser and the fan shaft, which may be attributed to losses in the fan, skin friction on the tunnel walls, losses in the turning vanes, and minor diffusion losses. The fan efficiency, obtained from total-pressure surveys ahead and behind the fan, is approximately 85 percent at transonic test-section Mach numbers. (See fig. 29.)

The increment in fan power associated with the addition of slots in the test section at a Mach number of 1.00 is approximately four times as great as the comparable increment in power loss at the downstream end of the test section (fig. 27), which leads to the additional loss at the fan. This comparison suggests that an appreciable improvement in the tunnel energy ratio might be obtained by removing the portions of the stream tube with the greatest deficiencies of total pressures from the tunnel circuit at the end of the test section and raising the pressure of this air to atmospheric pressure by a compressor rather than by the diffuser and fan.

With the final diffuser-entrance nose installed, the increase in power losses due to the addition of the slots is most rapid in the forward portions of the slotted throat. (See fig. 27.) This distribution suggests that further reductions in the additional power losses associated with the installation of the slots might be accomplished by altering the forward portions of the slot configurations.

Lateral and radial variations of losses.- The lateral variations of power losses at various streamwise stations, with the final diffuser-entrance nose installed as presented in figure 28, indicate cross flows of the low-energy air from the slots toward the center lines of the panels as was present with the original nose. The flow is less severe with the revised configurations (fig. 18), probably because of the smaller lateral pressure gradients. The radial variations of total-pressure deficiency obtained with the final diffuser-entrance nose for a Mach number of 1.10 (fig. 30) indicate that, at the center line of the slot, $y'/b = 0$, at the point of tangency of the diffuser-entrance nose with the diffuser wall, streamwise station 150, the downstream motion in the boundary layer is relatively low over a wide radial region. The slow, irregular motion of the tufts observed in this region also indicated the presence of these low velocities. The retarded motion in this region is associated primarily with severe positive pressure gradients just ahead of this measurement station. At stations farther downstream, the total pressures of the elements in the boundary layer increase markedly because of mixing, and, as a result, the velocities in this region are considerably higher than those just downstream of the slot.

The contours of equal total pressure obtained in the vicinity of a slot at the 90-inch streamwise station at a Mach number of 0.60 (fig. 31)

indicate that the transfer of energy from the stream tube to the essentially still air in the test chamber does not progress from the slot with equal speed in all radial directions as might be expected. Outside the slot the progress is more rapid in a direction at approximately 45° to the plane of symmetry than along the plane of symmetry. The magnitude of this difference is shown in figure 32. The expansion of the stream tube through the slot at a Mach number of 1.10 results in an expansion of the region of mixing along the plane of symmetry but causes little change in the development of the mixing region outside the slots in a direction at 45° to plane of symmetry. (See fig. 32.)

The distributions of total pressure at the leading edge of the diffuser-entrance nose at a Mach number of 1.10 (fig. 33) indicate that for the stream which reenters the tunnel circuit, a minimum of 8 percent of the stream kinetic energy is recovered at the end of the slot.

Pressure and temperature variations.- A comparison of the distributions of static pressures in the diffuser downstream of the slotted throat with the original and final diffuser-entrance-nose configurations (figs. 16 and 34) indicate better pressure recoveries with the final nose for all stations at transonic Mach numbers as would be expected. In the forward portion of the diffuser, at a Mach number of 0.60, the recovery with final nose is not as rapid as with the original nose.

The radial distributions of temperature at various stations in the circuit with the final diffuser-entrance nose installed (fig. 35) are similar to those measured with the original nose (fig. 10). At the 90-inch streamwise station, the temperature gradients near the center line of the tunnel do not appear to be large. The results of tests of models placed in this region should be only slightly affected by this gradient. Near the tunnel wall the temperature gradient is relatively severe at a Mach number of 1.10. At the atmospheric condition for which these measurements were made, the absolute temperature varies by 10 percent from the wall to a point 0.5 radius off the wall.

CONCLUSIONS

The results of an investigation of stream-tube power losses and a program of development of improved diffuser-entrance noses in the Langley 8-foot transonic tunnel with a slotted test section form the basis for the following general conclusions:

1. With the early diffuser-entrance nose installed, a large part of the power loss associated with the installation of the slotted test section was caused by the inefficient induction of the part of the stream tube outside the slots into the diffuser.

[redacted]

2. The installation of improved diffuser-entrance noses substantially reduced the losses directly caused by the induction of the stream tube into the diffuser.

3. With the improved diffuser-entrance noses installed, the increase in power loss due to the addition of the slots is most pronounced in the forward portions of the slotted throat.

4. As for a closed throat tunnel, the major part of the stream tube power loss in the slotted throat tunnel occurs in the diffuser.

Langley Aeronautical Laboratory
National Advisory Committee for Aeronautics
Langley Field, Va.

REFERENCES

1. Wright, Ray H., and Ritchie, Virgil S.: Characteristics of a Transonic Test Section With Various Slot Shapes in the Langley 8-Foot High-Speed Tunnel. NACA RM L51H10, 1951.

2. Ritchie, Virgil S., and Pearson, Albin O.: Calibration of the Slotted Test Section of the Langley 8-Foot Transonic Tunnel and Preliminary Experimental Investigation of Boundary-Reflected Disturbances. NACA RM L51K14, 1952.

[redacted]

TABLE I

POSITIONS TESTED WITH ORIGINAL DIFFUSER-ENTRANCE NOSE INSTALLED

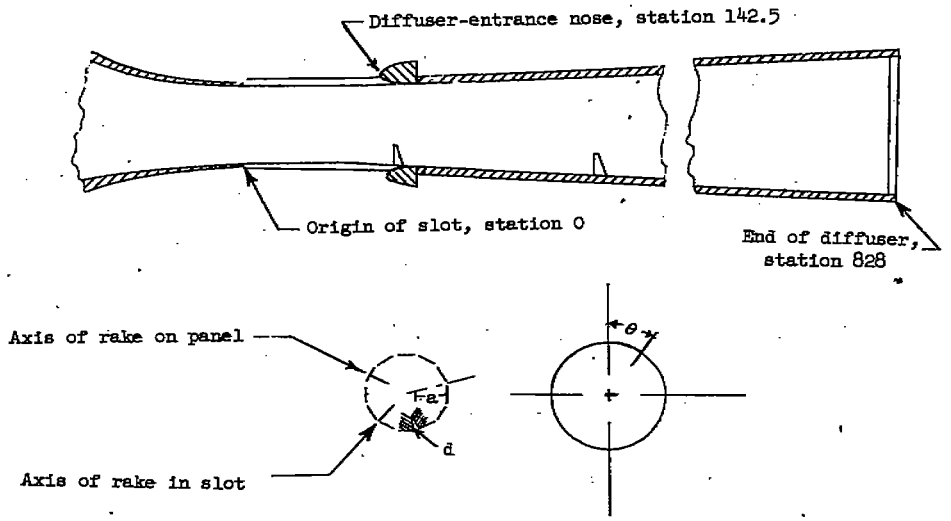

Positions in test section		Positions in diffuser	
Longitudinal station, in. from origin	Lateral station on panel, percent distance from panel center line to slot center line	Longitudinal station, in. from origin	Radial station, θ, deg from top center
145	0 43.79 81.35	169	45.00 51.60 55.77 60.00 180.00 300.00 312.48 315.00
Positions in slot		193	55.01 60.00 309.90 315.00
Longitudinal station, in. from origin	Normal station in slot, percent distance from center line to edge of slot	241	54.99 60.00 309.90 315.00
145	0 100	337	45.00 60.00 315.00
		828	0 90.00 180.00 270.00

TABLE II

POSITIONS TESTED WITH REVISED DIFFUSER-ENTRANCE NOSE INSTALLED

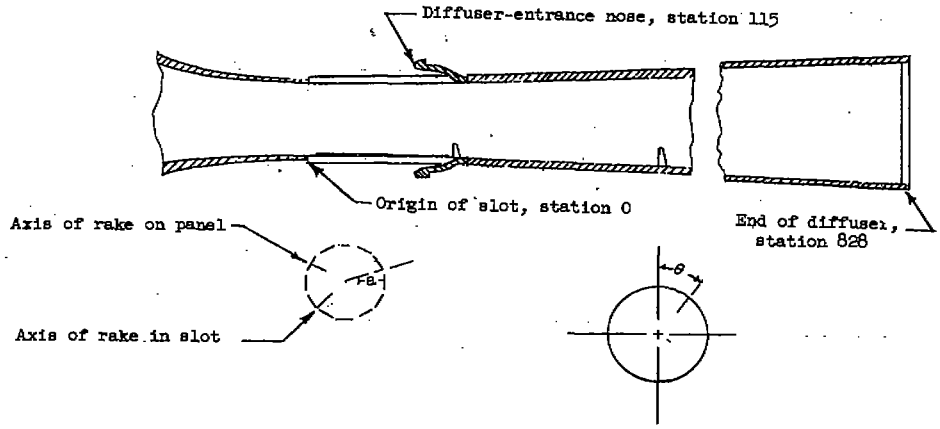

Positions in test section		Positions in diffuser	
Longitudinal station, in. from origin	Lateral station on panel, percent distance from panel center line to slot center line	Longitudinal station, in. from origin	Radial station, θ, deg from top center
90	0 41.908 88.586	193	55.01 60.00 309.90 315.00
117	0 47.791 88.683	337	60.00 315.00
150	0 1.964 52.938 79.542	828	0 90 180 270

Positions in slot

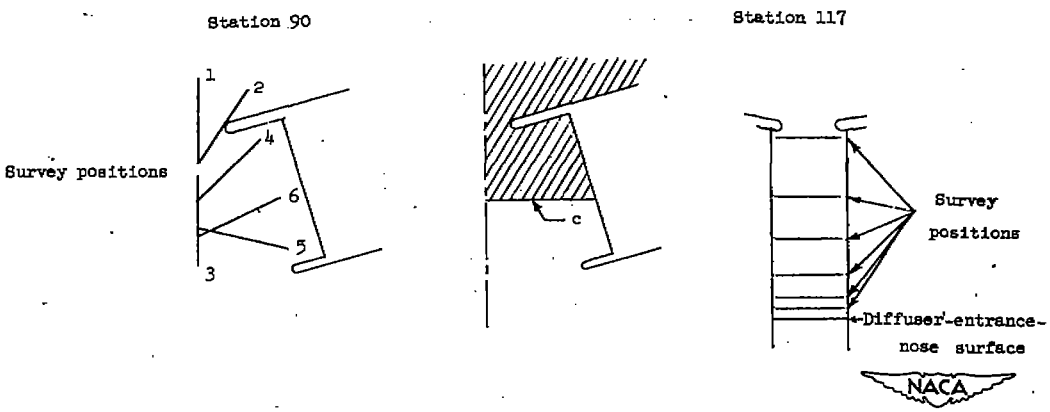

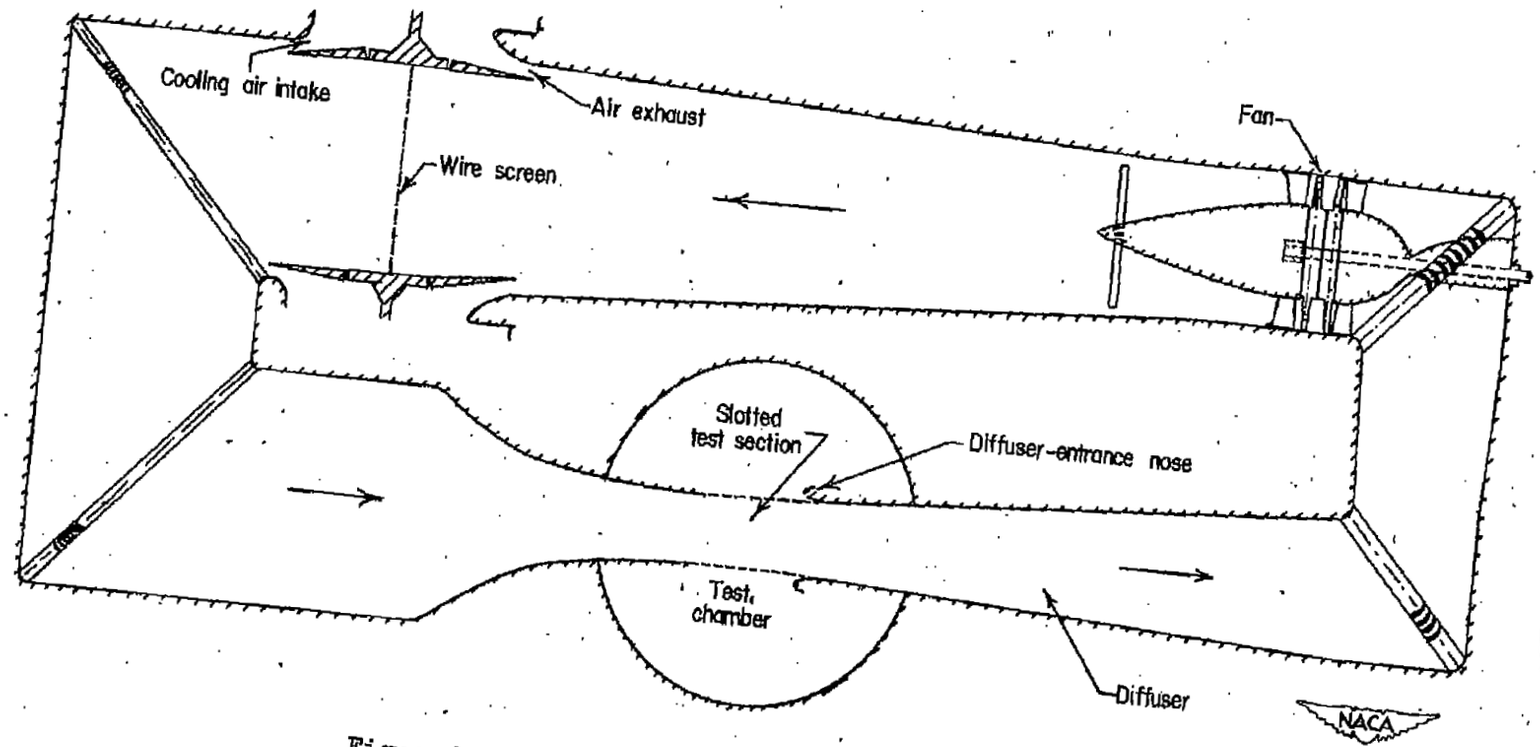

Figure 1.- Sketch of the Langley 8-foot transonic tunnel.

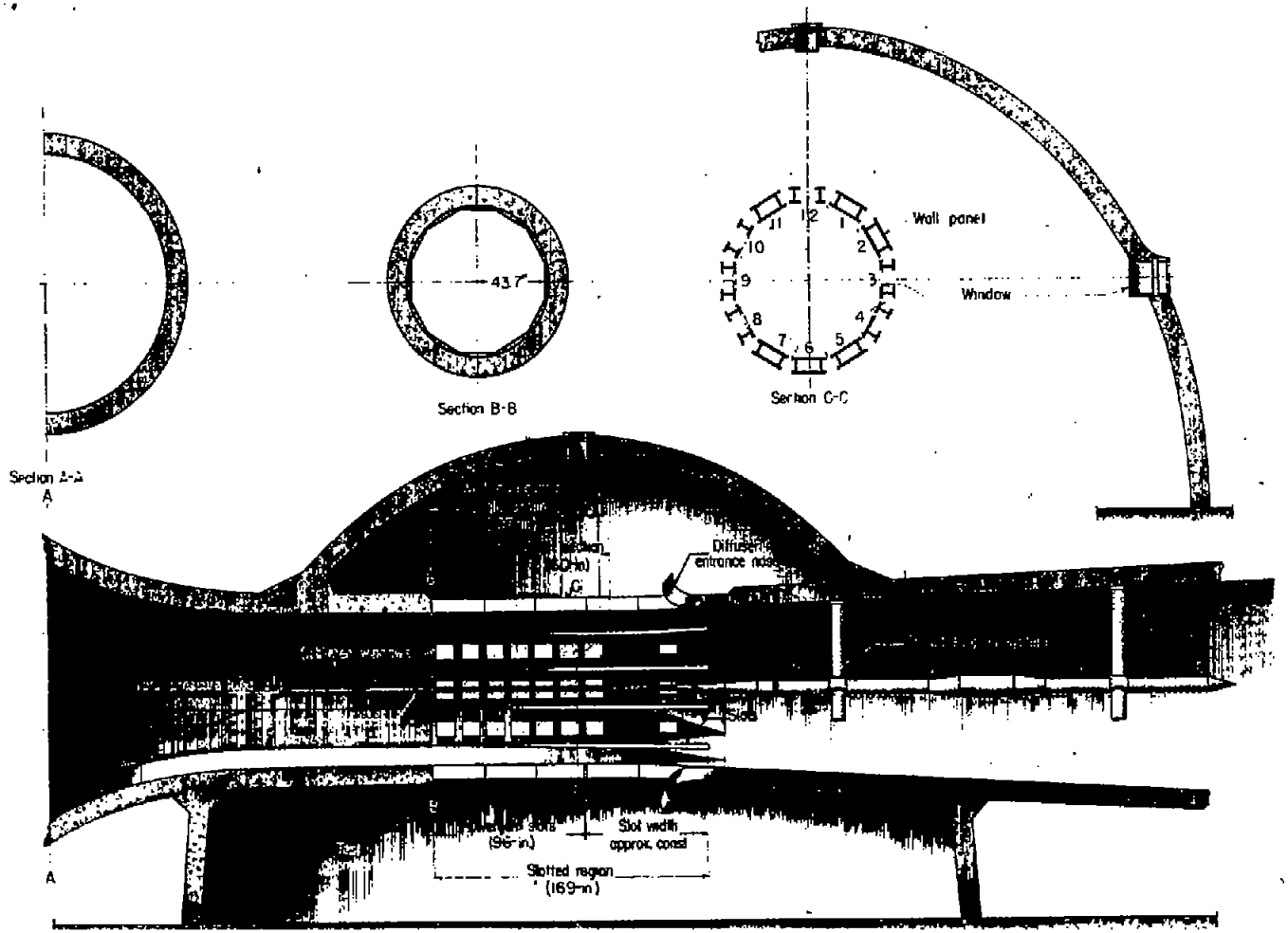

NACA

L-72677

Figure 2.- Views of throat region of 8-foot transonic tunnel showing slotted test section, cylindrical survey tube, and support system.

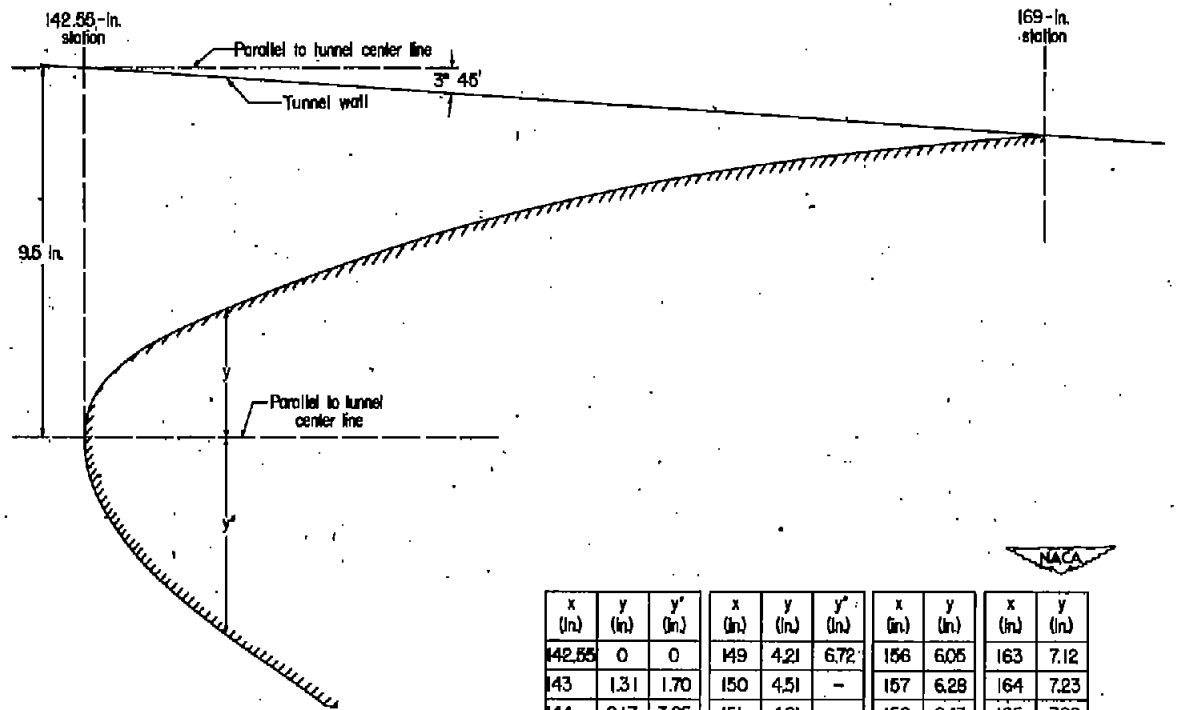

NACA

x (in.)	y (in.)	y' (in.)	x (in.)	y (in.)	y' (in.)	x (in.)	y (in.)	x (in.)	y (in.)
142.55	0	0	149	4.21	6.72	156	6.05	163	7.12
143	1.31	1.70	150	4.51	–	157	6.28	164	7.23
144	2.17	3.05	151	4.81	–	158	6.43	165	7.26
145	2.71	4.00	152	5.12	–	159	6.62	166	7.38
146	3.14	4.78	153	5.39	–	160	6.79	167	7.44
147	3.50	5.49	154	5.62	–	161	6.92	168	7.50
148	3.87	6.13	155	5.88	–	162	7.04	169	7.59

x=Distance downstream of station 0
y=Distance from diffuser-entrance-nose reference line to inner surface.
y'=Distance from diffuser-entrance-nose reference line to outer surface

(a) Original diffuser-entrance nose. Shape A.

Figure 3.- Coordinates of diffuser-entrance nose shapes.

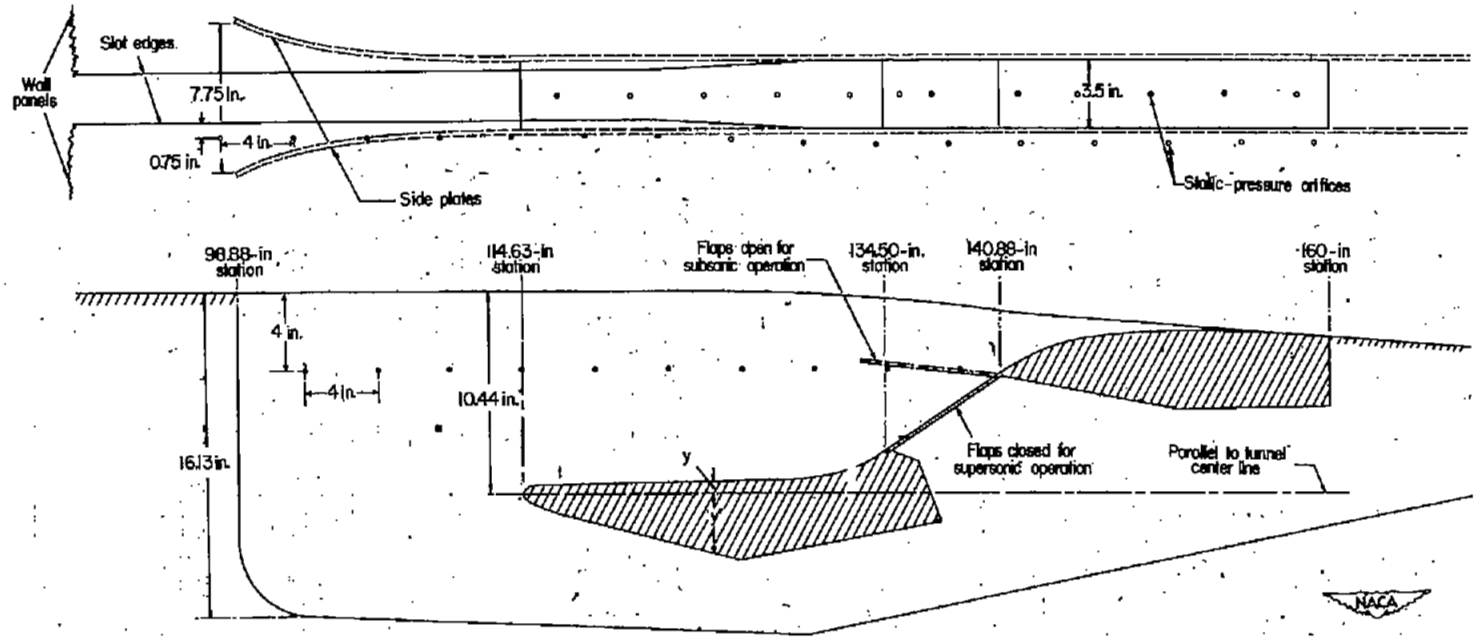

x (in.)	y (in.)	y' (in.)	x (in.)	y (in.)	y' (in.)	x (in.)	y (in.)
114.63	0	0	126	.65	3.33	146	8.00
115.63	.42	.47	128	.71	3.82	148	8.20
115.50	.47	.67	130	.82	–	150	8.29
116	.48	.85	132	1.07	–	152	8.31
118	.52	1.36	134.50	2.12	–	154	8.30
120	.55	1.86	140.88	6.30	–	156	8.28
122	.59	2.33	142	6.66	–	158	8.15
124	.62	2.83	144	7.58	–	160	8.03

x = Distance downstream of station 0
y = Distance from diffuser-entrance-nose reference line to inner surface
y' = Distance from diffuser-entrance-nose reference line to outer surface

(b) Revised diffuser-entrance nose. Shape B.

Figure 3.- Concluded.

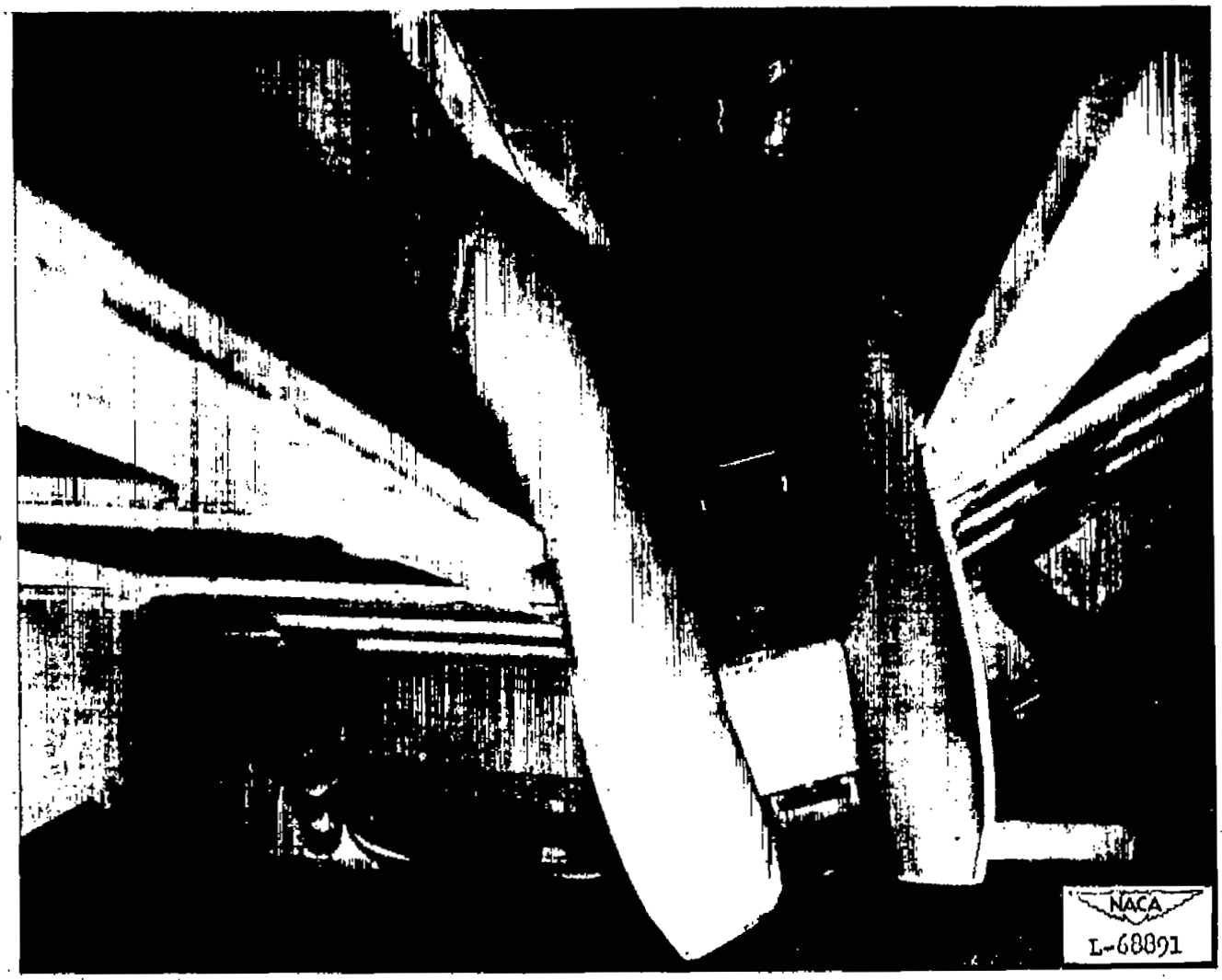

Figure 4.- Front view of final diffuser-entrance nose placed between steel plates.

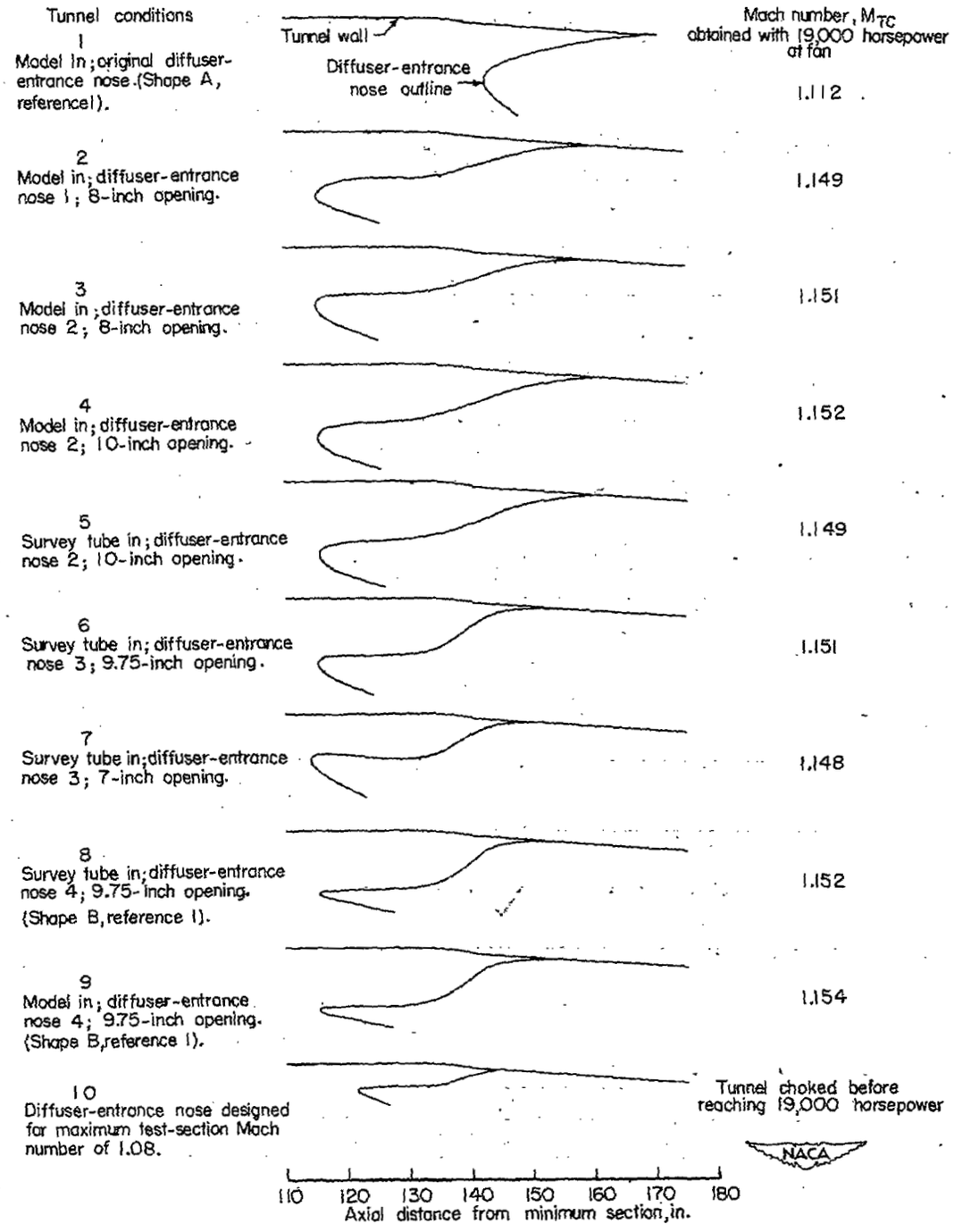

Figure 5.- Sketches of configurations investigated during development of final diffuser-entrance-nose shape.

[redacted]

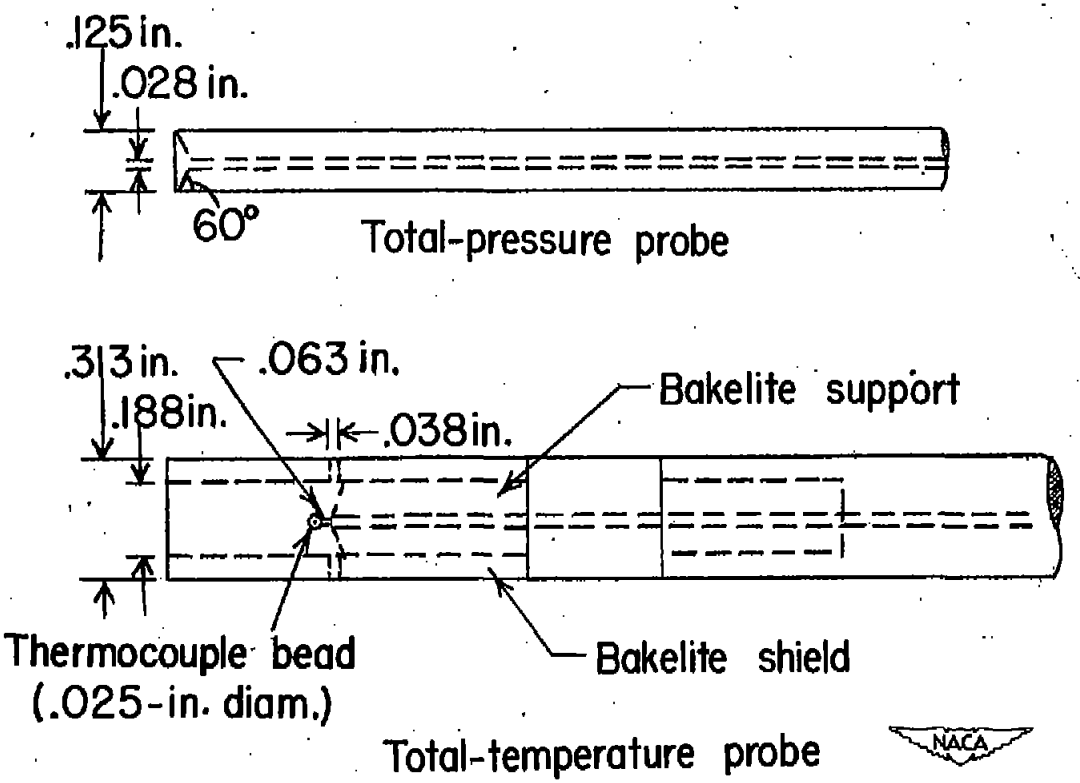

Figure 6.- Details of total pressure and temperature probes.

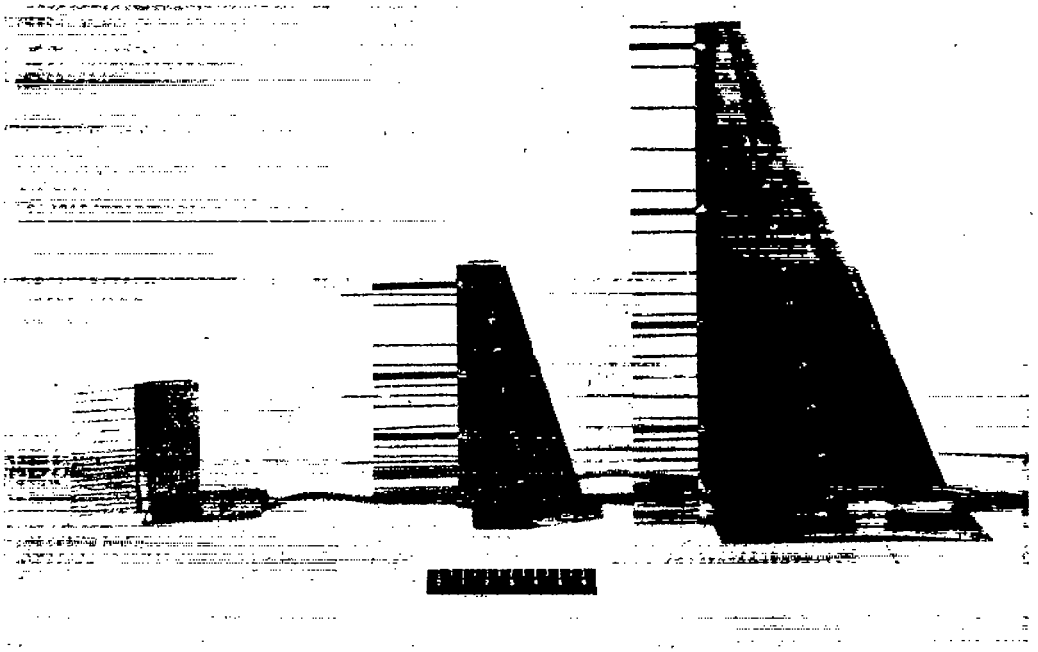

NACA L-71526

(a) Rakes for surveying boundary layer.

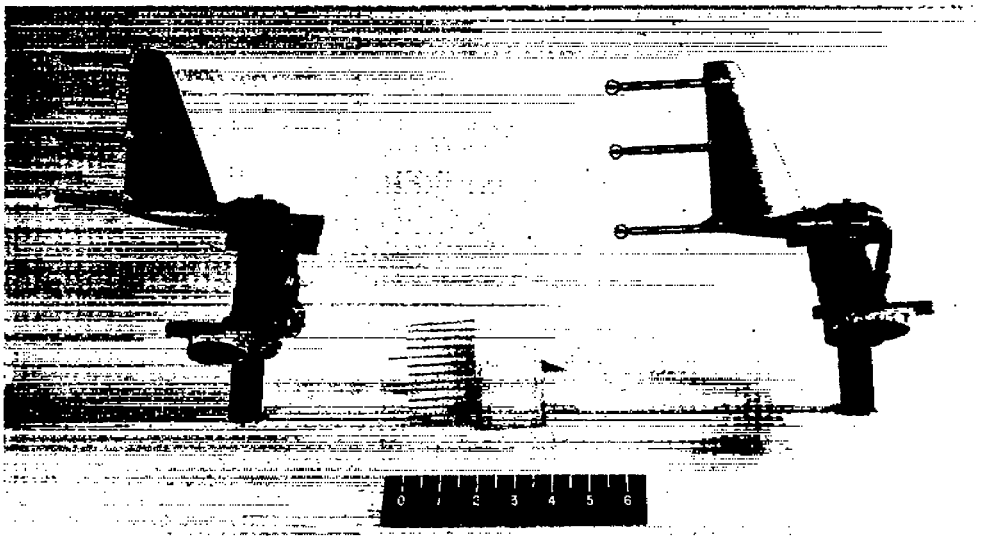

NACA L-71527

(b) Rakes for survey of flow in slots.

Figure 7.- Rakes used for flow surveys.

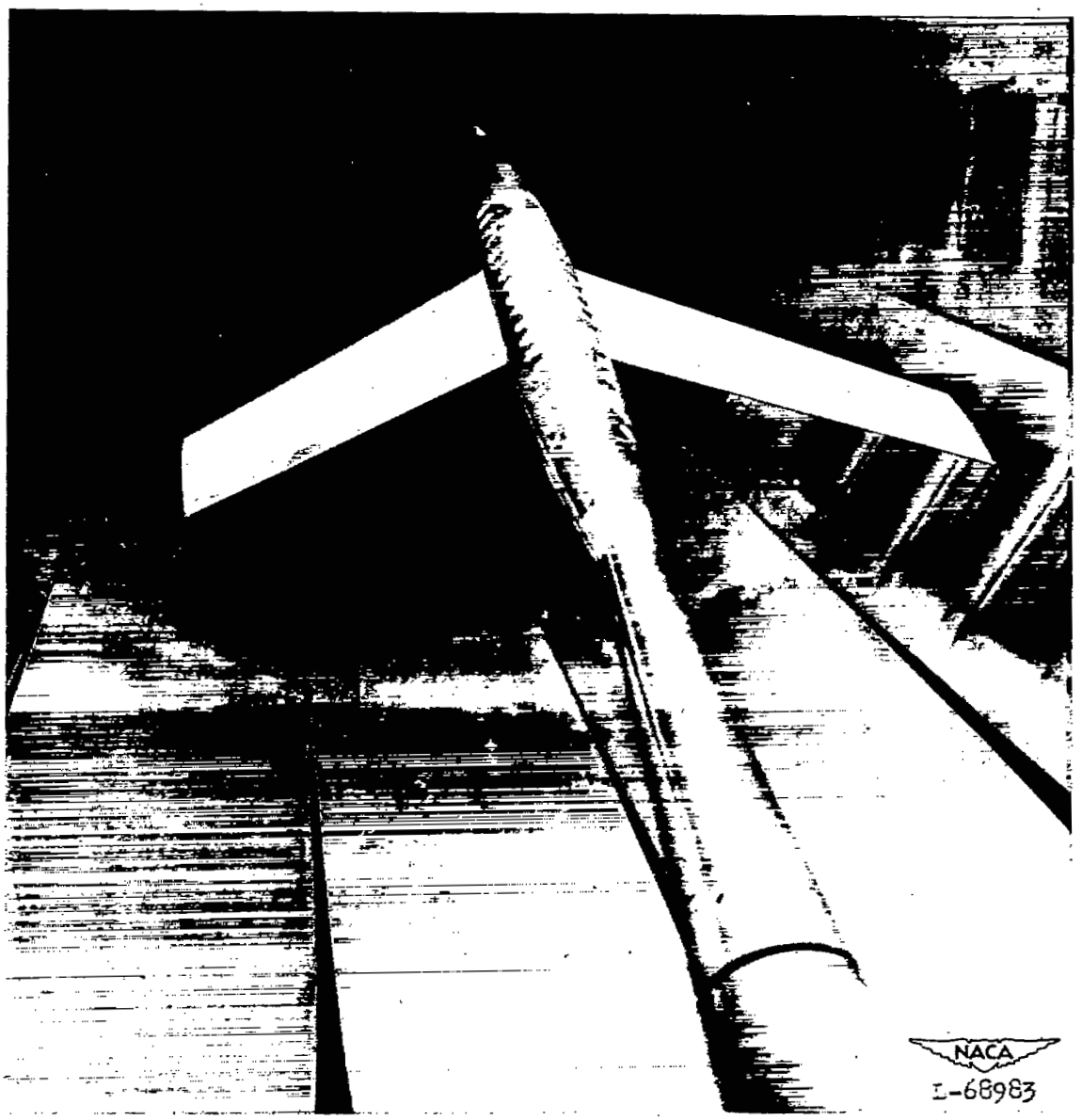

Figure 8.- Wing-fuselage combination mounted on the sting-support system in the 8-foot slotted test section.

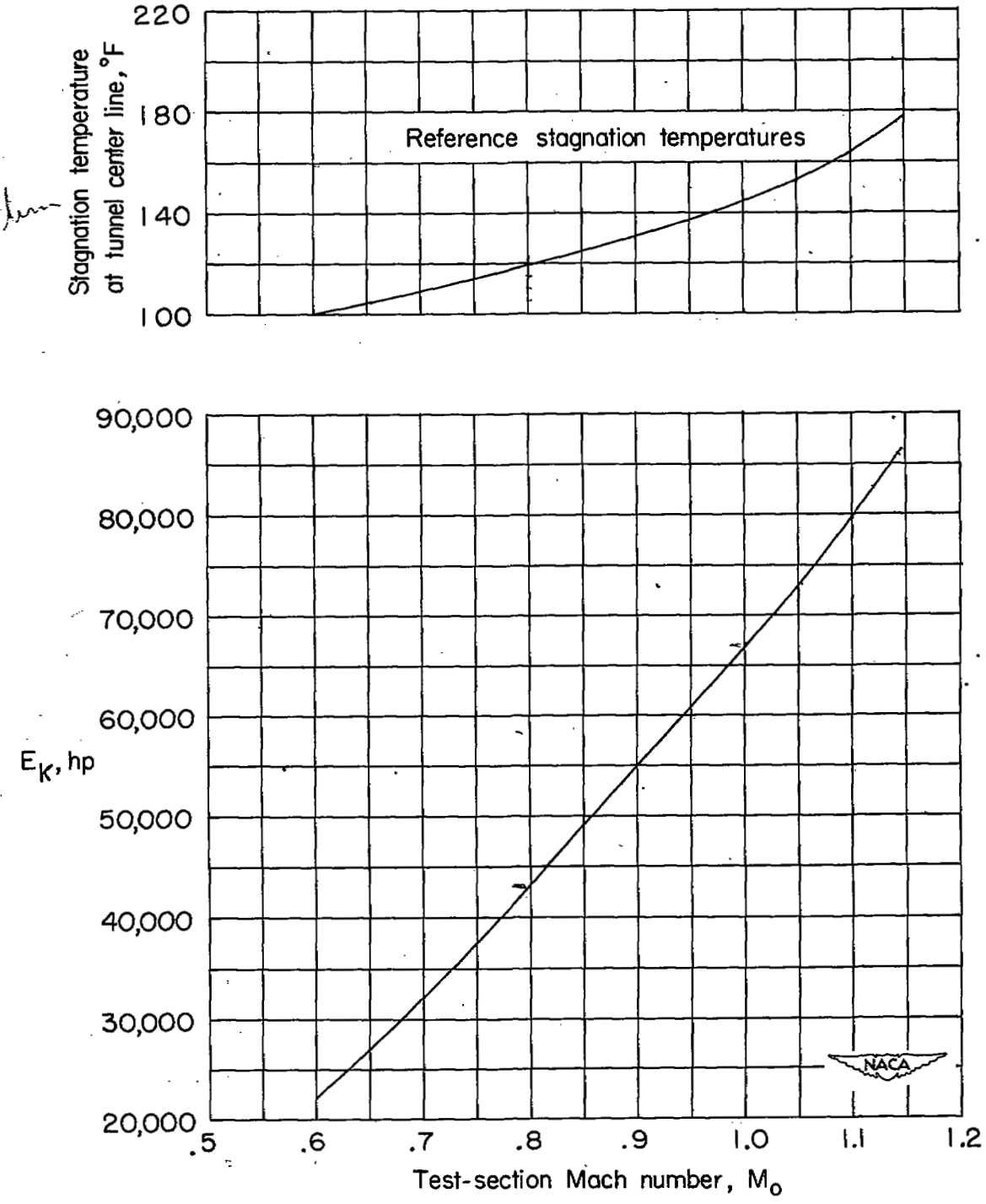

Figure 9.- Kinetic power of stream tube at test section assuming no losses and reference temperatures.

[redacted]

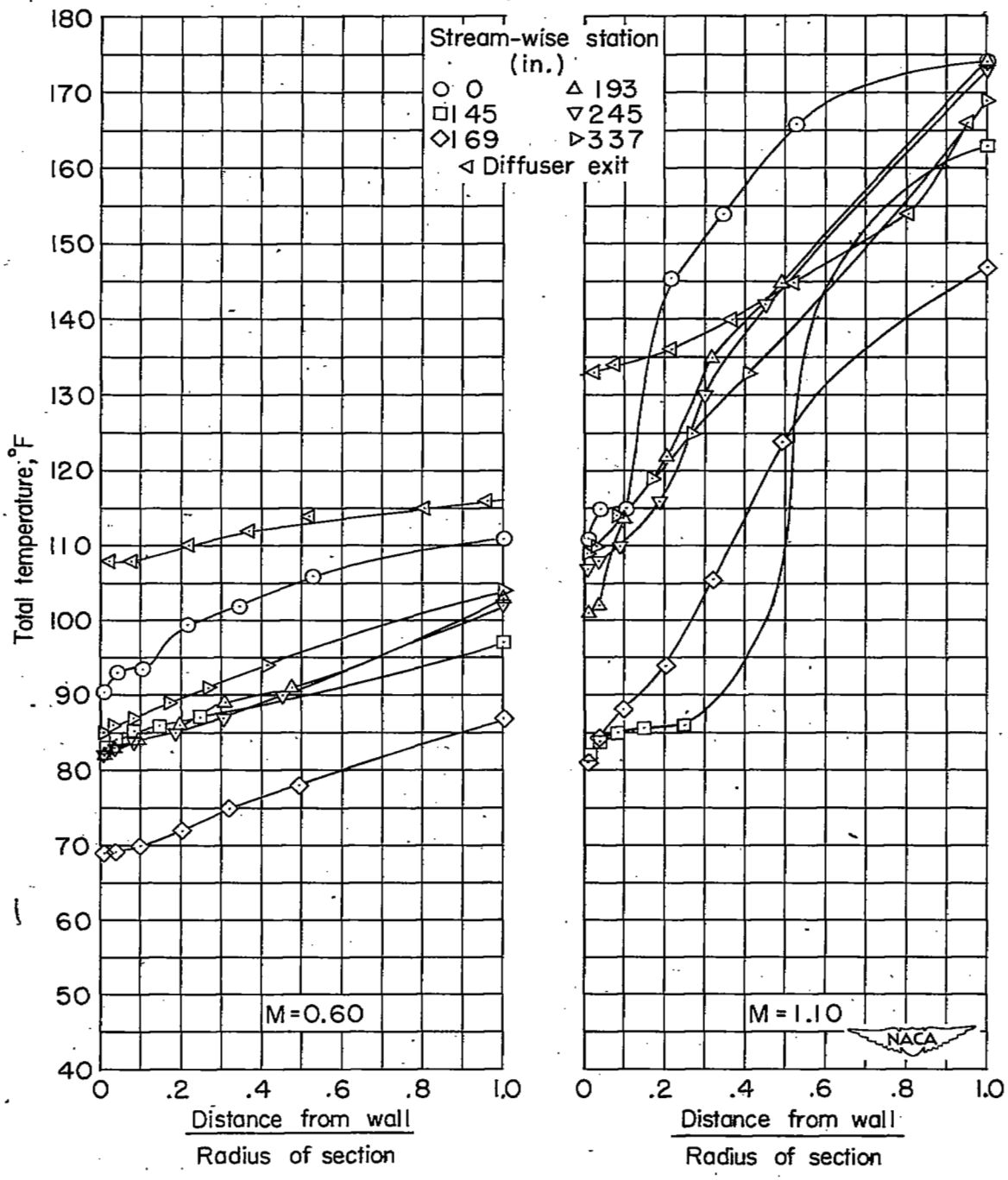

Figure 10.- Radial variations of local total temperature measured at various rake locations in tunnel with original diffuser-entrance noses installed.

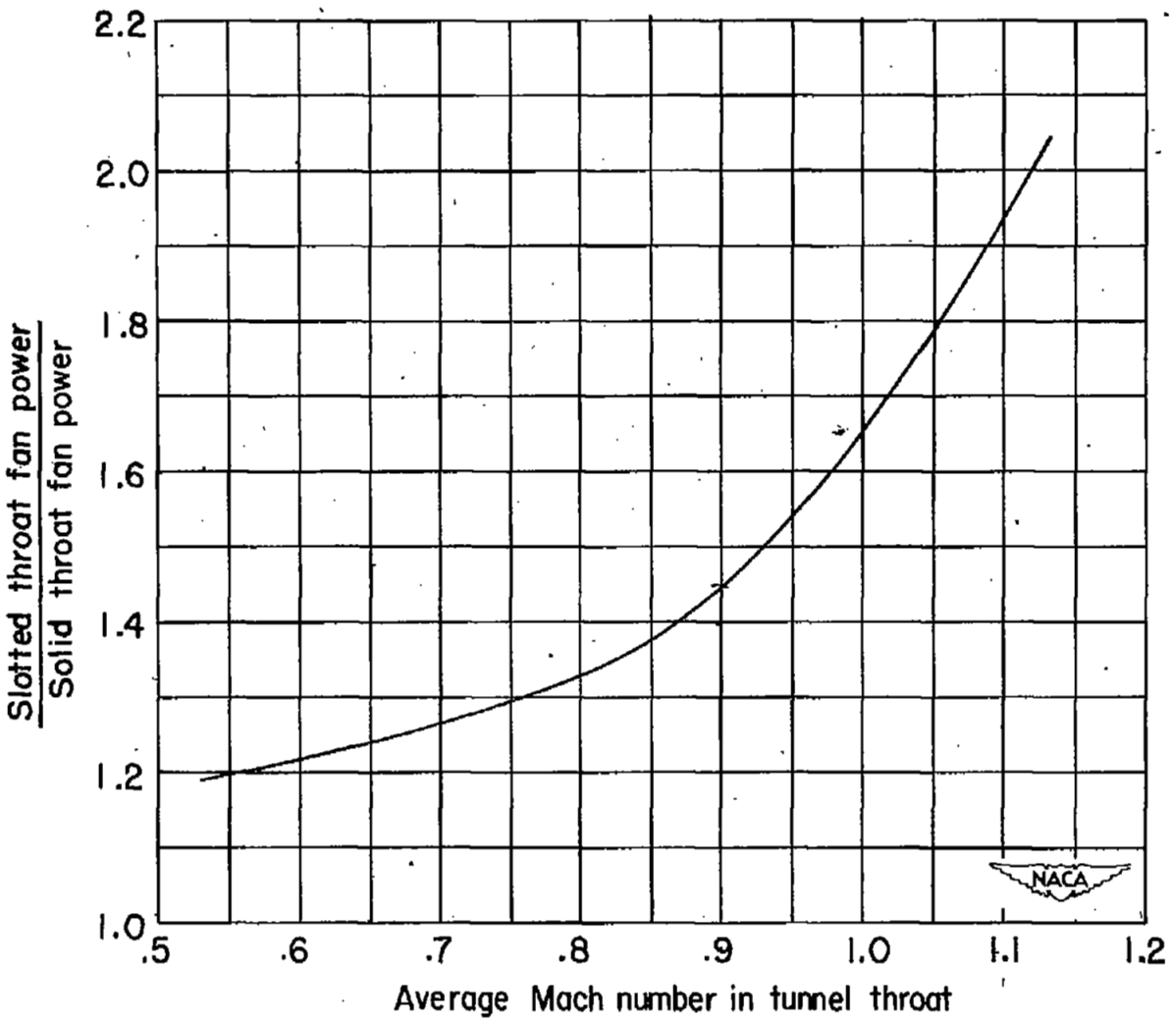

Figure 11.- Effect of installation of slotted test section on fan power with original diffuser-entrance nose.

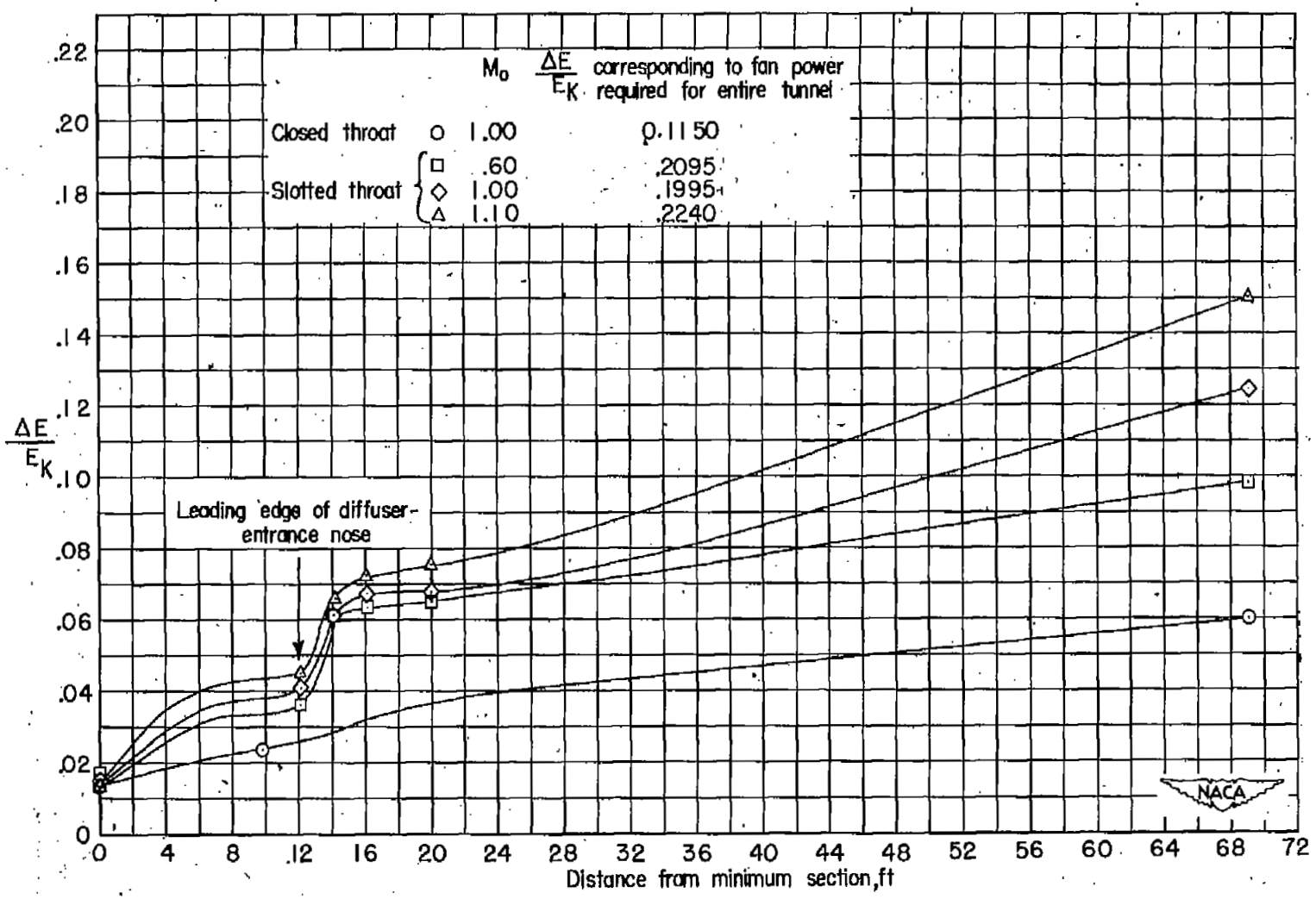

Figure 12.- Streamwise variations of energy required to raise local total pressures in the stream tube to atmospheric pressure for closed throat and slotted throat with original diffuser-entrance nose installed.

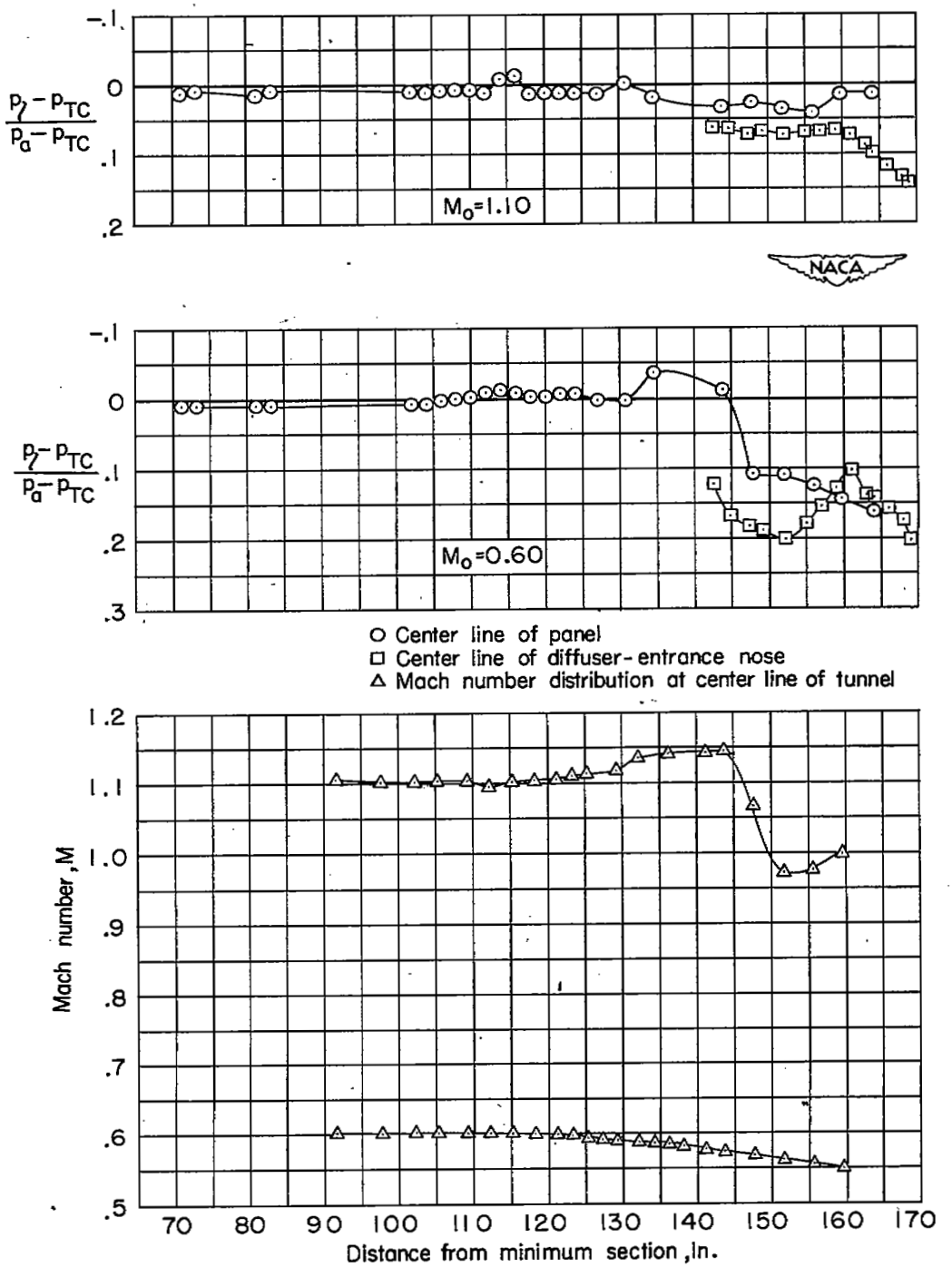

Figure 13.- Pressure distributions on panel and diffuser-entrance nose and center-line Mach number distributions with original diffuser-entrance noses installed.

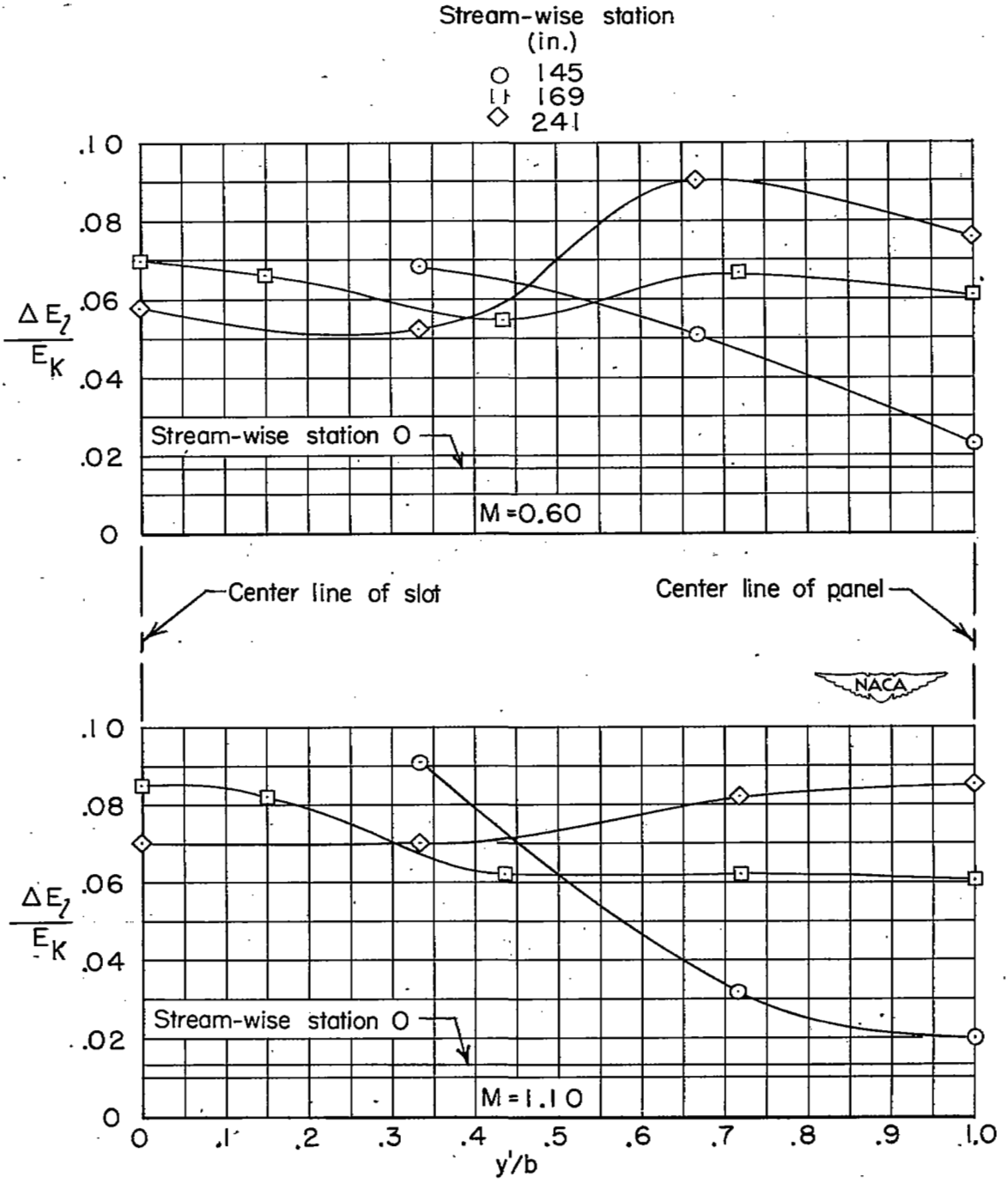

Figure 14.- Lateral variations of energy deficiencies measured at various rake locations for several streamwise stations in tunnel with original diffuser-entrance noses installed.

[redacted]

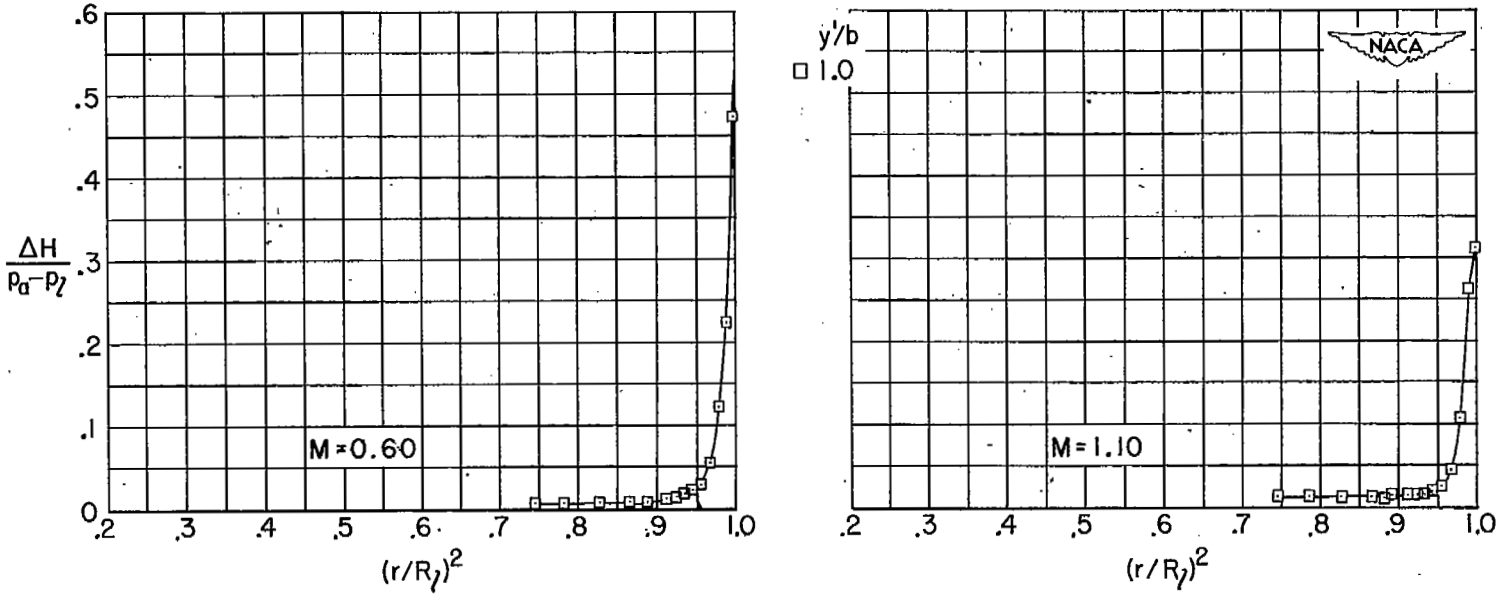

(a) Streamwise station 0.

Figure 15.- Radial variations of the local total pressure deficiencies measured at various rake locations in tunnel with original diffuser-entrance noses installed.

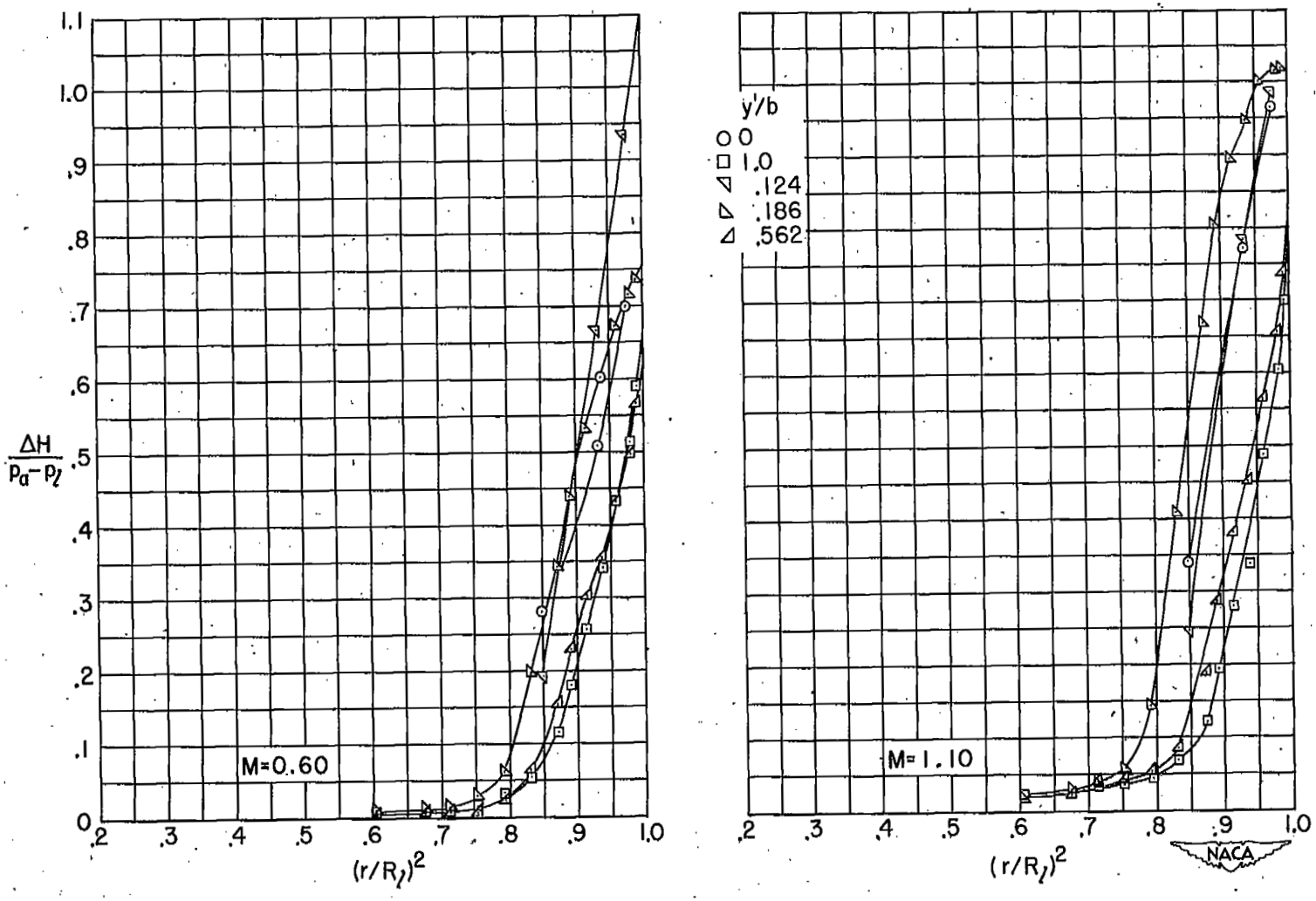

(b) Streamwise station 145.

Figure 15.- Continued.

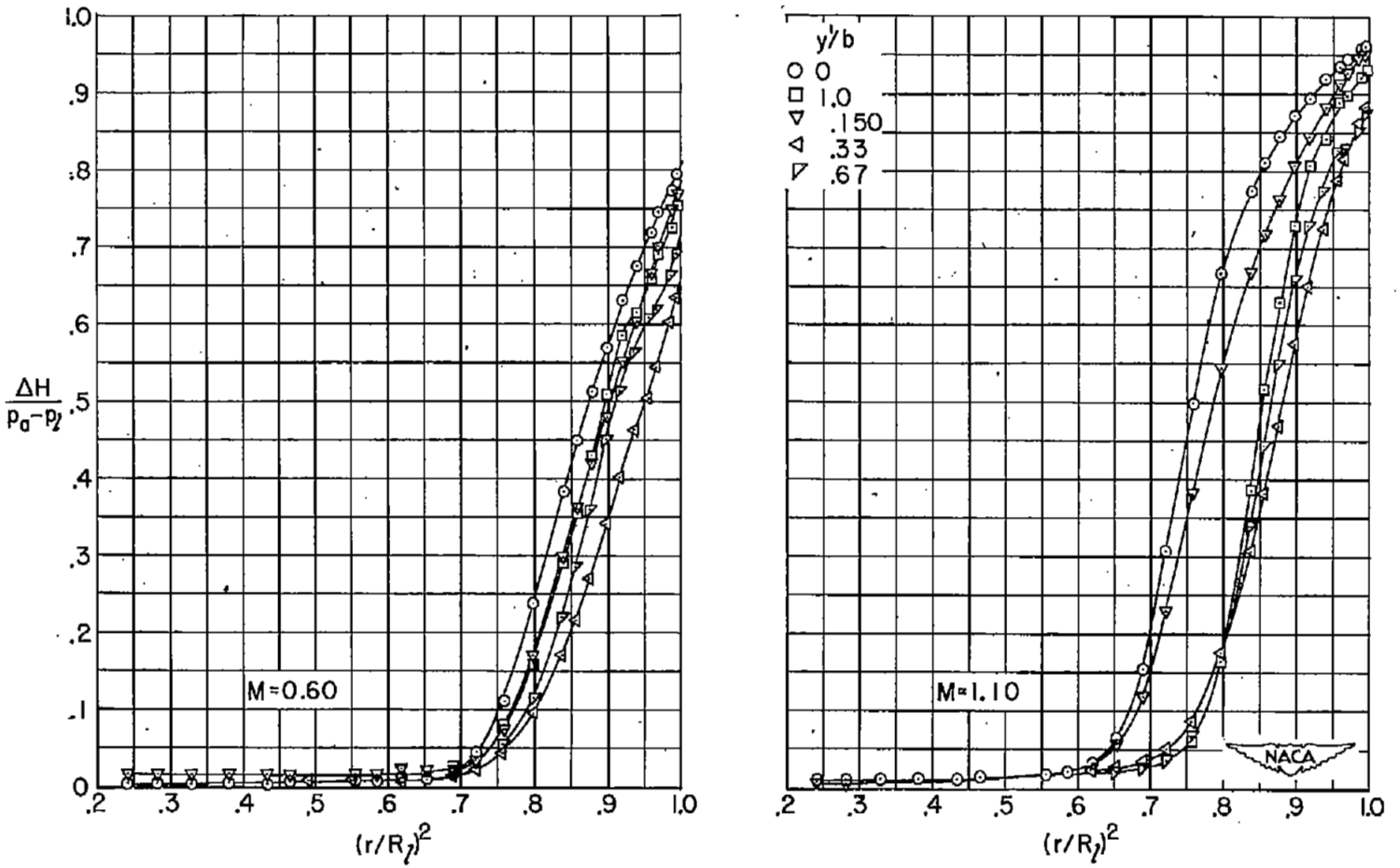

(c) Streamwise station 169.

Figure 15.- Continued.

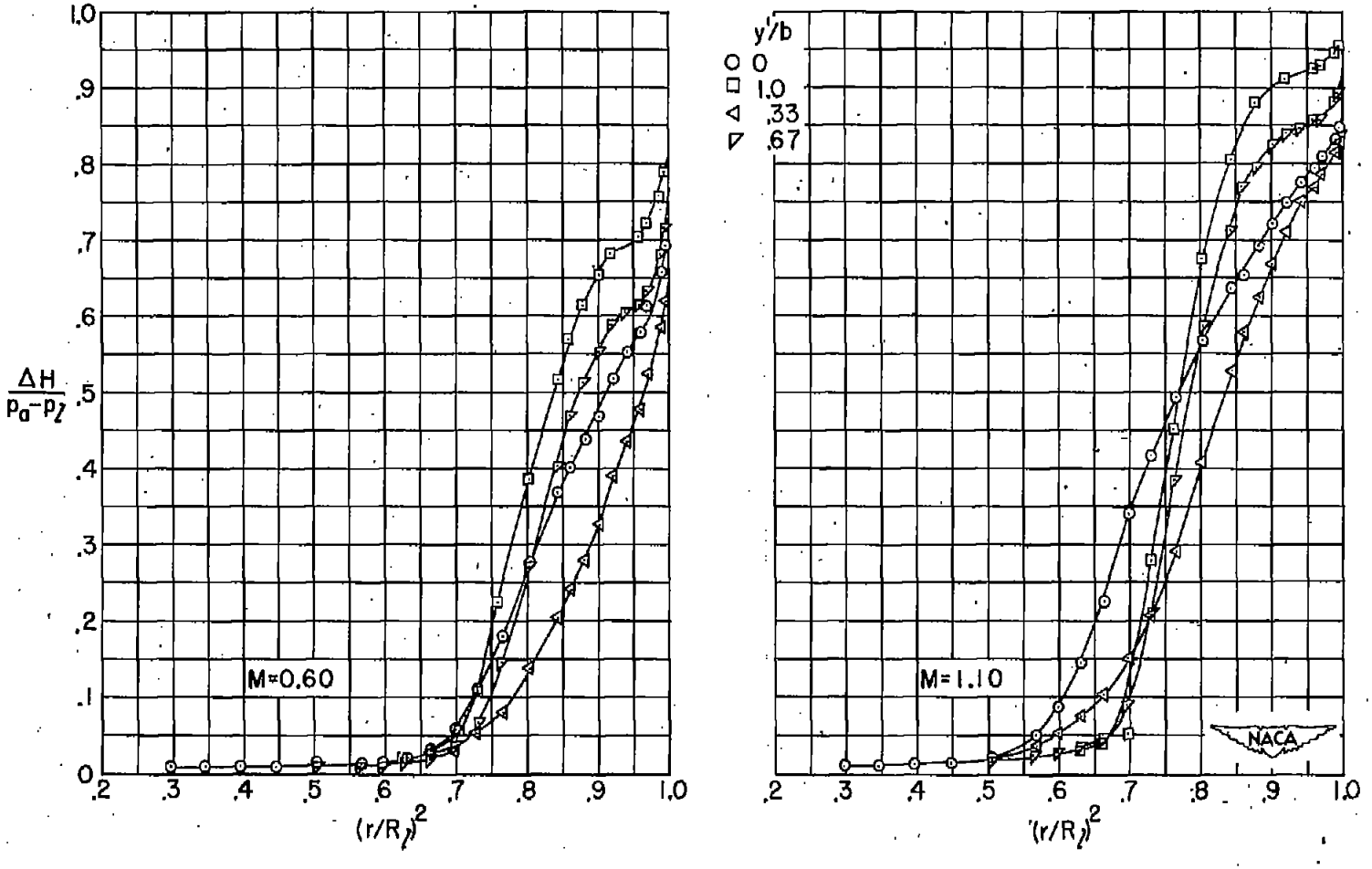

(d) Streamwise station 193.

Figure 15.- Continued.

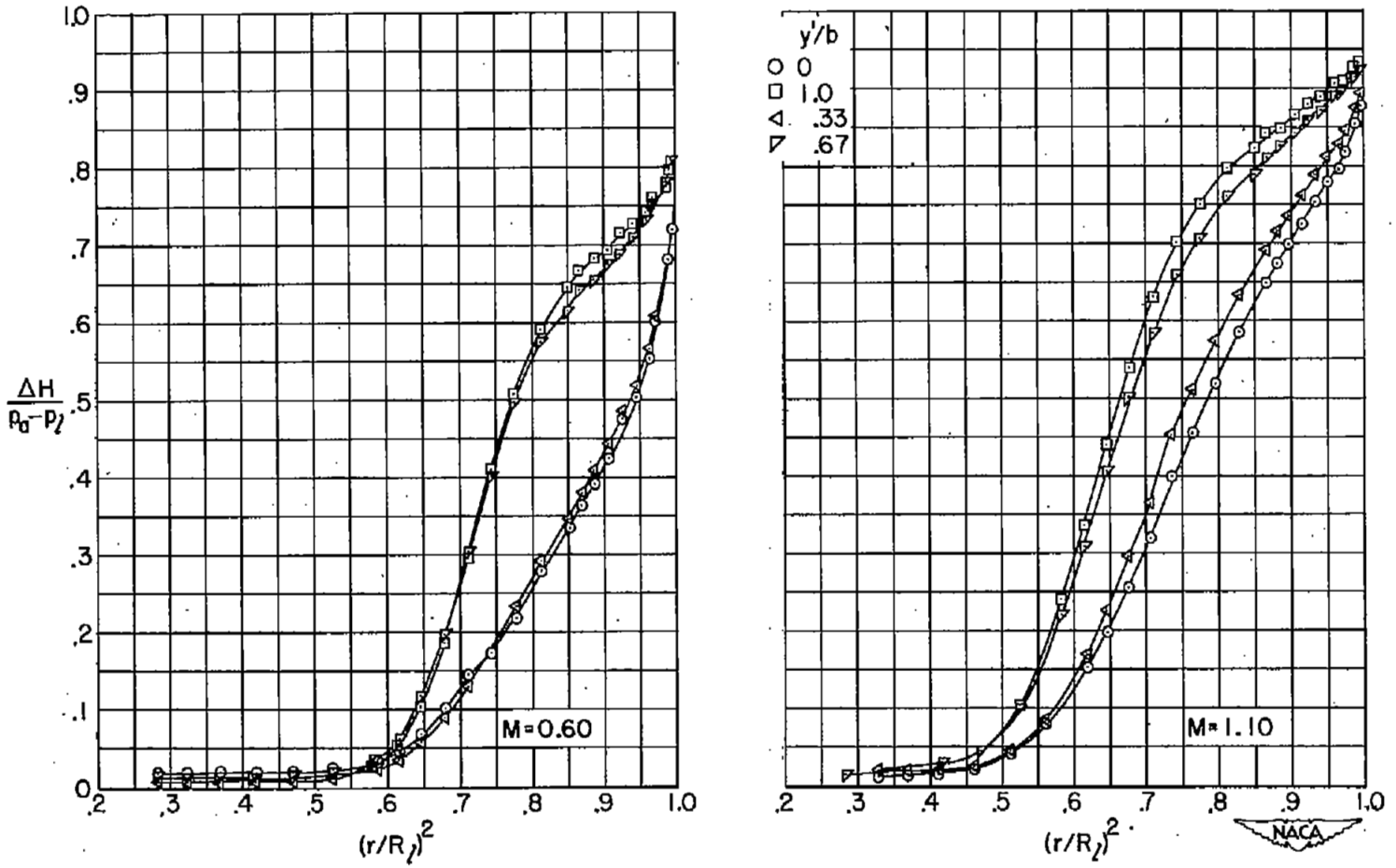

(e) Streamwise station 241.

Figure 15.- Continued.

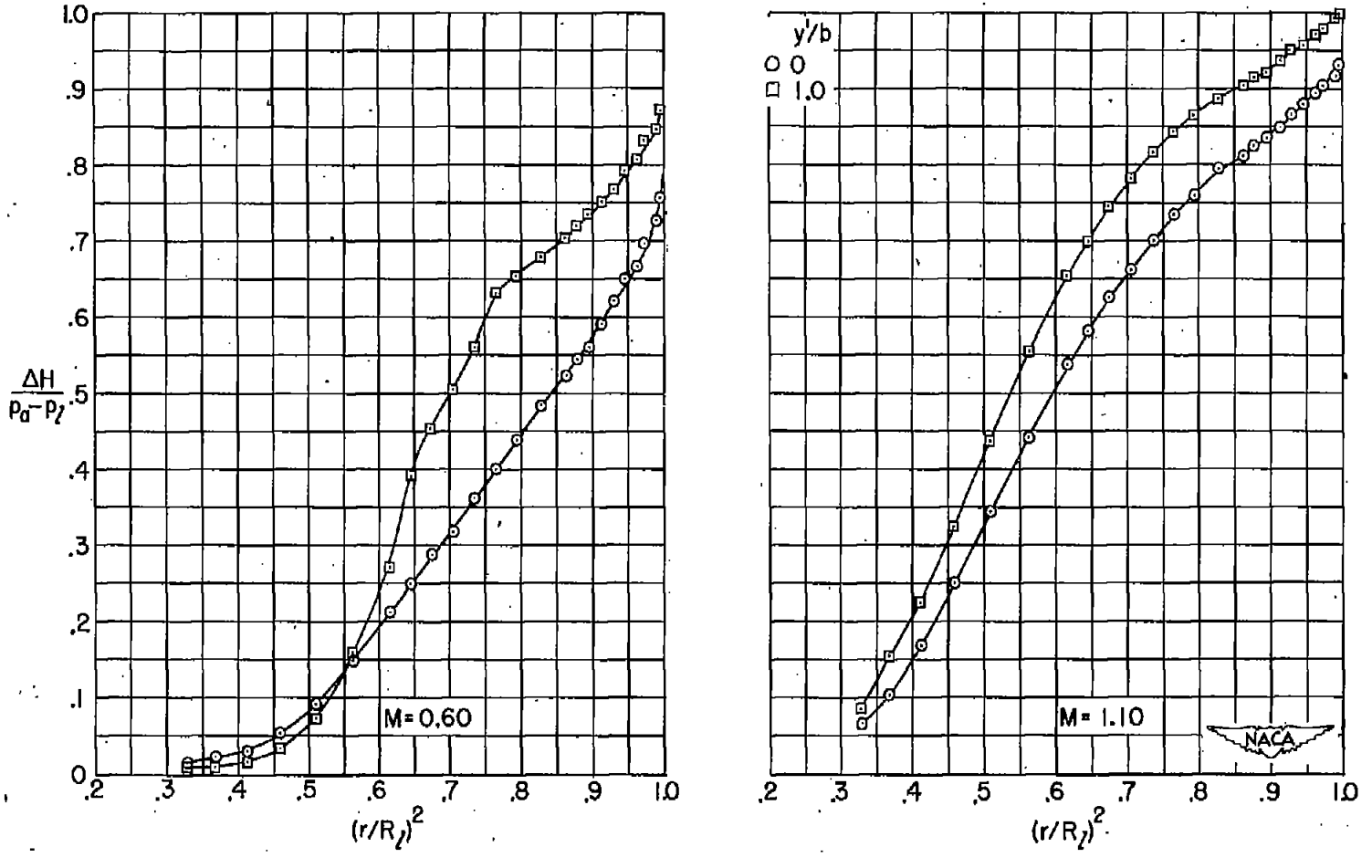

(f) Streamwise station 337.

Figure 15.- Continued.

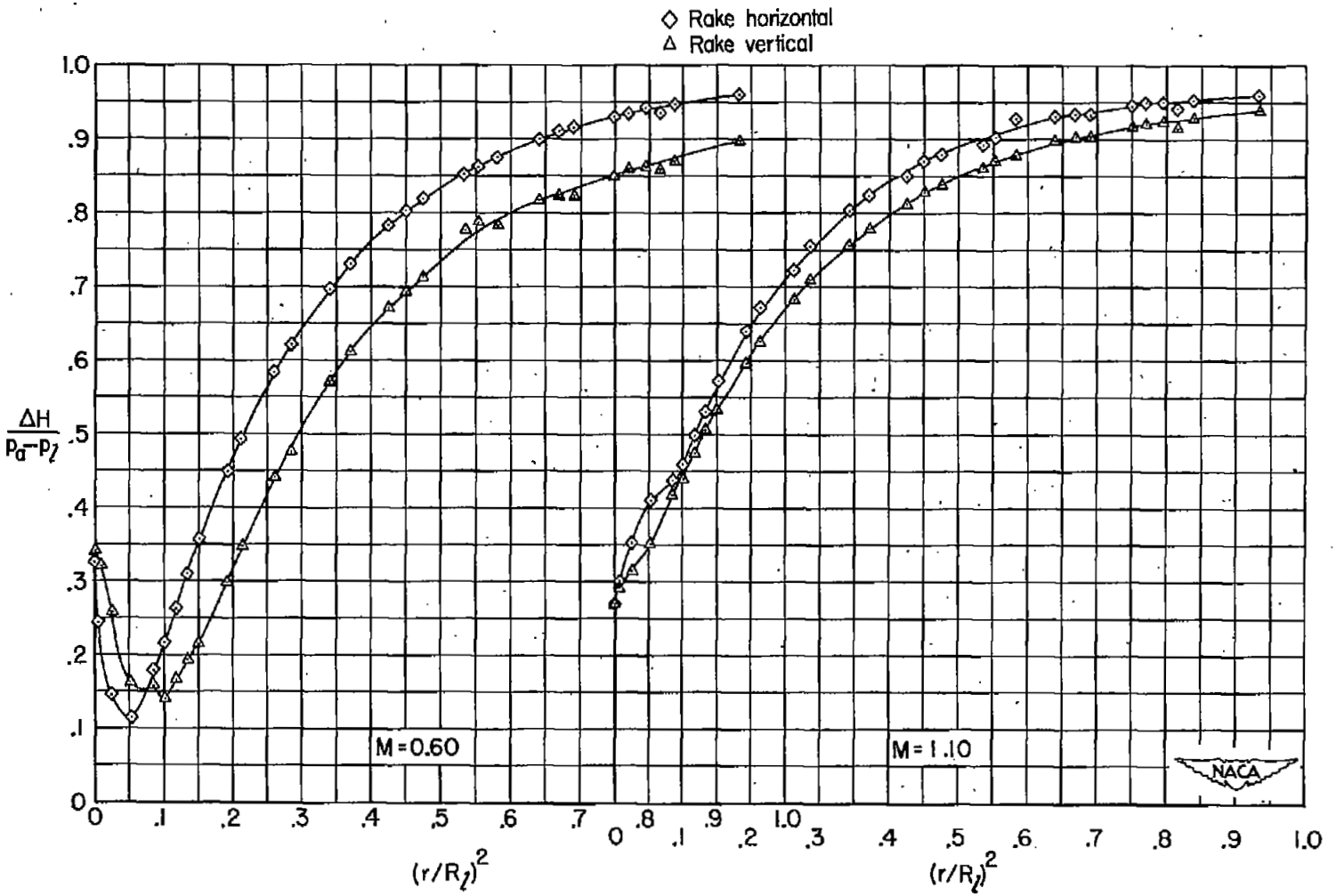

(g) Diffuser exit.

Figure 15.- Concluded.

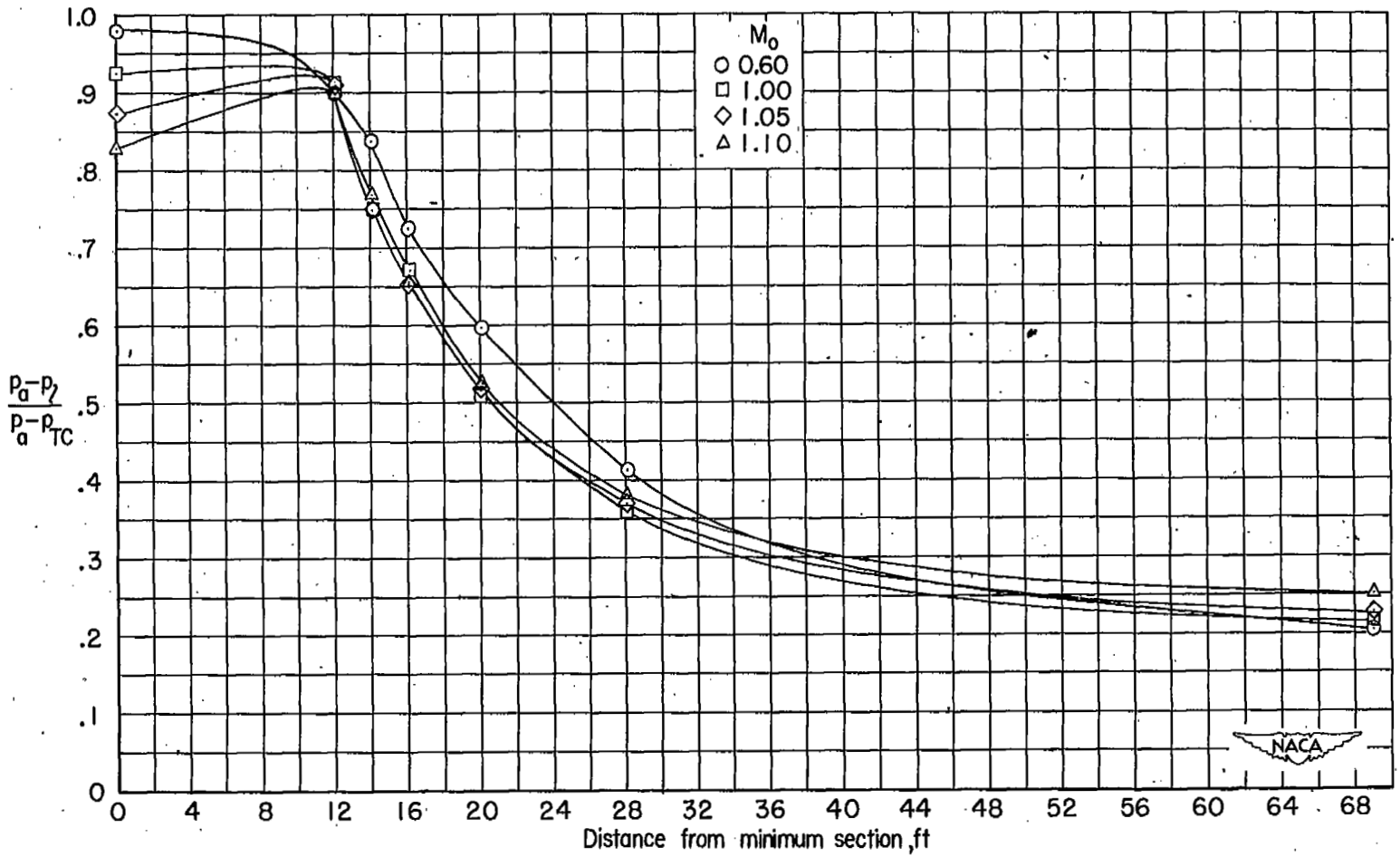

Figure 16.- Streamwise variations of static pressures in the diffuser of tunnel with original diffuser-entrance noses installed.

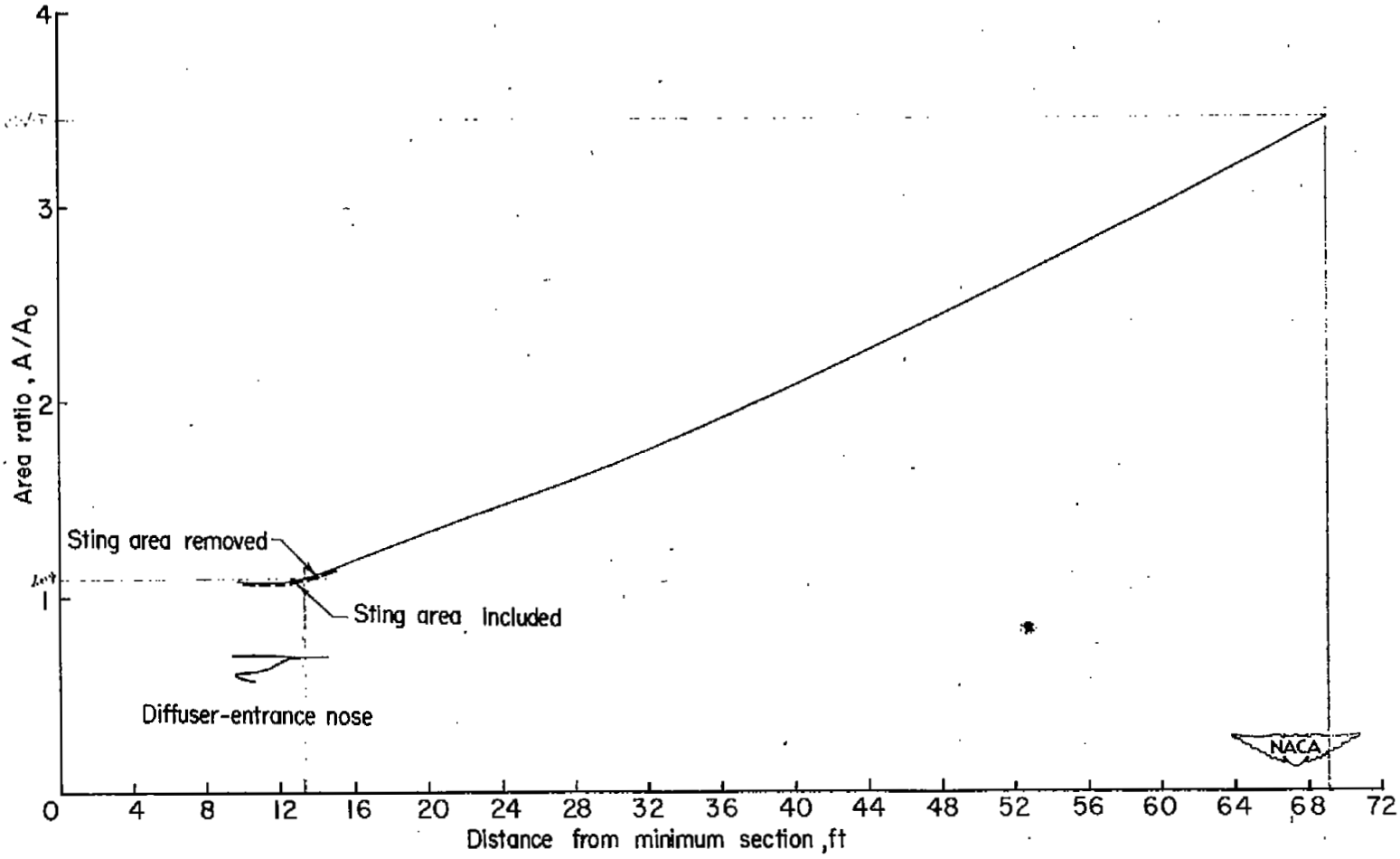

Figure 17.- Streamwise variation of tunnel cross-sectional area with final diffuser-entrance noses installed.

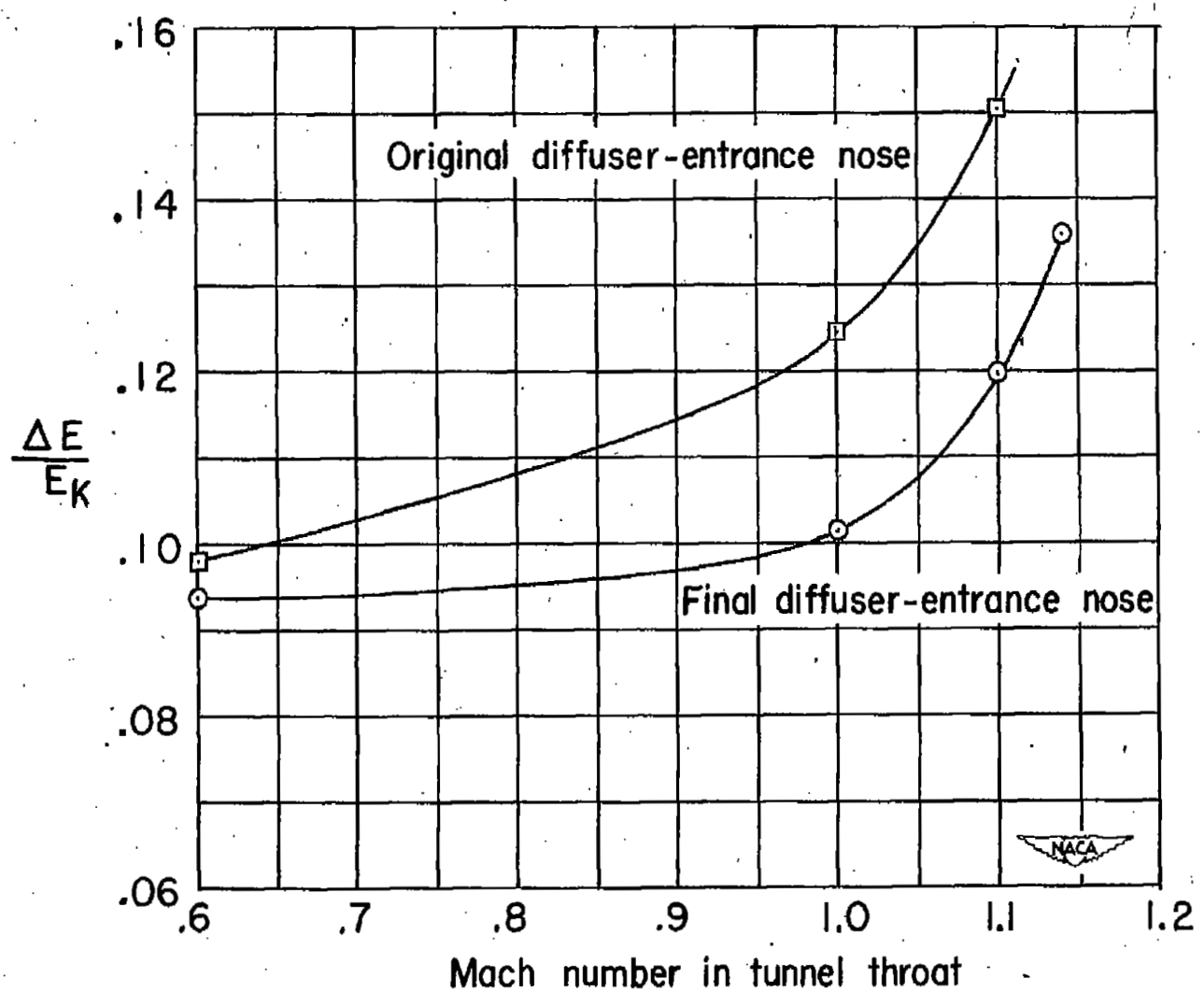

Figure 18.- Comparison of energy losses at end of diffuser with original and final diffuser-entrance noses.

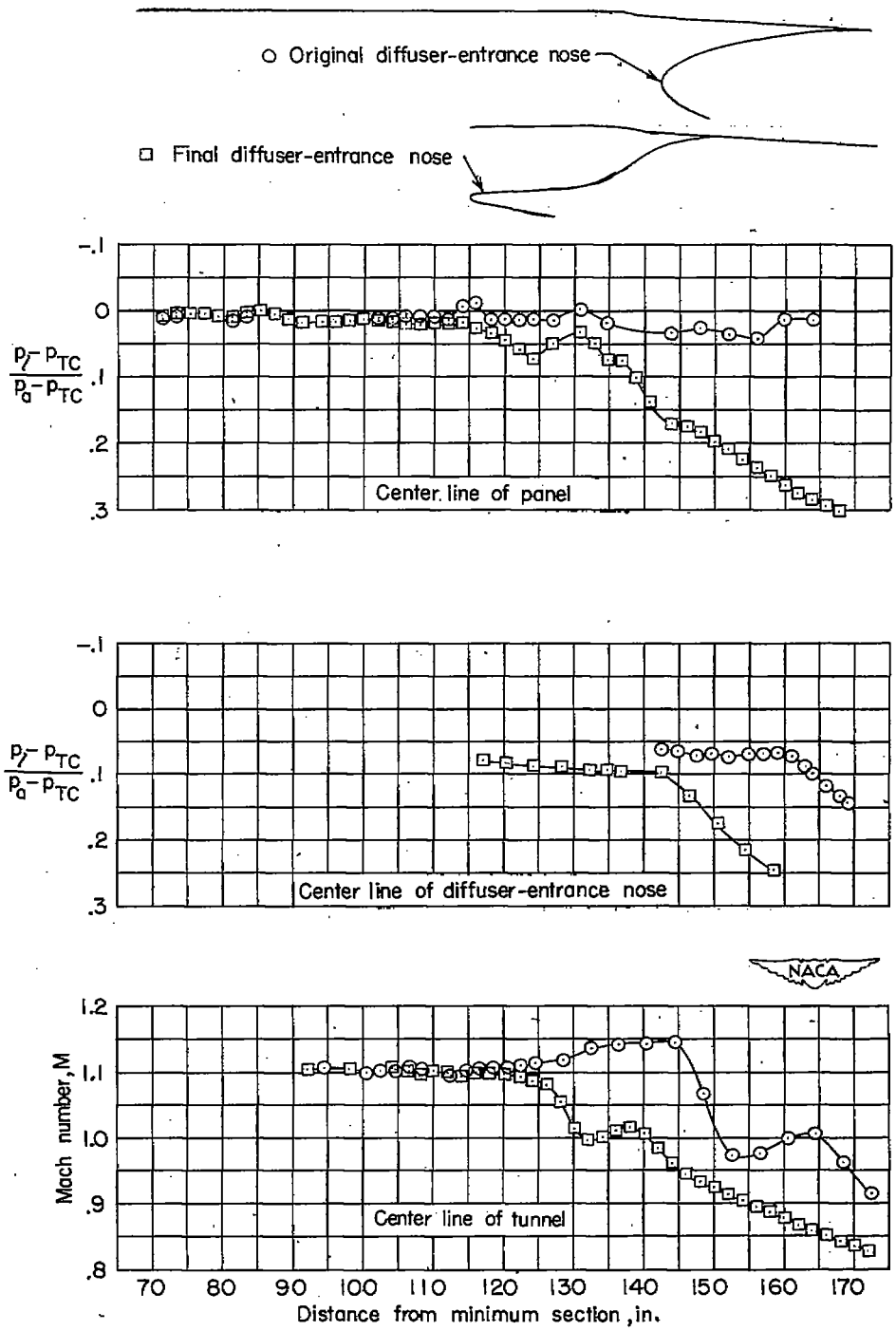

Figure 19.- Comparison of pressure distributions on panel and diffuser-entrance nose and center-line Mach number distributions with the original and final diffuser-entrance noses installed. $M_o = 1.10$.

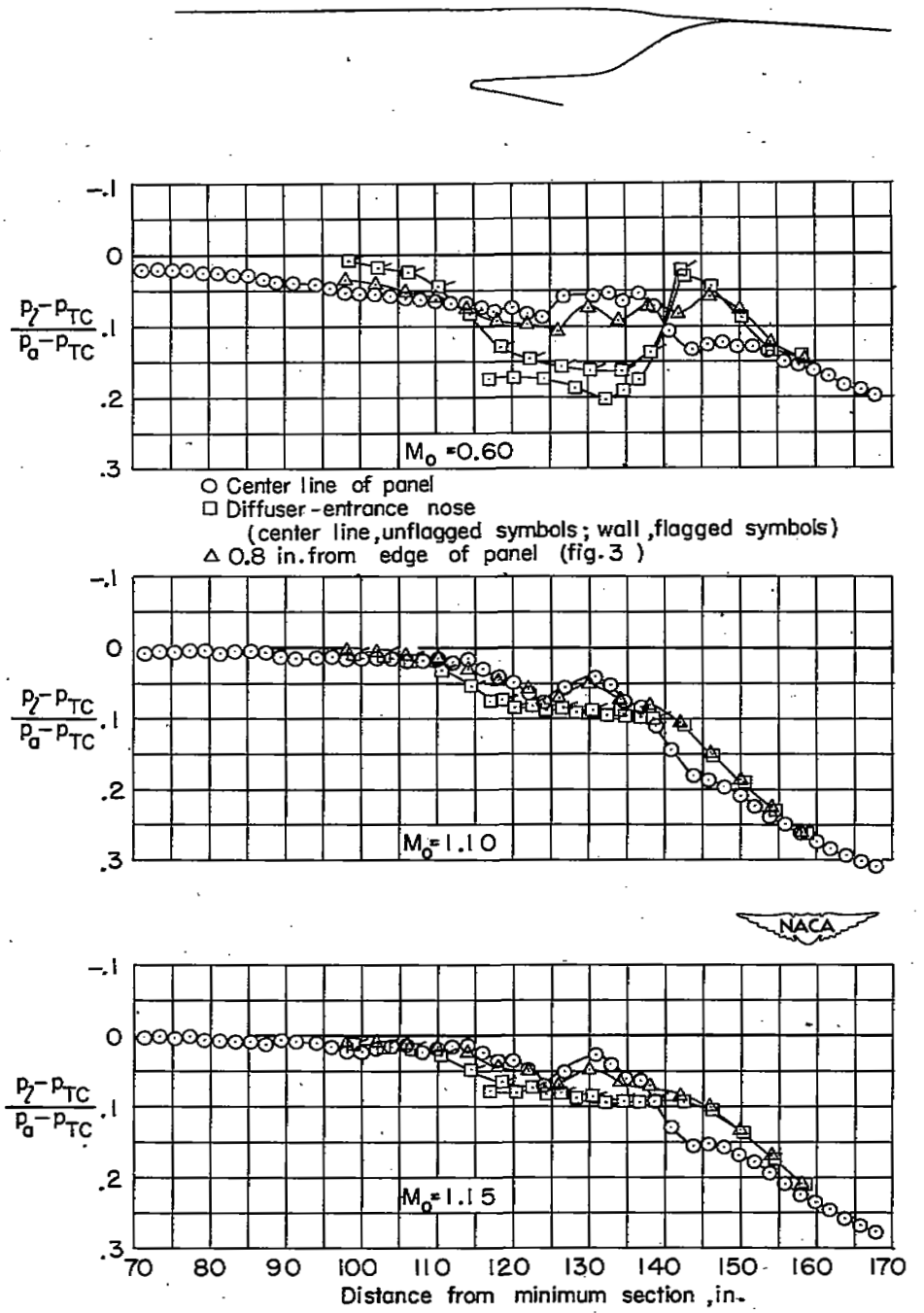

Figure 20.- Pressure distributions on panel and diffuser-entrance nose at several Mach numbers for tunnel with final diffuser-entrance noses installed.

[redacted]

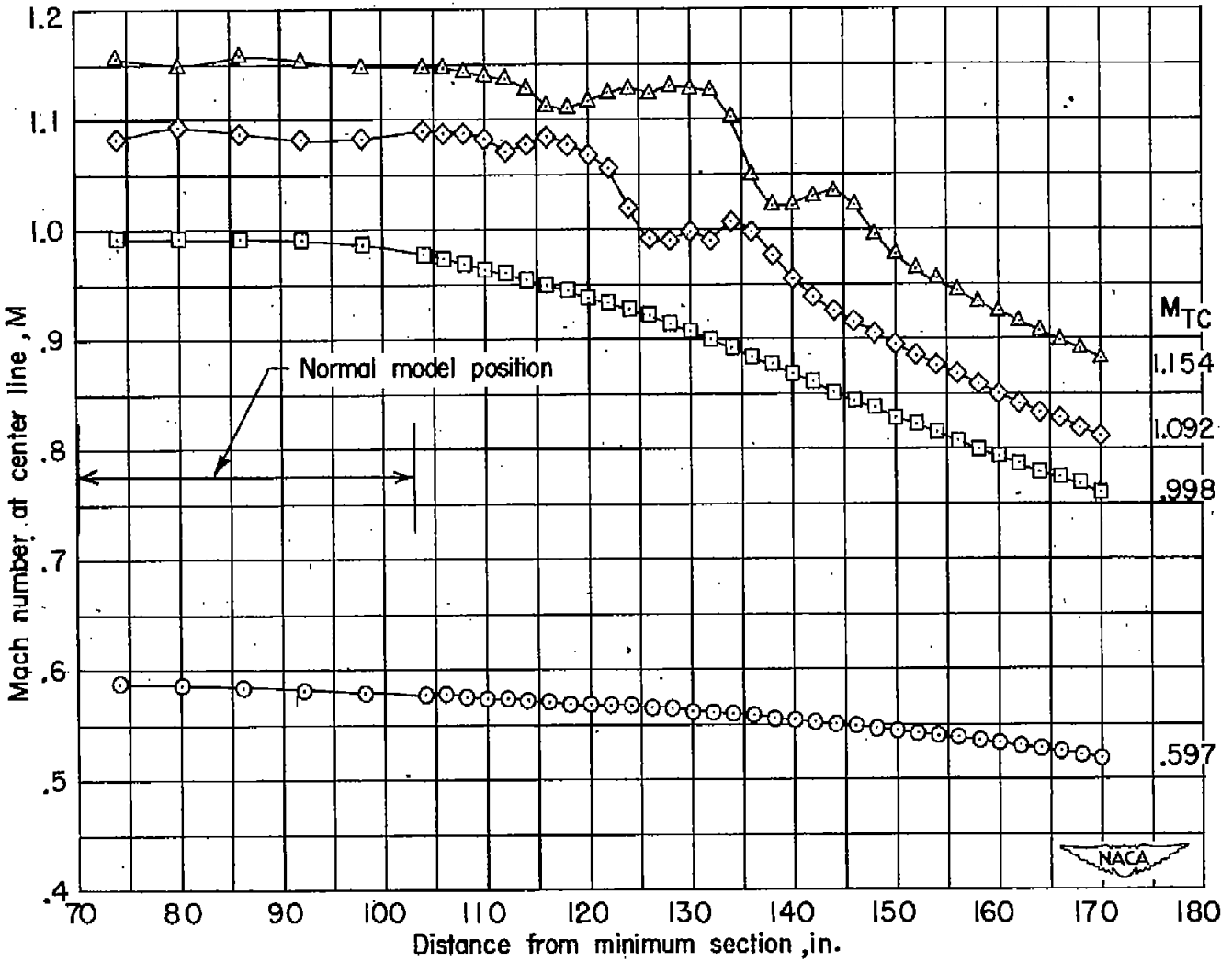

Figure 21.- Center-line Mach number distributions at several test-chamber Mach numbers for tunnel with final diffuser-entrance noses installed.

Tunnel condition	Body in tunnel	Diffuser-entrance nose	Distance between nose and tunnel surface, (in.)
5	Survey tube	2	10
7	Survey tube	3	7
8	Survey tube	4	9.75
9	Wing-body	4	9.75

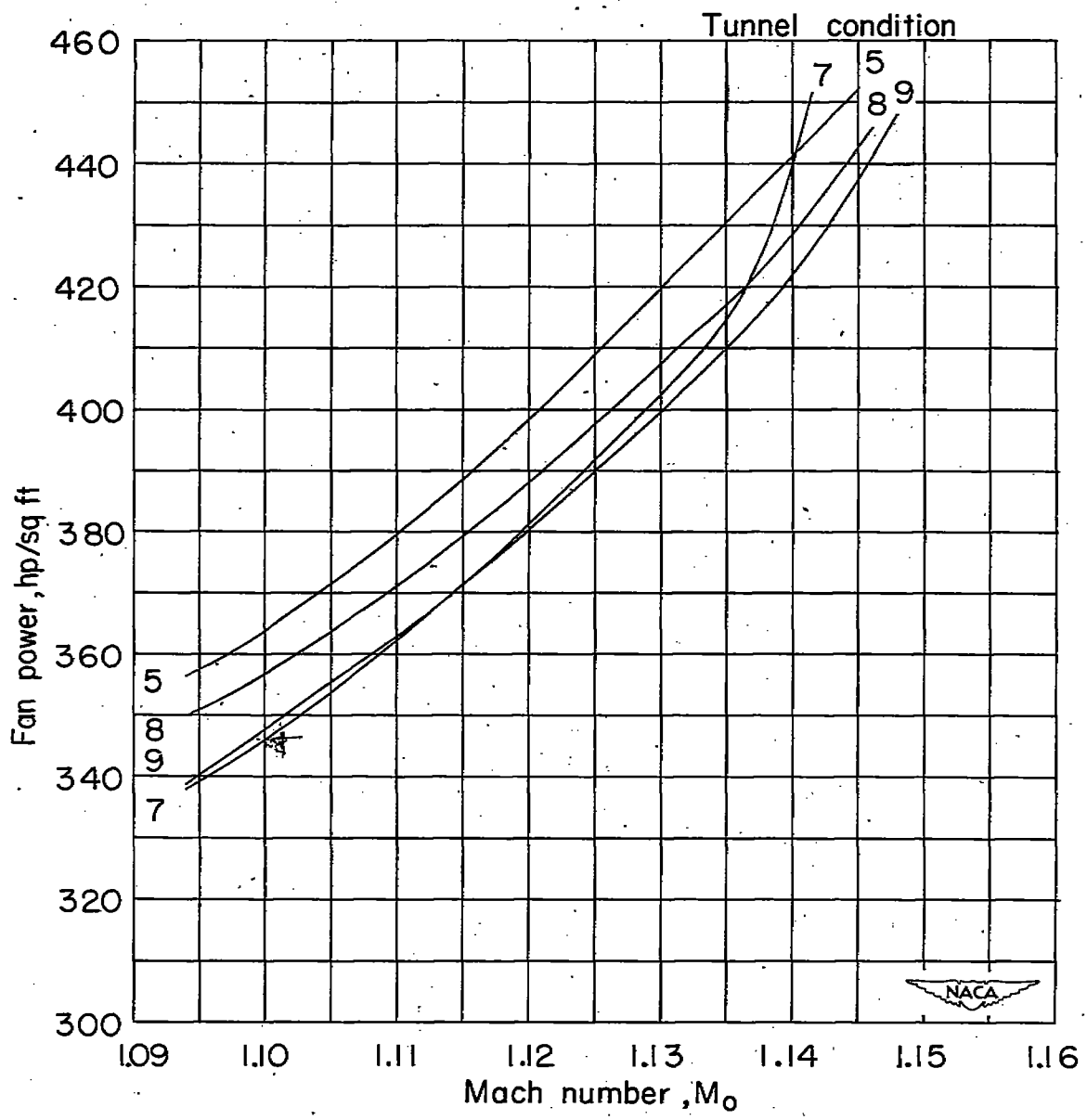

Figure 22.- Variation of fan power with Mach number for several variations of the revised diffuser-entrance noses.

[redacted]

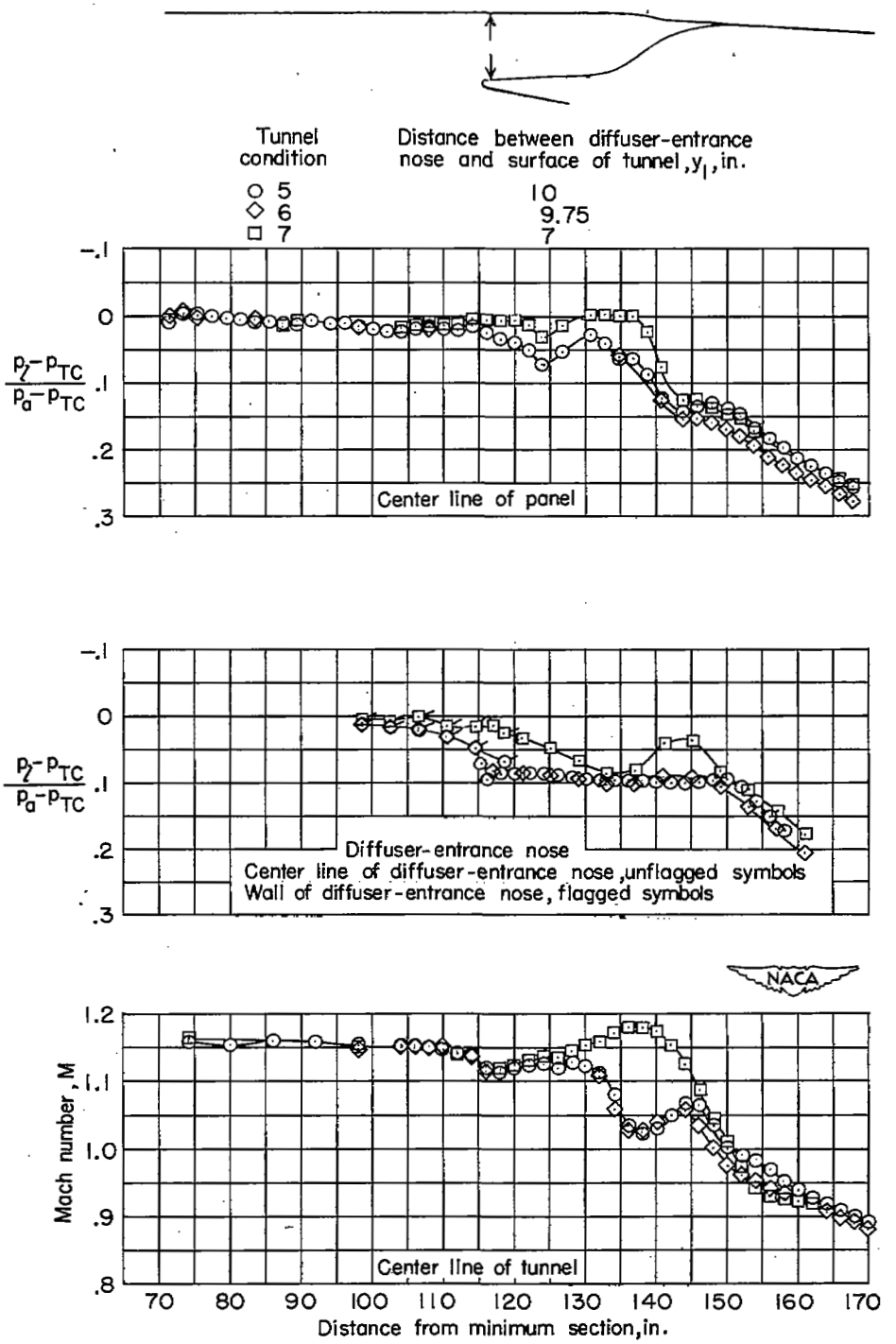

Figure 23.- Pressure distributions on panel and diffuser-entrance nose and center-line Mach number distribution for tunnel with several revised diffuser-entrance-nose configurations. $M_o = 1.15$.

[redacted]

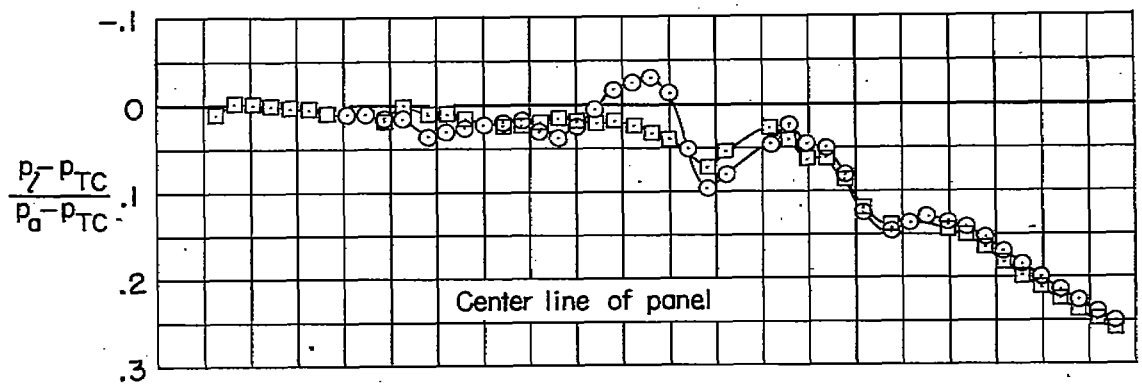

○ Wing-body model in test region
□ Static-pressure tube in test region

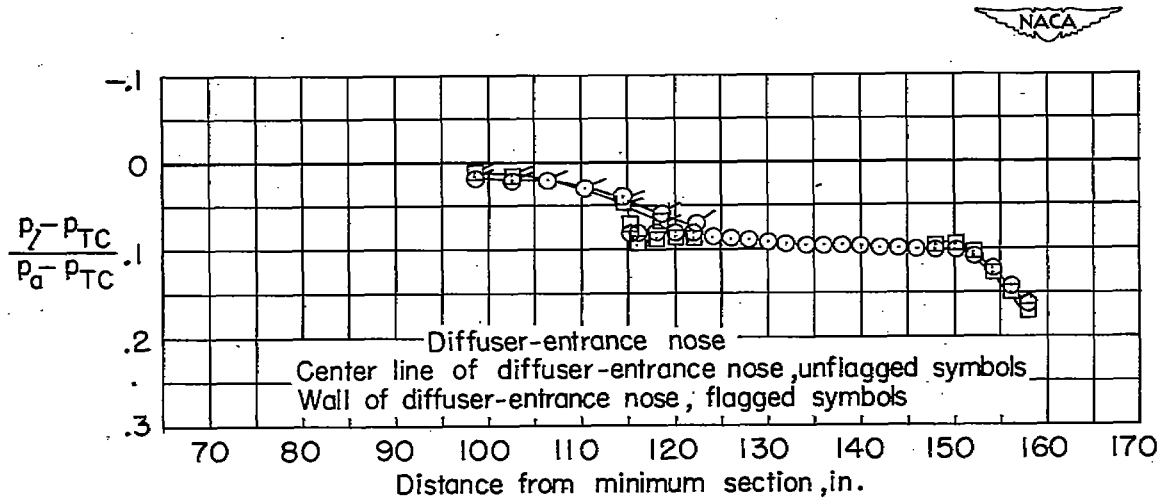

Figure 24.- The effect of a sweptback-wing-body model in test section on the pressure distributions on the panel and diffuser-entrance nose. $M_o = 1.15$.

Error

An error occurred while processing this page. See the system log for more details.

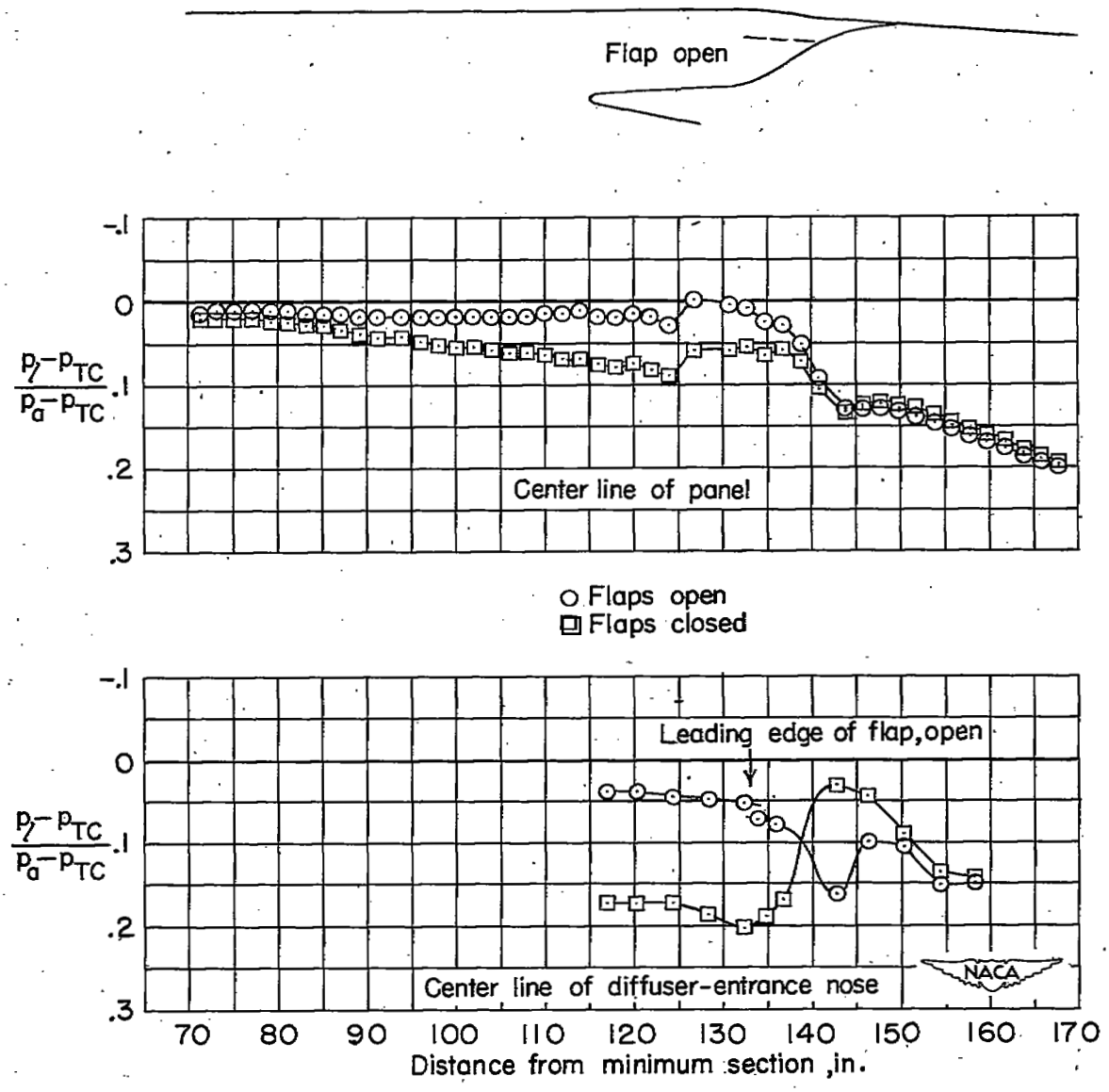

Figure 26.- The effect of opening flaps in the final diffuser-entrance noses on pressure distributions on panel and diffuser-entrance nose. M = 0.60.

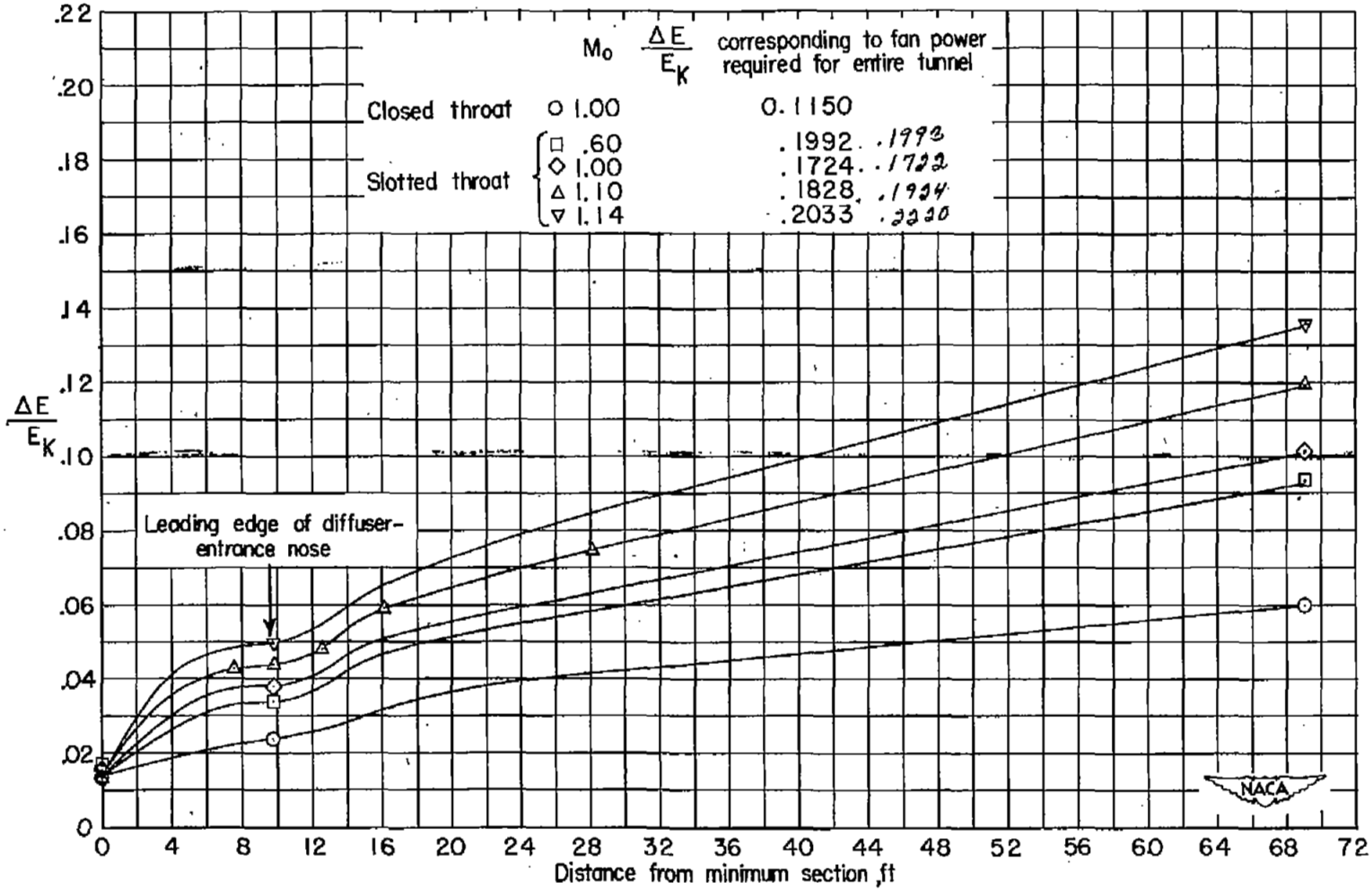

Figure 27.- Streamwise variations of power required to raise local total pressures in the stream tube to atmospheric pressure for closed throat and slotted throat with final diffuser-entrance nose installed.

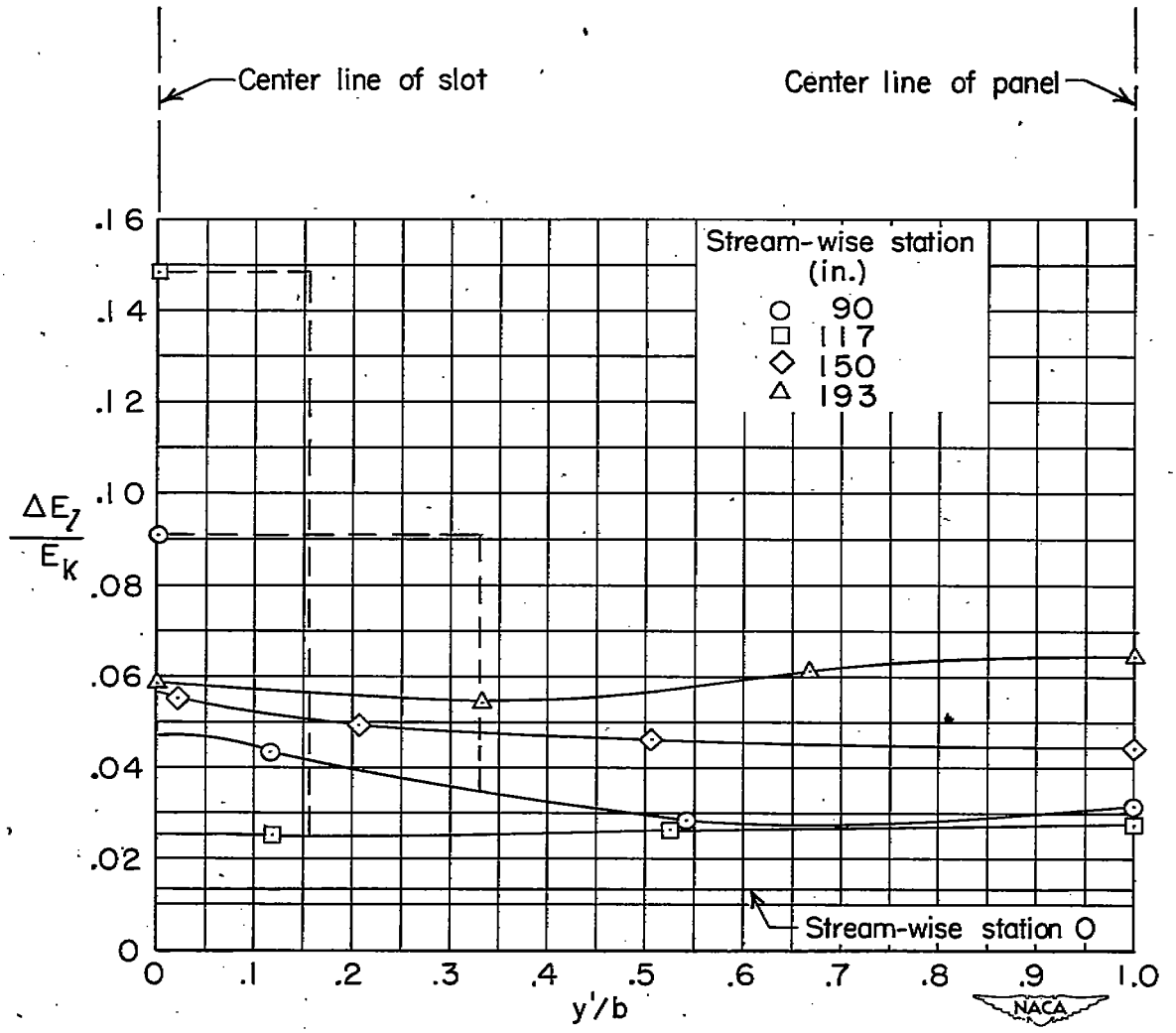

Figure 28.- Lateral variations of power deficiencies measured at various rake locations for several streamwise stations in tunnel with final diffuser-entrance noses installed. M_o = 1.10.

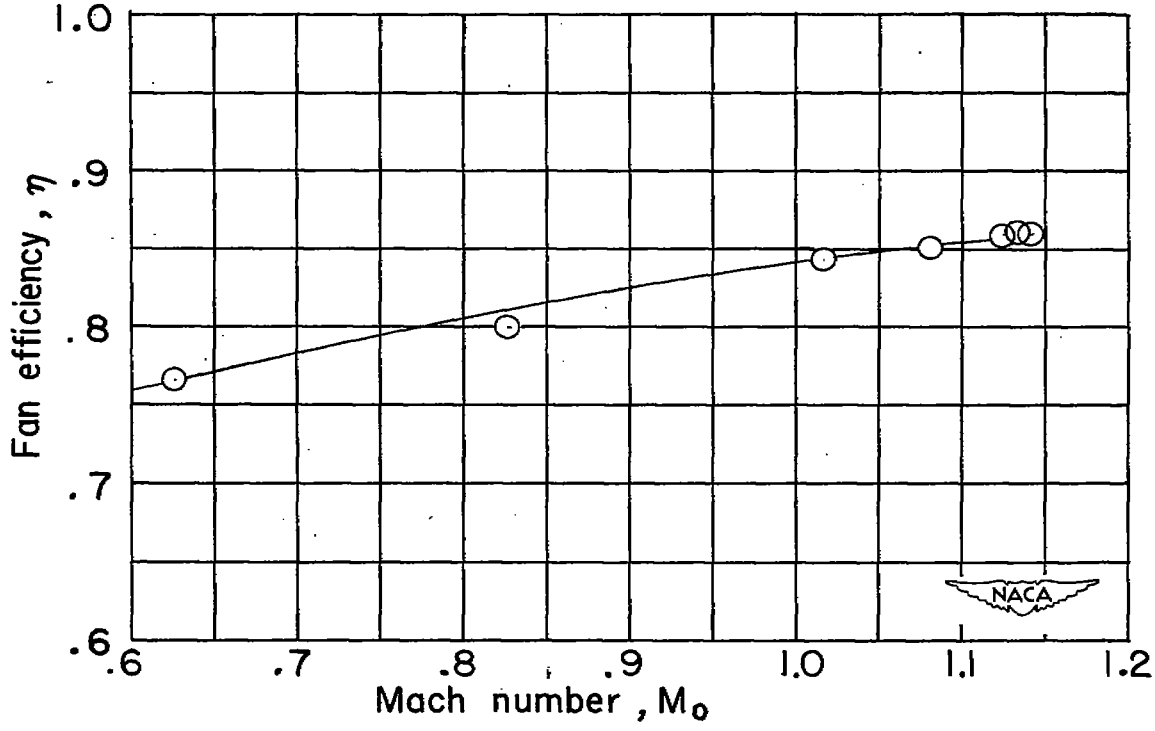

Figure 29.- Variation of fan efficiency with Mach number.

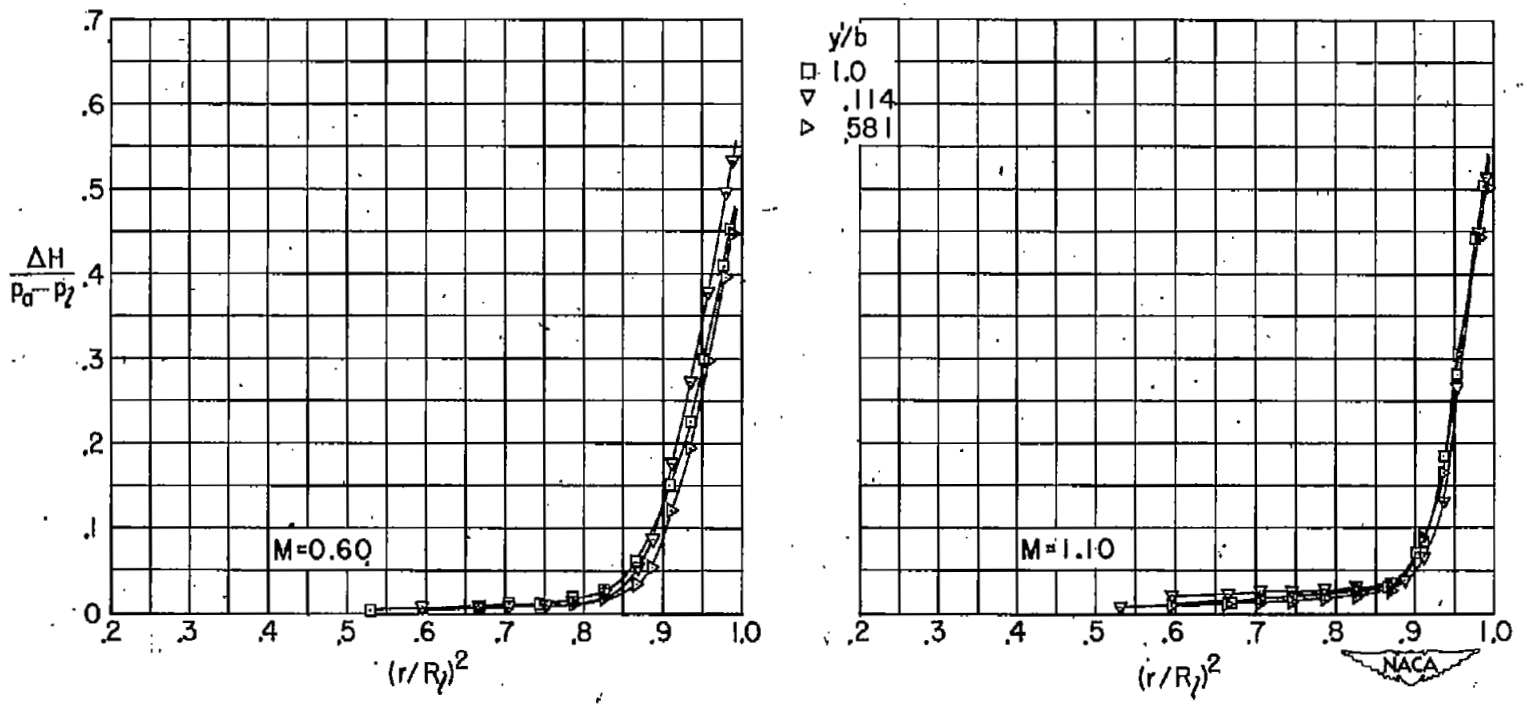

(a) Streamwise station 90.

Figure 30.- Radial variations of local total pressure deficiencies measured at various rake locations in tunnel with final diffuser-entrance nose installed.

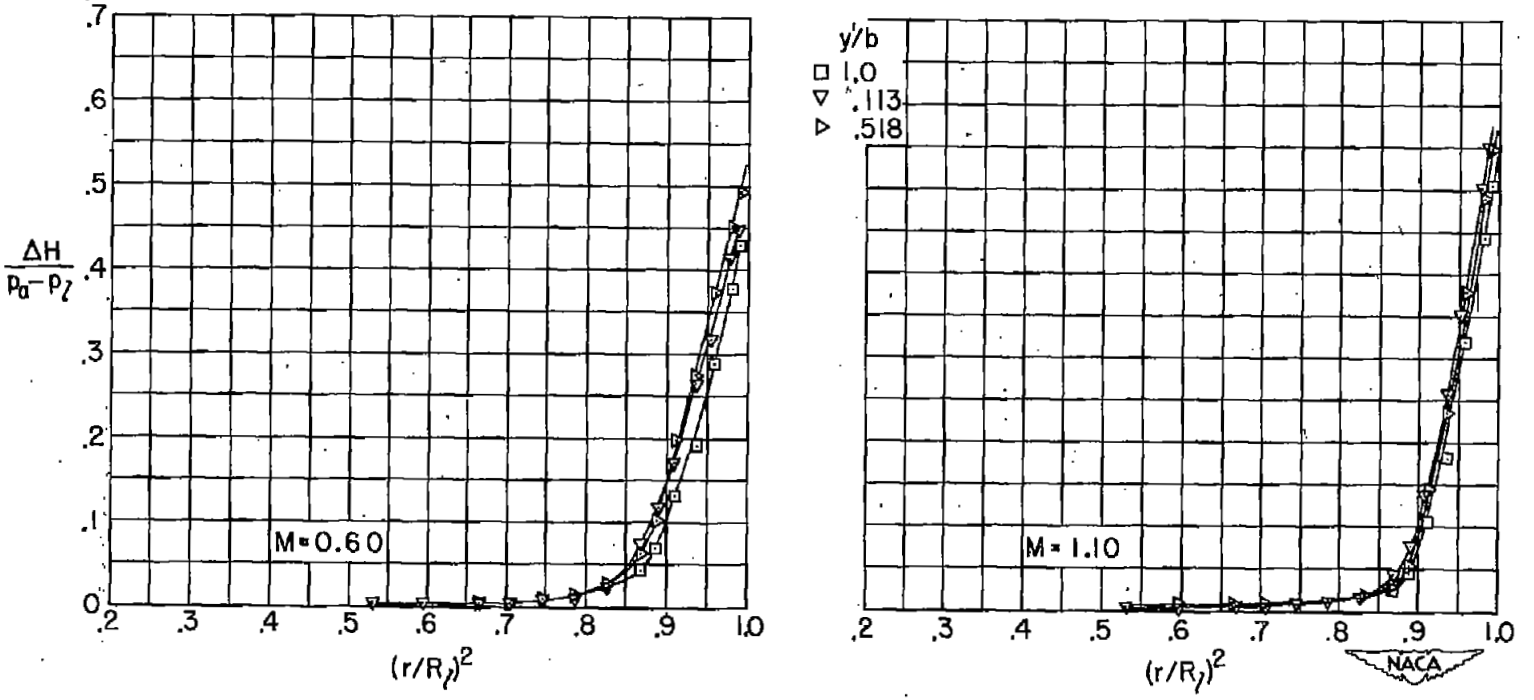

(b) Streamwise station 117.

Figure 30.- Continued.

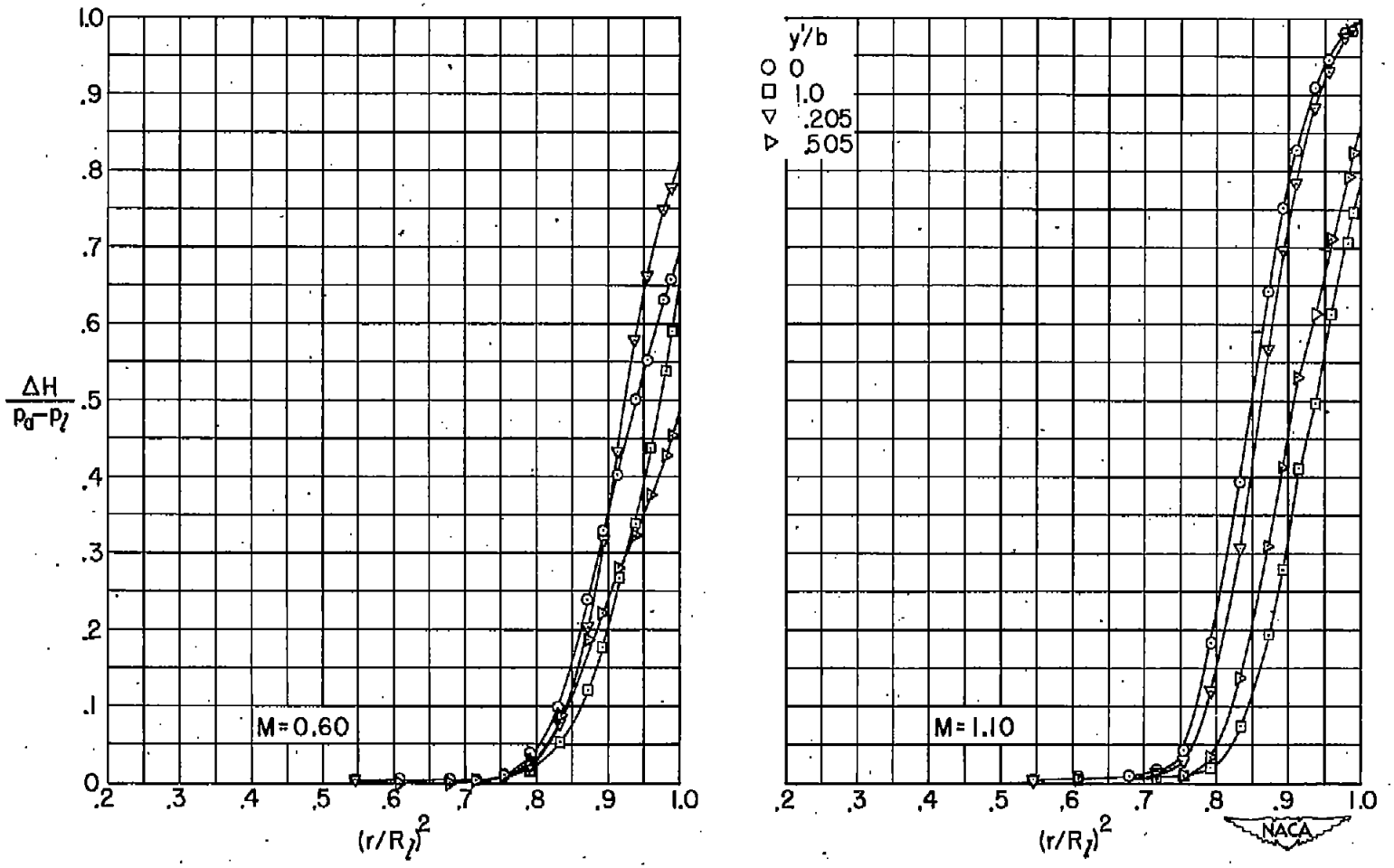

(c) Streamwise station 150.

Figure 30.- Continued.

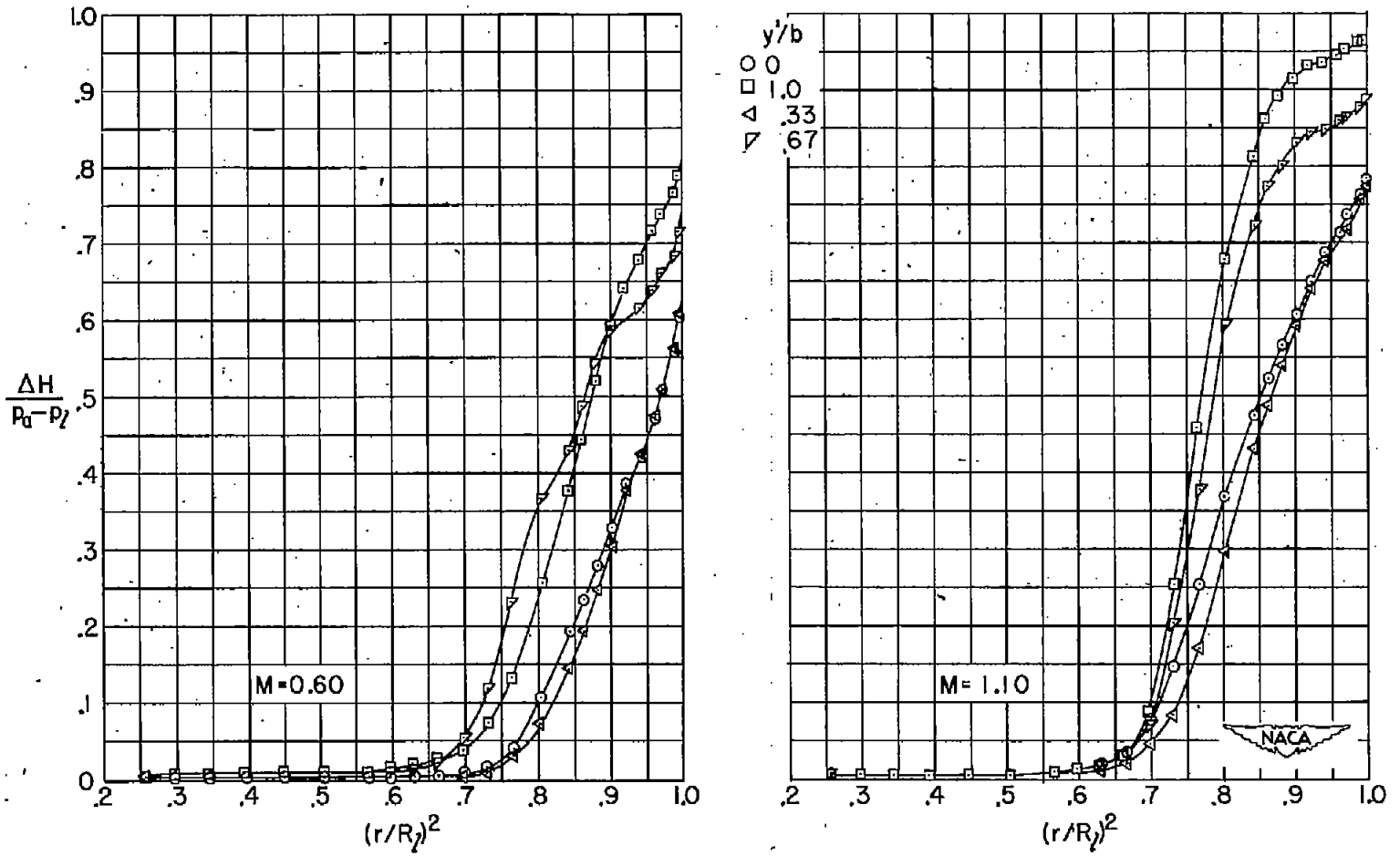

(d) Streamwise station 193.

Figure 30.- Continued.

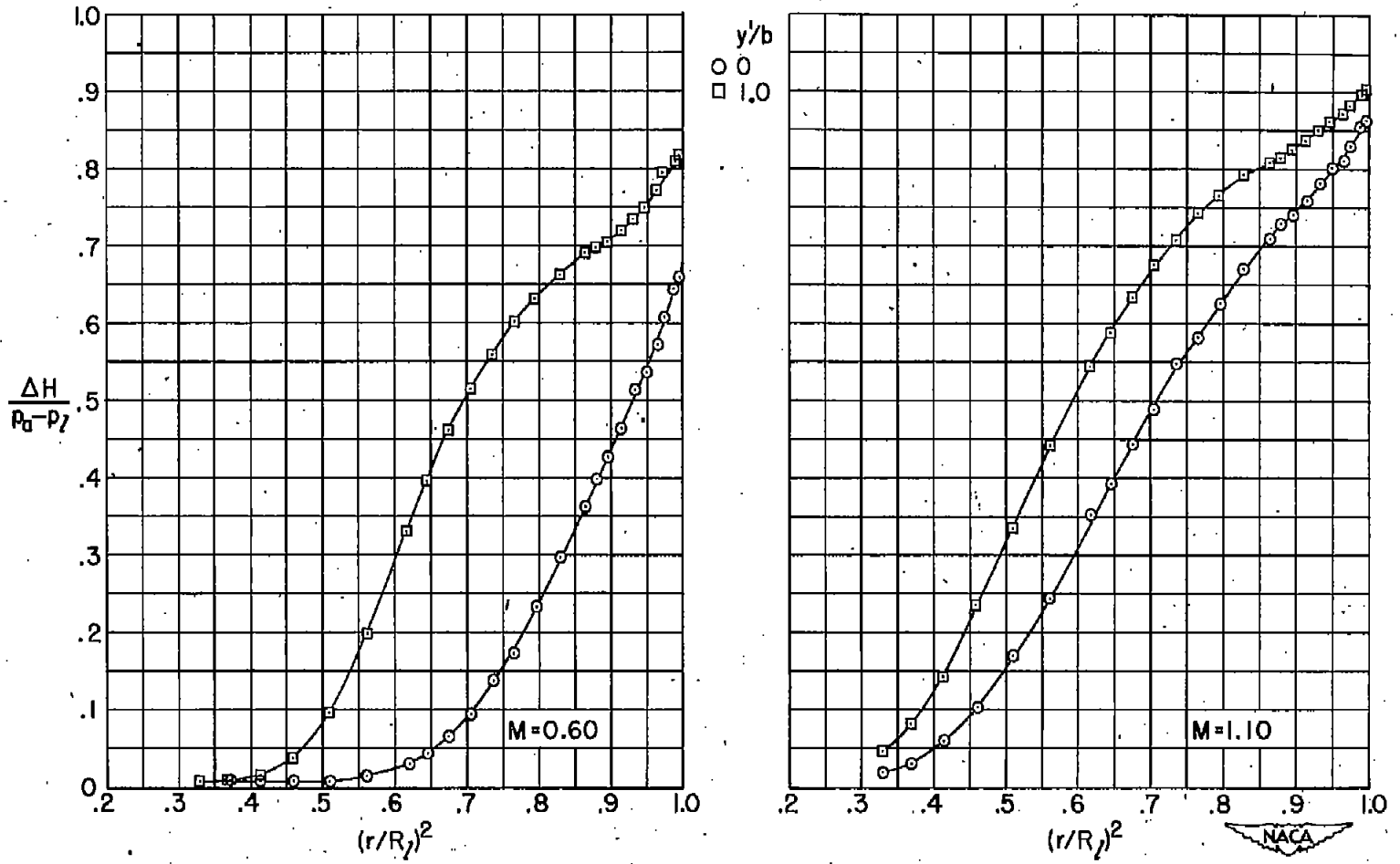

(e) Streamwise station 337.

Figure 30.- Continued.

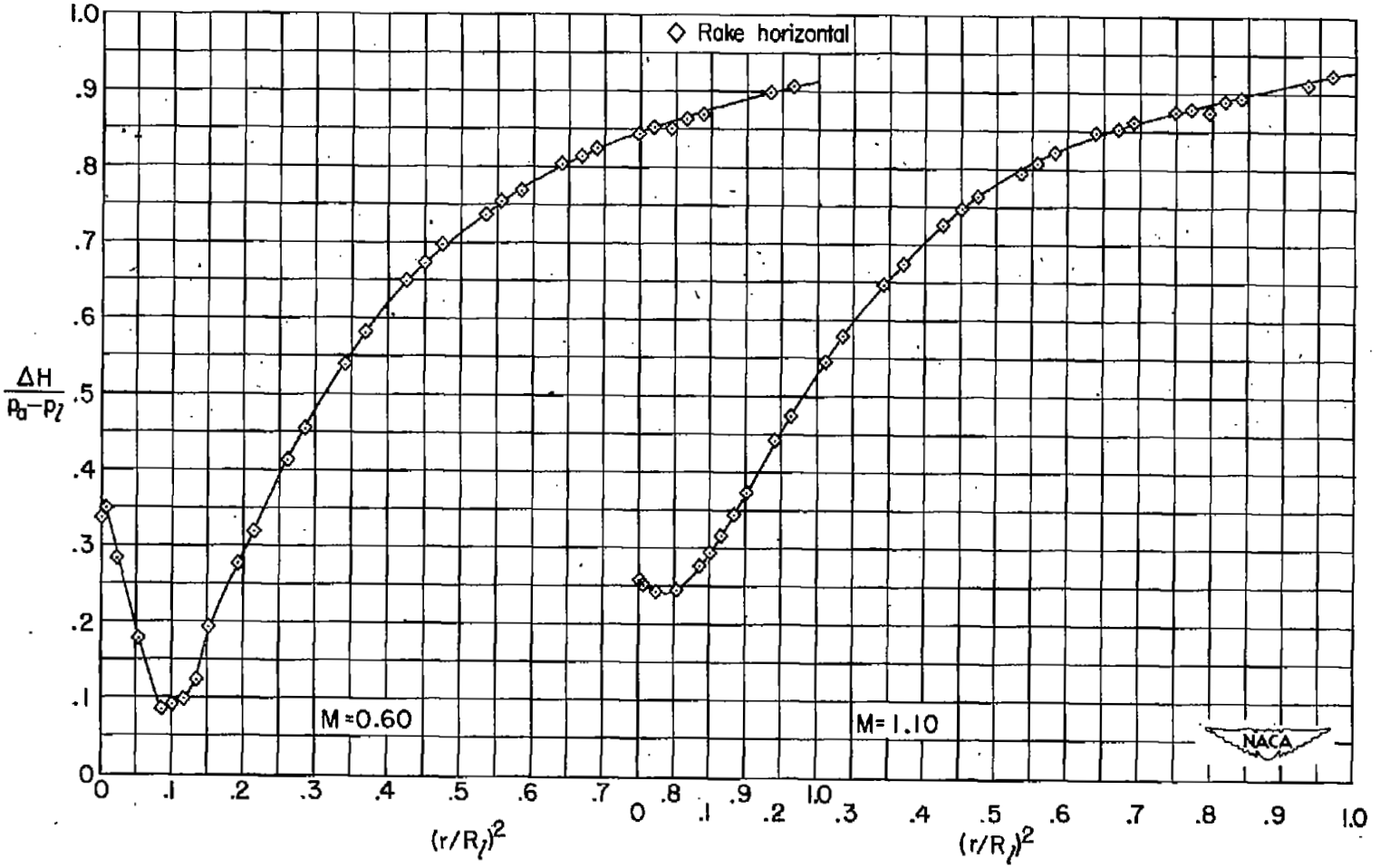

(f) Diffuser exit.

Figure 30.- Concluded.

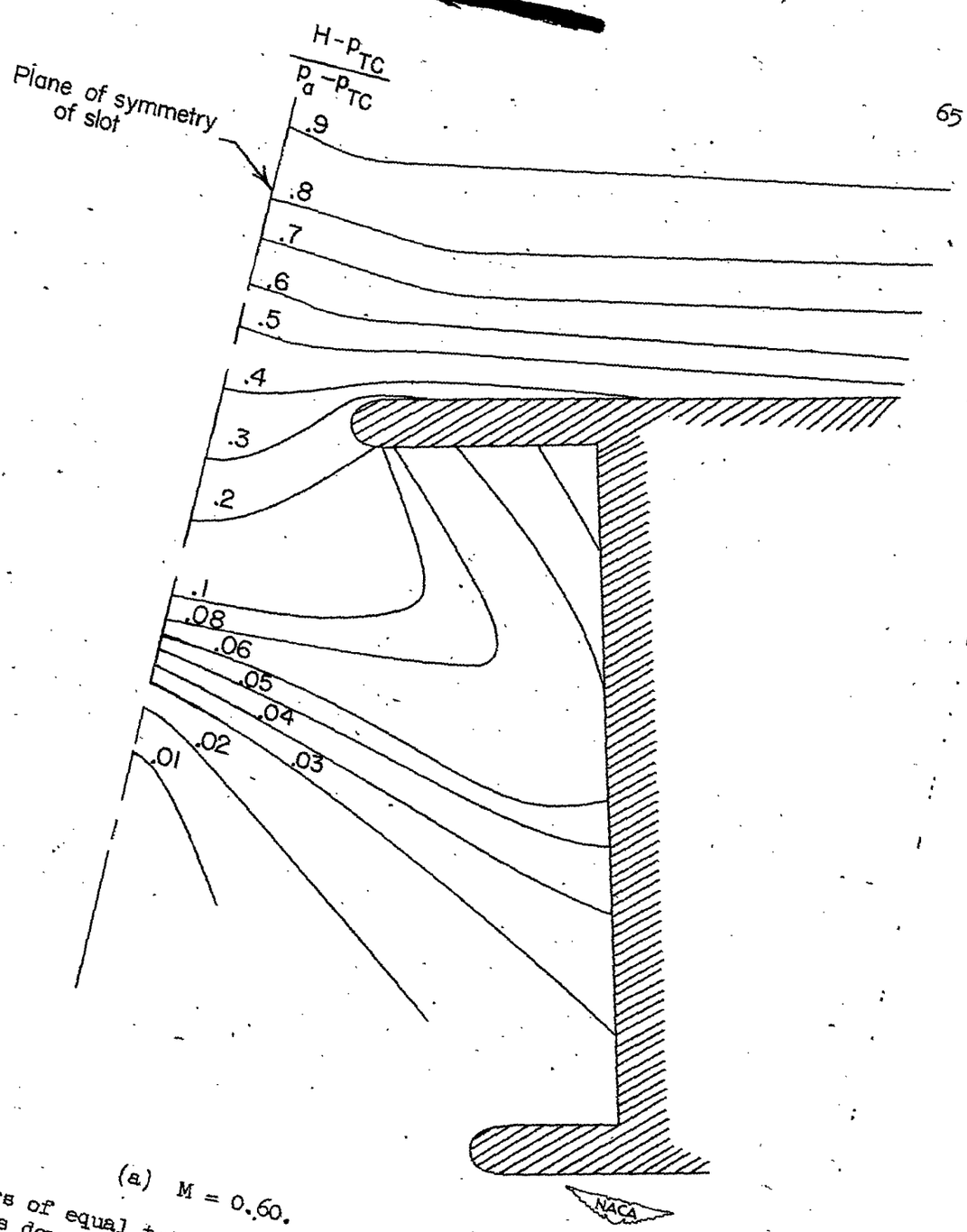

(a) M = 0.60.

Figure 31.- Contours of equal total pressure in regions of slot at a station 90 inches downstream of the origin of the slots for the tunnel with final diffuser-entrance noses installed.

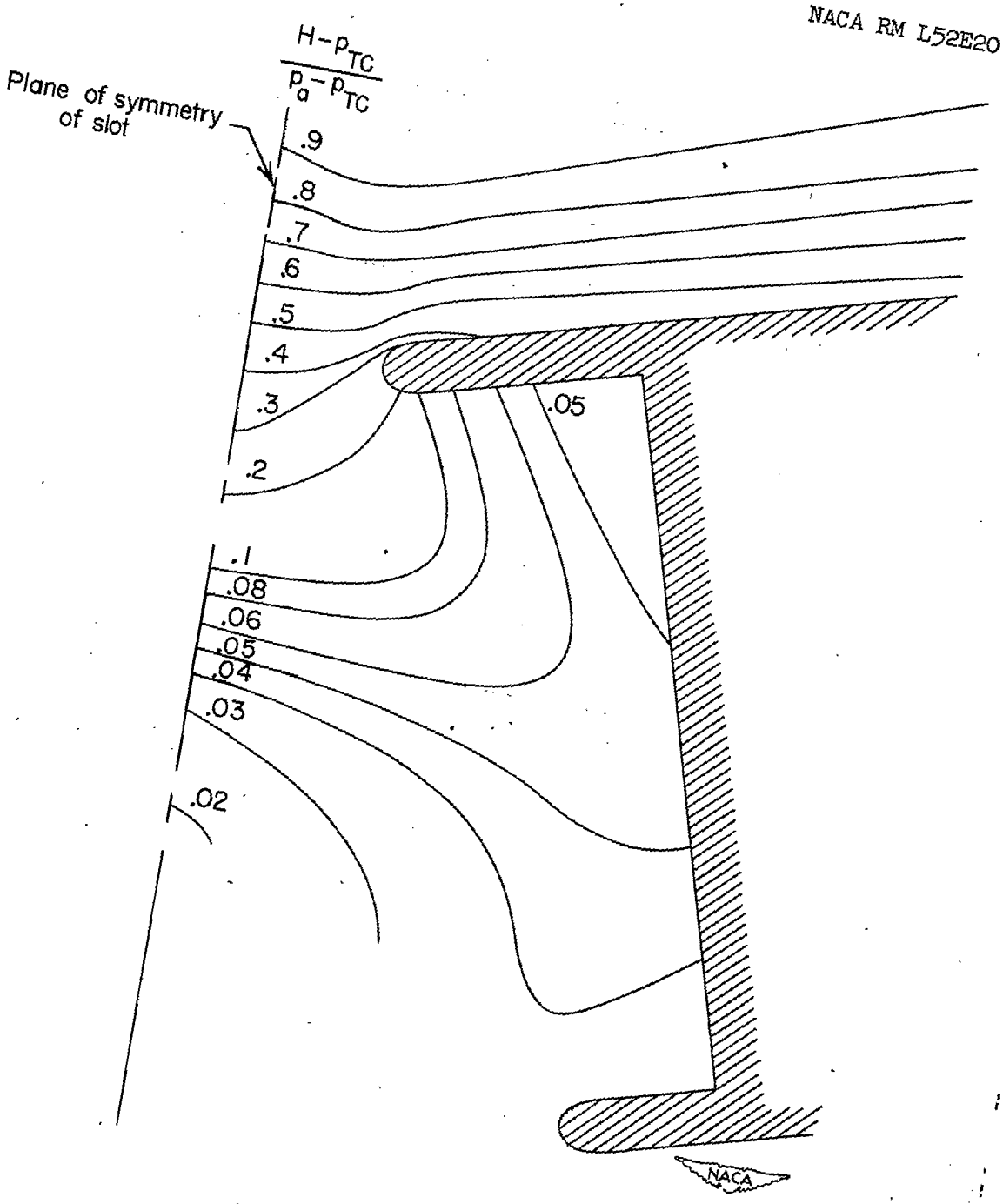

(b) $M = 1.10$.

Figure 31.- Concluded.

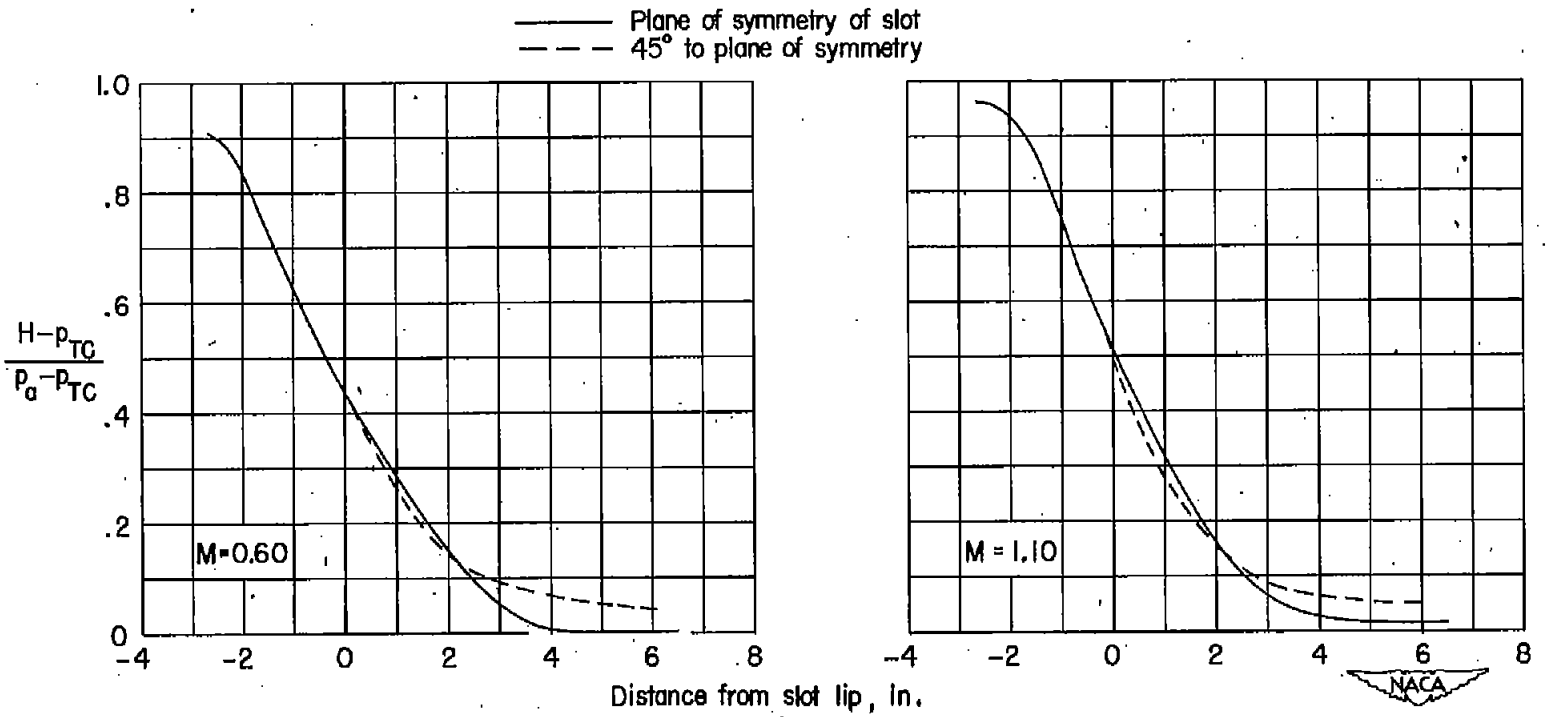

Figure 32.- Variations of total pressure in region of slot at a station 90 inches downstream of the origin of the slots for the tunnel with final diffuser-entrance noses installed.

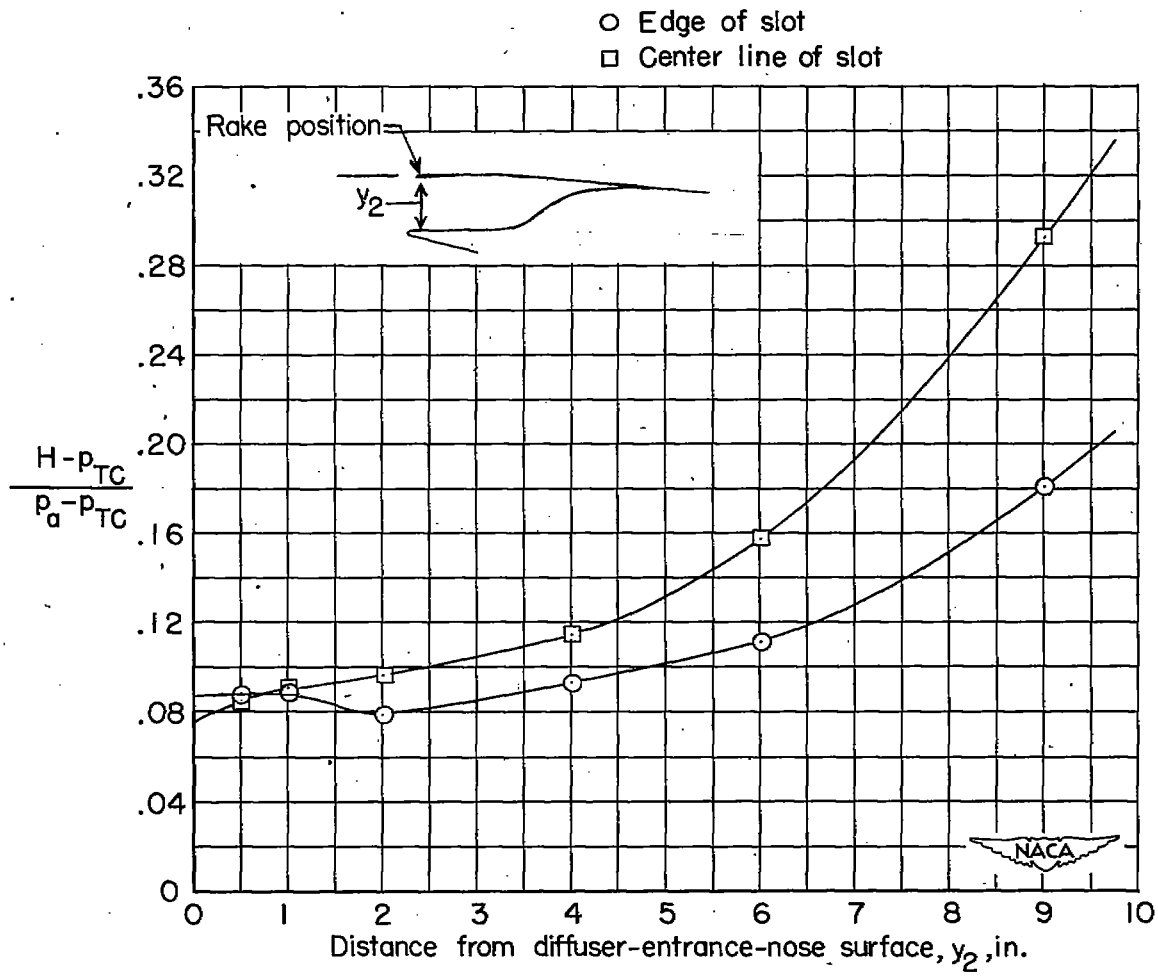

Figure 33.- Variations of total pressure normal to tunnel axis at leading edge of final diffuser-entrance nose. $M_o = 1.10$.

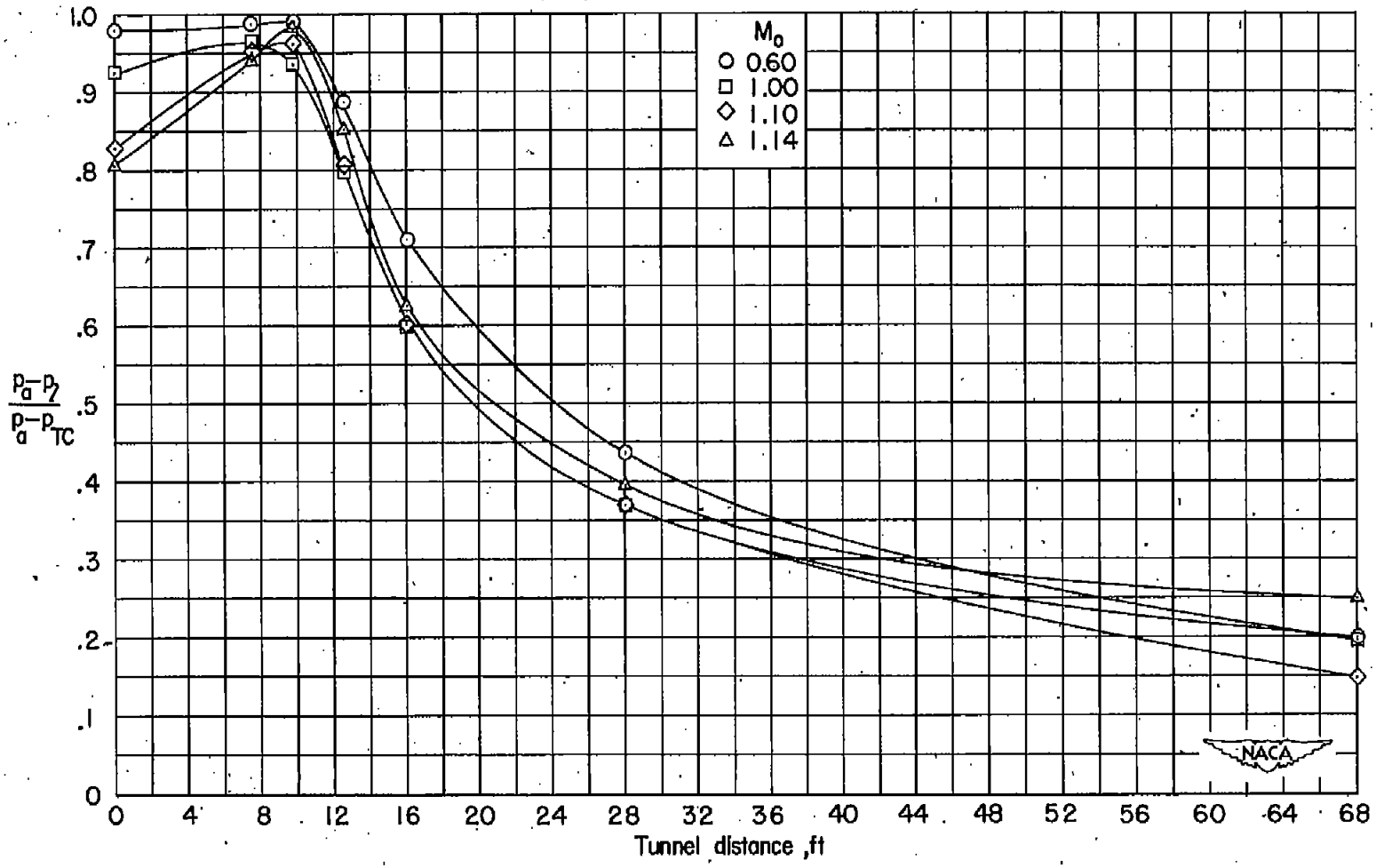

Figure 34.- Streamwise variations of static pressures in the diffuser of tunnel with final diffuser-entrance noses installed.

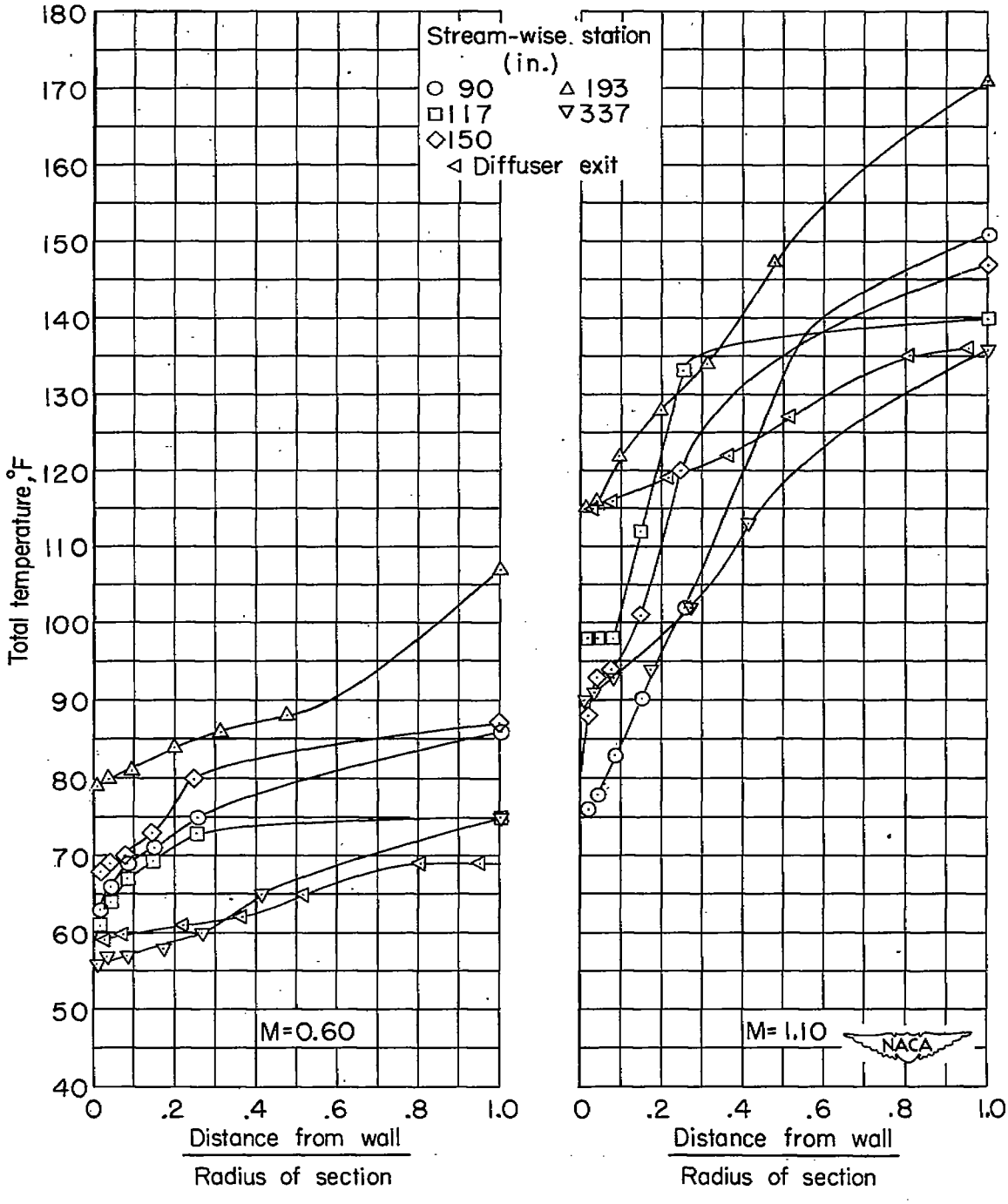

Figure 35.- Radial variations of local total temperature measured at various rake locations in tunnel with final diffuser-entrance noses installed.